Application of Overset Grid Methods to Wind Turbine Rotors

C.P. “Case” van Dam

Mechanical & Aerospace Engineering
University of California, Davis

cpvandam@ucdavis.edu

2010 Overset Grid Symposium
Moffett Field, CA

22 September 2010

Acknowledgements

- Mike Zuteck, MDZ Consulting
- Kevin Jackson, Dynamic Design Engineering, Inc.
- Earl Duque, Northern Arizona University
- Wind Energy Technology Dep., Sandia National Laboratories, Albuquerque
- National Wind Technology Center, NREL
- TPI Composites, Inc.
- K&C Wind Group
- UC Davis, Past & Present
  - Edward Mayda, Frontier Wind
  - Jonathan Baker, Frontier Wind
  - Kevin Standish, Siemens Windpower
  - David Chao, Vestas Windpower
  - Scott Larwood, University of the Pacific
  - Dora Yen Nakafuji, HECO
  - Syta Saephan,Wind Energy Consultant
  - Jose Zayas, SNL Albuquerque
  - Myra Blaylock
  - Ray Chow
  - Aubryn Cooperman
  - Scott Johnson
  - Henry Shiu
  - Et al.

Outline

- Wind Energy Overview
- Advanced Rotor Designs
  - BSDS blade
  - STAR blade
  - Active aerodynamic load control
  - Inboard flow separation mitigation
- Concluding Remarks

Source: Mayda

Why Wind Energy?

- Renewable
  - Guaranteed “fuel” availability
  - Large available resource in USA
  - No cost volatility
  - Does not rely on water
- Clean
  - Emission free operation
  - No waste generation
- Installation
  - Rapidly deployed
- Security
  - Non-centralized installation and operation
  - No imported fuel requirement
- Economics
  - Cost effective energy
  - Local economic benefits

Installed Wind Power Capacity

- In the 1980s, USA was the leader in installed wind-based electric power generation capacity
- From the 1990s until recently, other countries outpaced the USA
- Over the last few years, pace of installation in the USA has increased rapidly

  Reasons:
  - Increase/uncertainty in fossil fuel prices
  - PTC (Federal)
  - RPS (States)

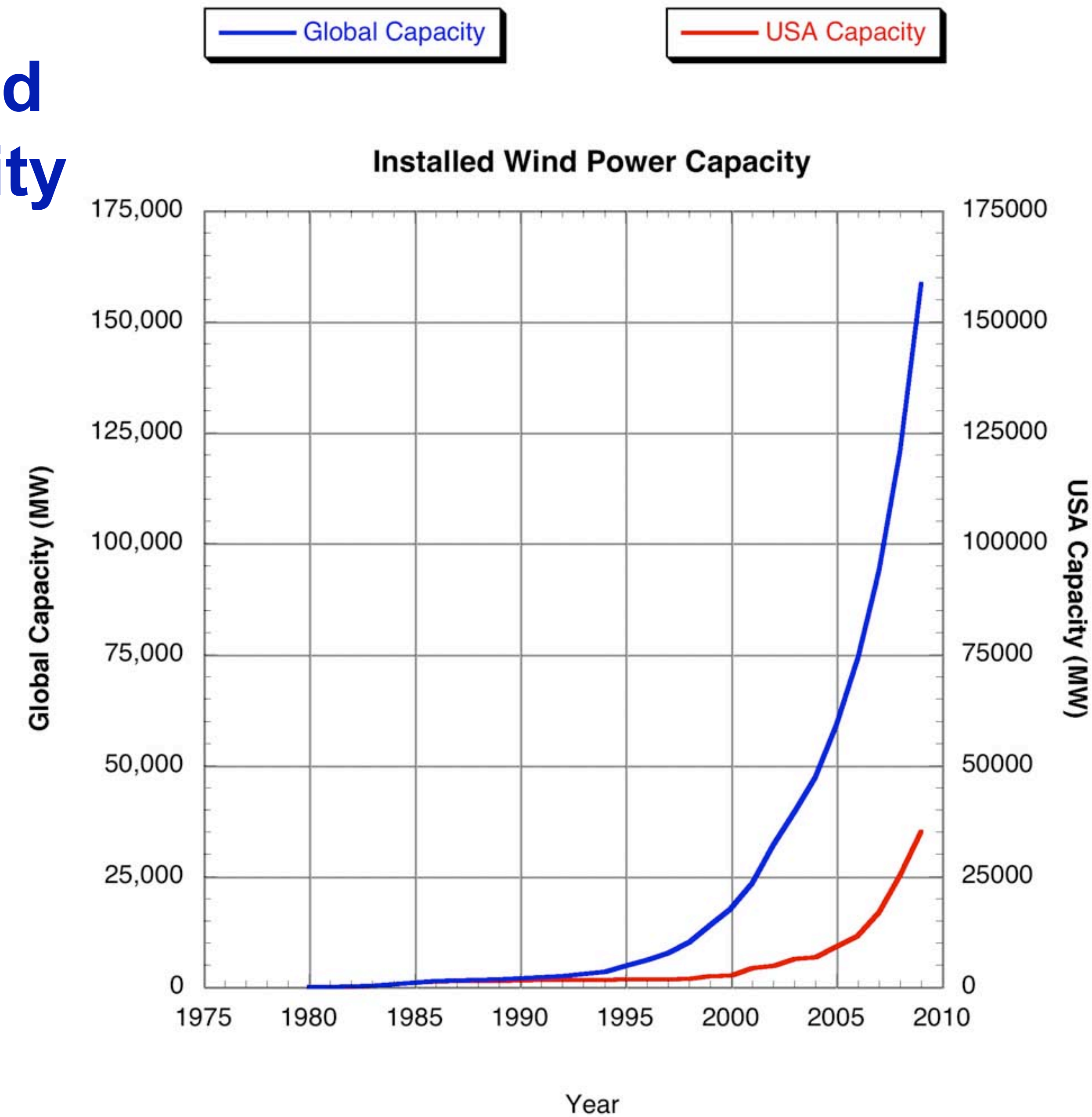

Global Installed Wind Energy Capacity

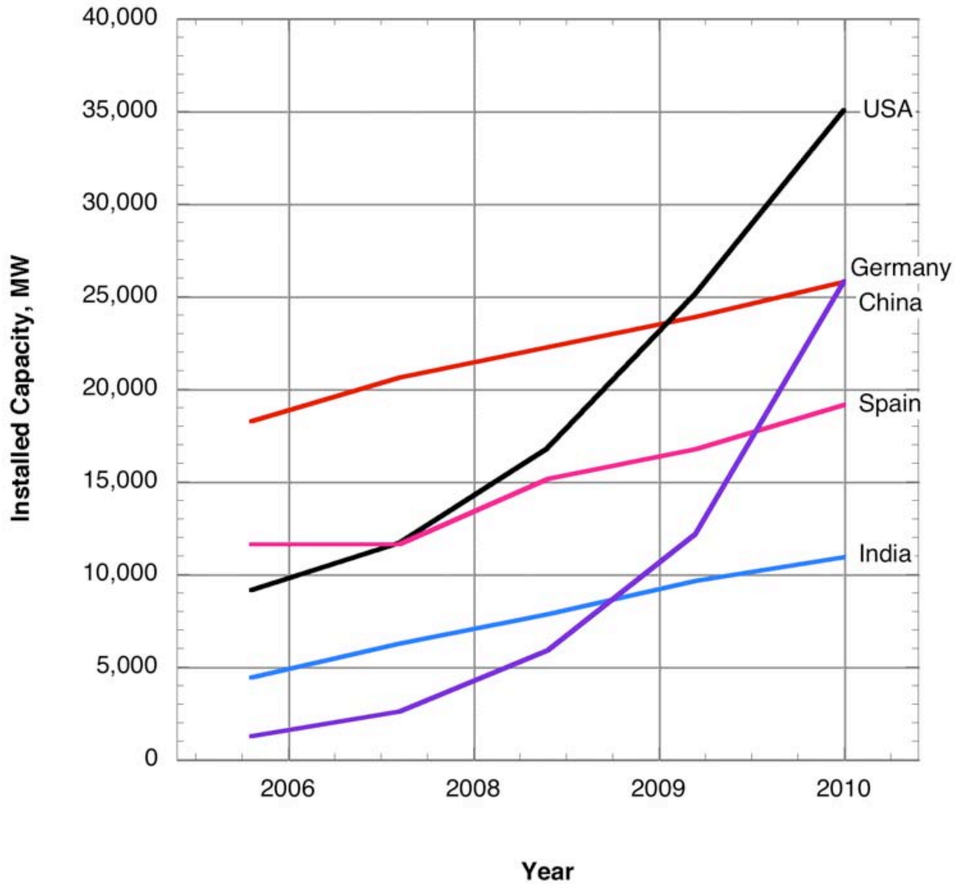

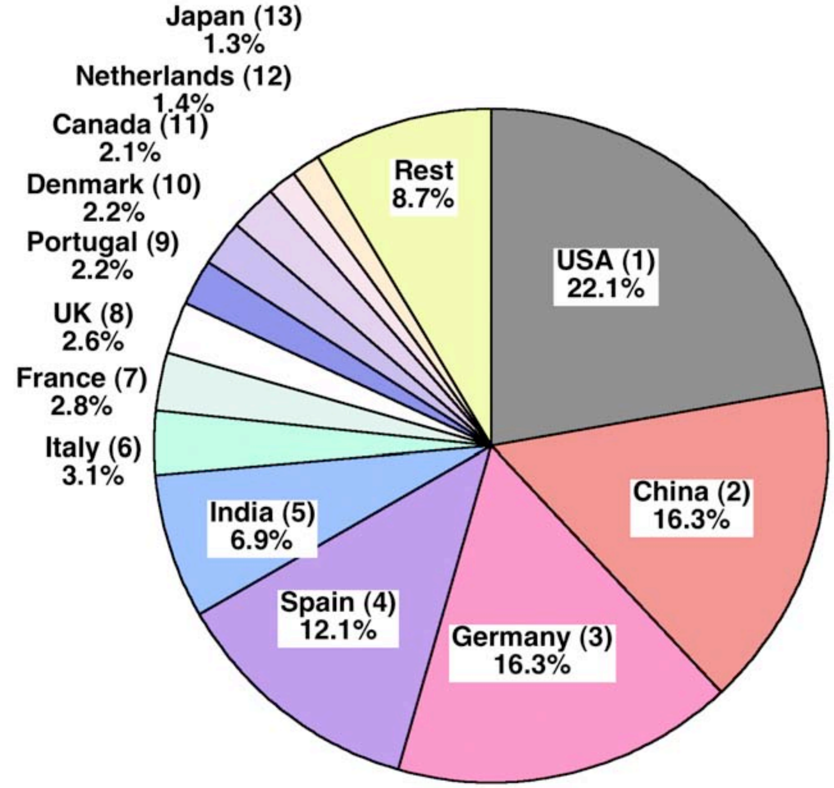

World Installed Capacity (159 GW) Start 2010

USA Installed Wind Energy Capacity

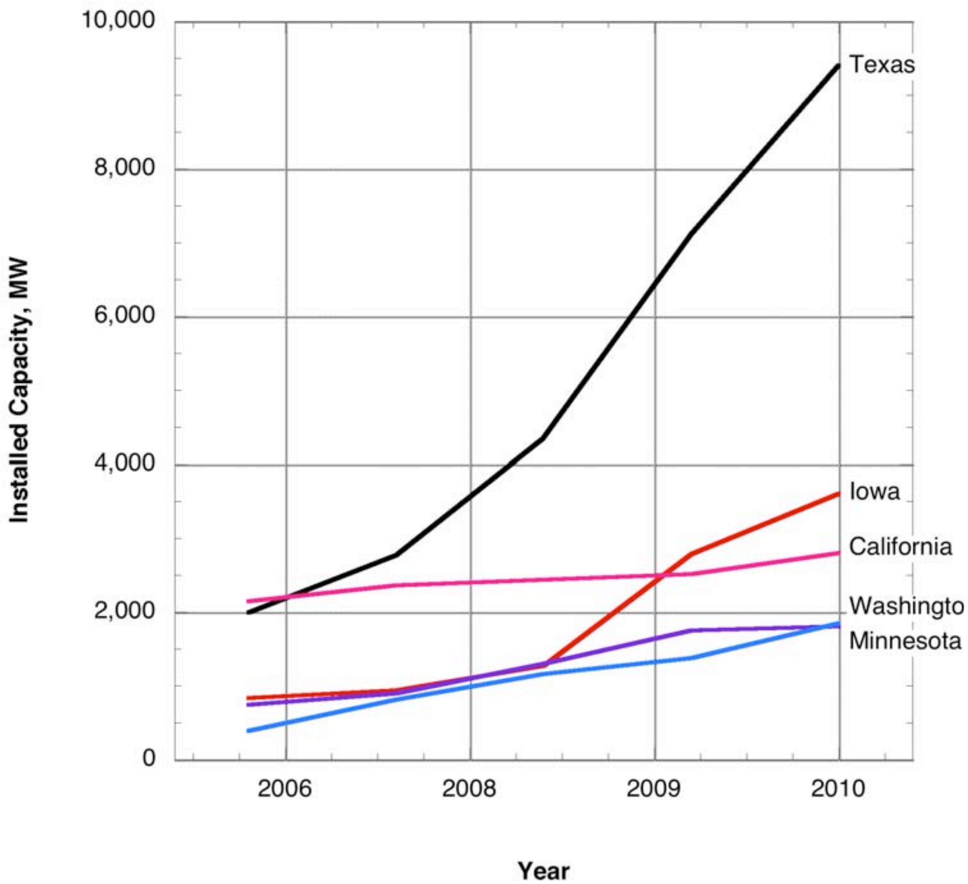

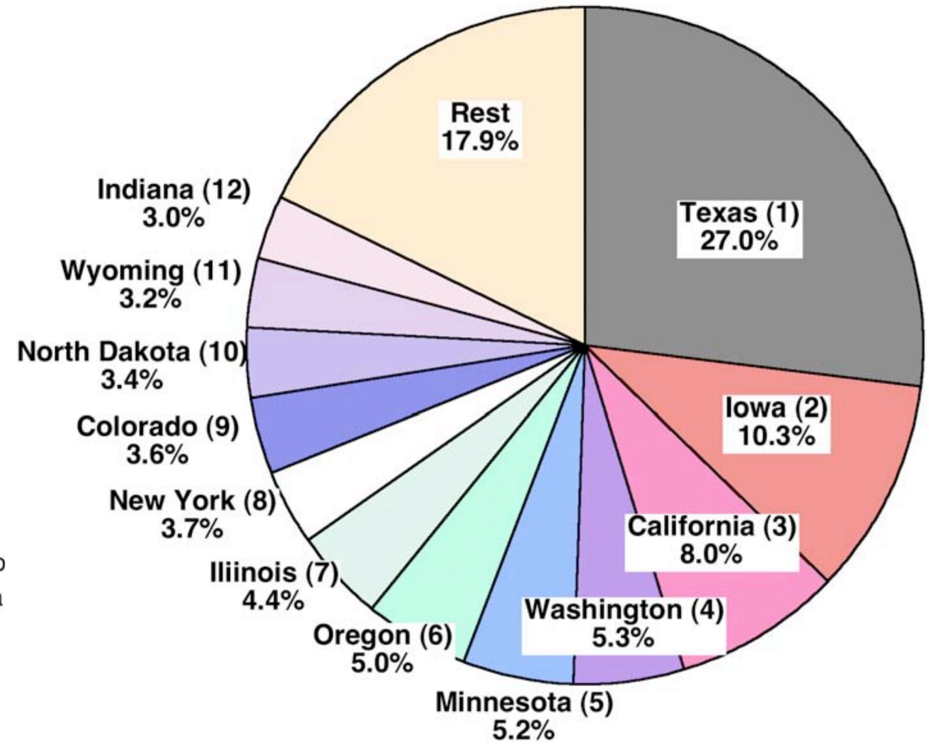

USA Installed Capacity (35 GW) Start 2010

Evolution of U.S. Utility-Scale Wind Turbine Technology

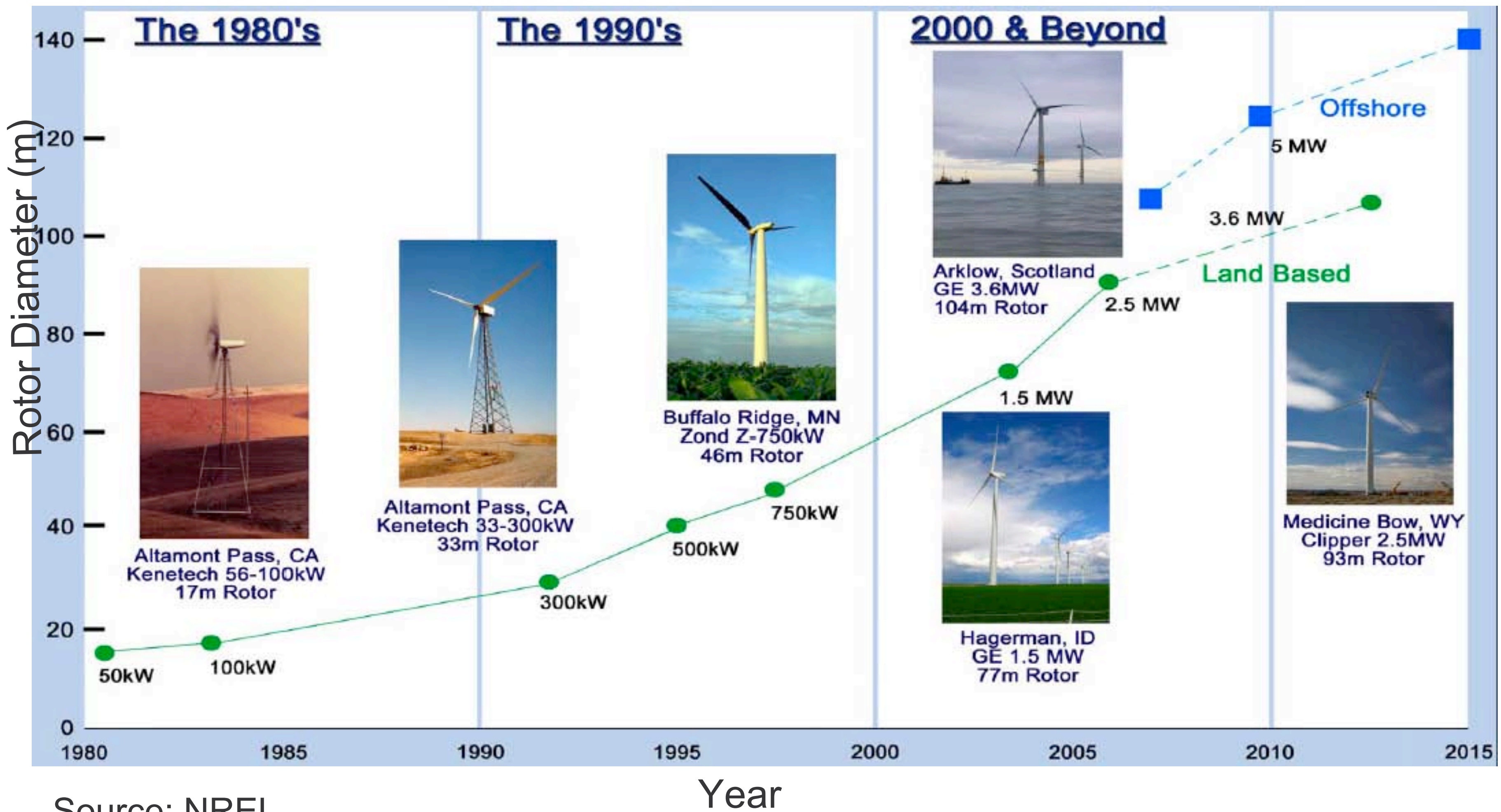

Source: NREL

Typical Wind Turbine Power Curve

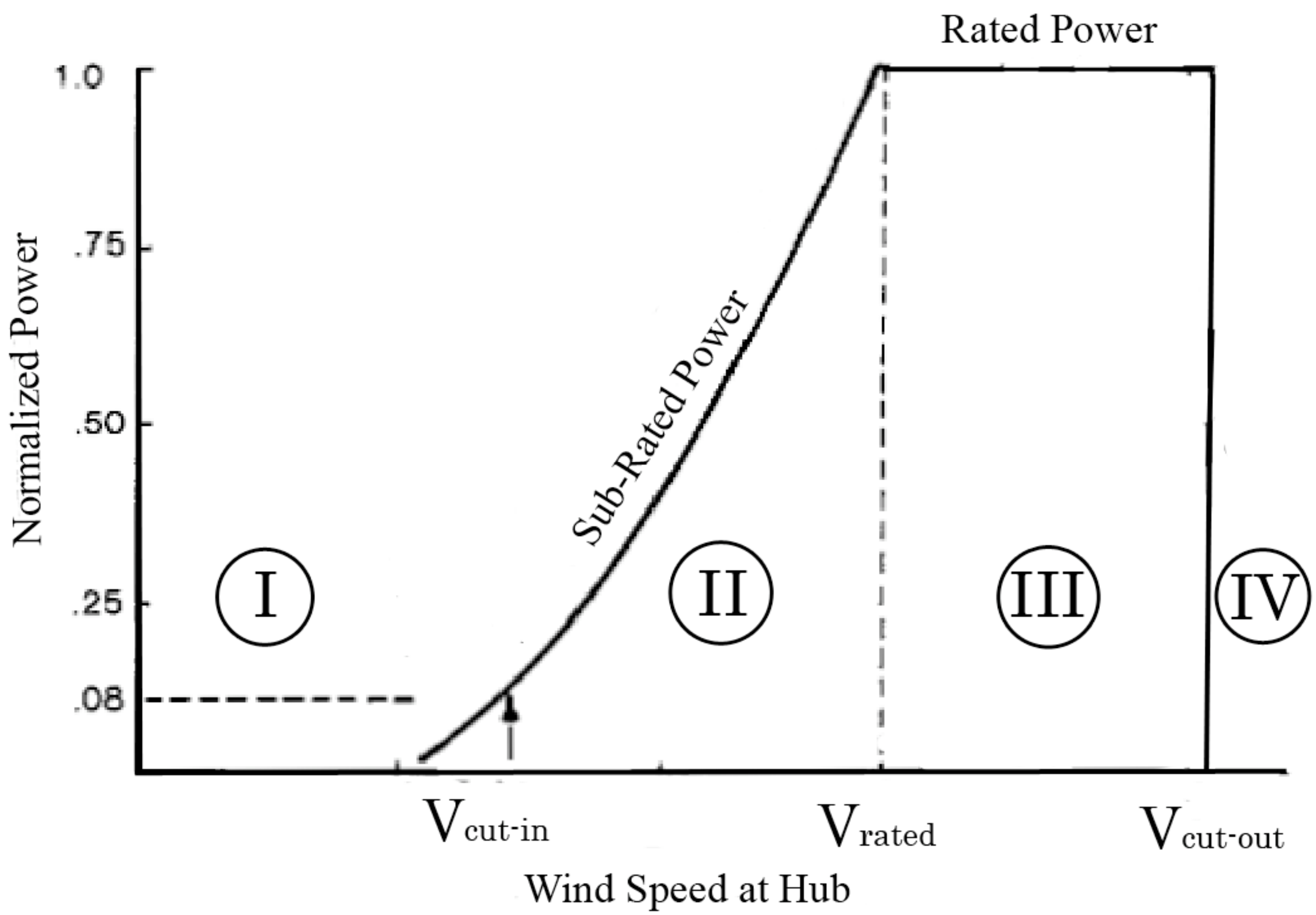

Basic Rotor Performance (Momentum Theory)

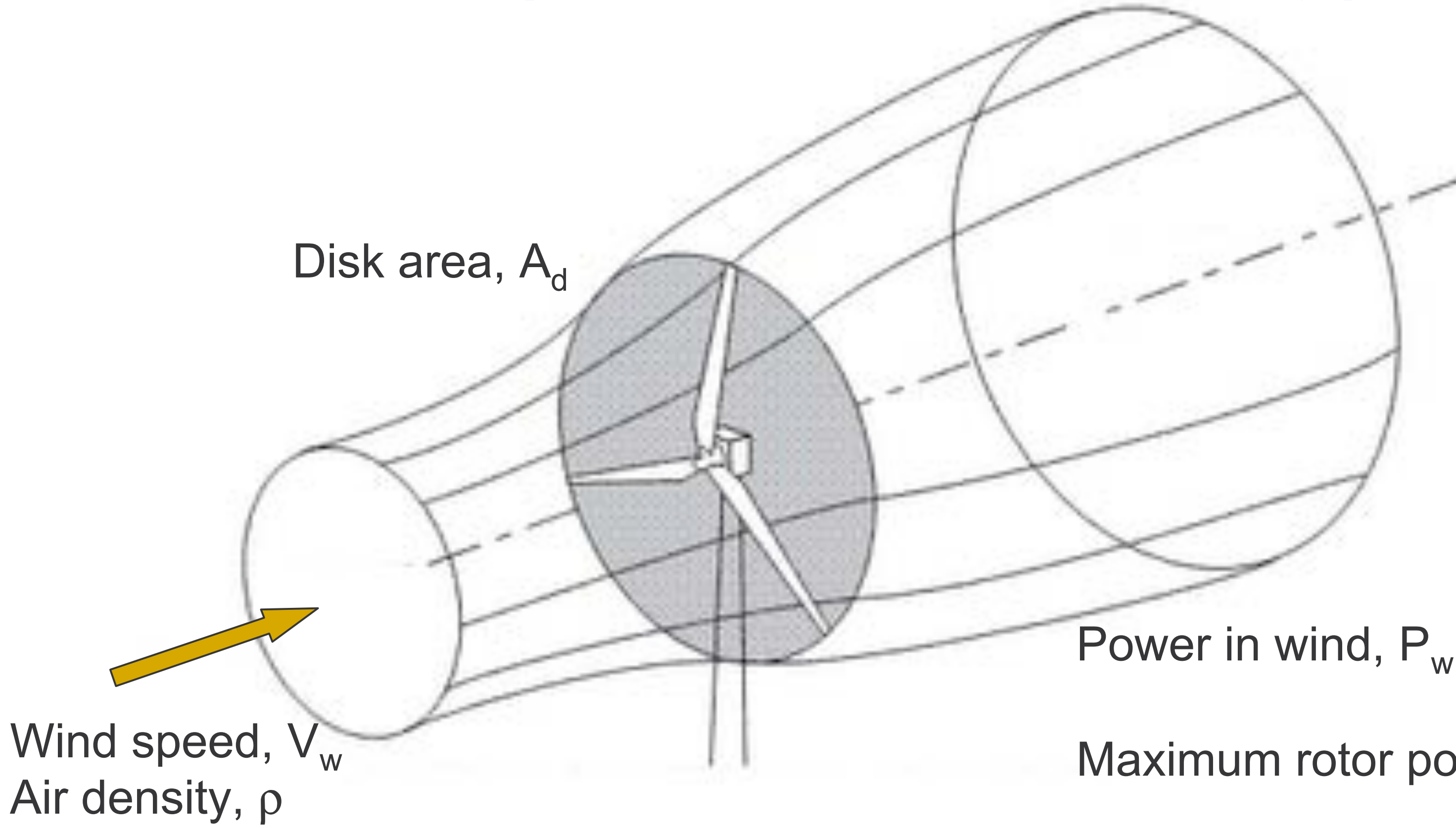

Power in wind, $P_w = {}^{1}/_{2}\ \rho\ V_w^{3}\ A_d$

Maximum rotor power, $P = {}^{16}/_{27}\ P_w$

Rotor efficiency, $C_p = P / P_w$

Betz limit, max $C_p = {}^{16}/_{27} = 59.3\%$

Efficiency of Various Rotor Designs

Butterfield (2008)

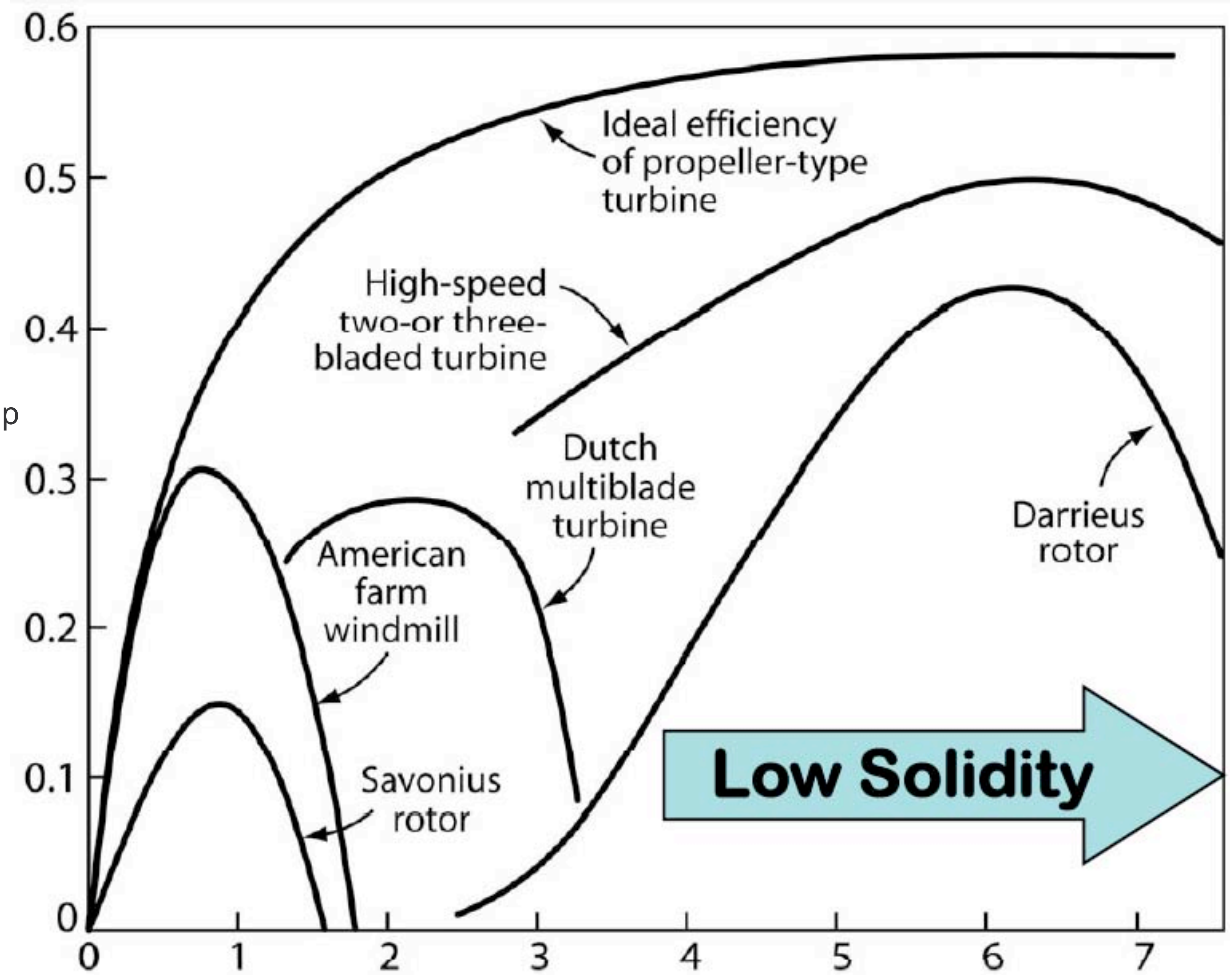

C_p

Tip Speed Ratio TSR = π D RPM / (60 V_w)

- $C_p = P_{rotor} / (1/2\ \rho\ V_w^3\ A_d)$
- Solidity = Blade Area / A_d
- TSR = Tip Speed / V_w
- High power efficiency for rotors with low solidity and high TSR
- Darrieus (VAWT) is less efficient than HAWT
- Current three-bladed rotors achieve high efficiency $C_p \Rightarrow 0.52$

Critical Performance Challenges to Meet Goal of 20% Wind by 2030

- Reduction in capital cost
  - Recently, turbine cost have increased sharply
- Increase in turbine capacity factor
  - Larger rotors for given rated power
- Reduced O&M cost
  - Rapid growth has resulted in reliability issues

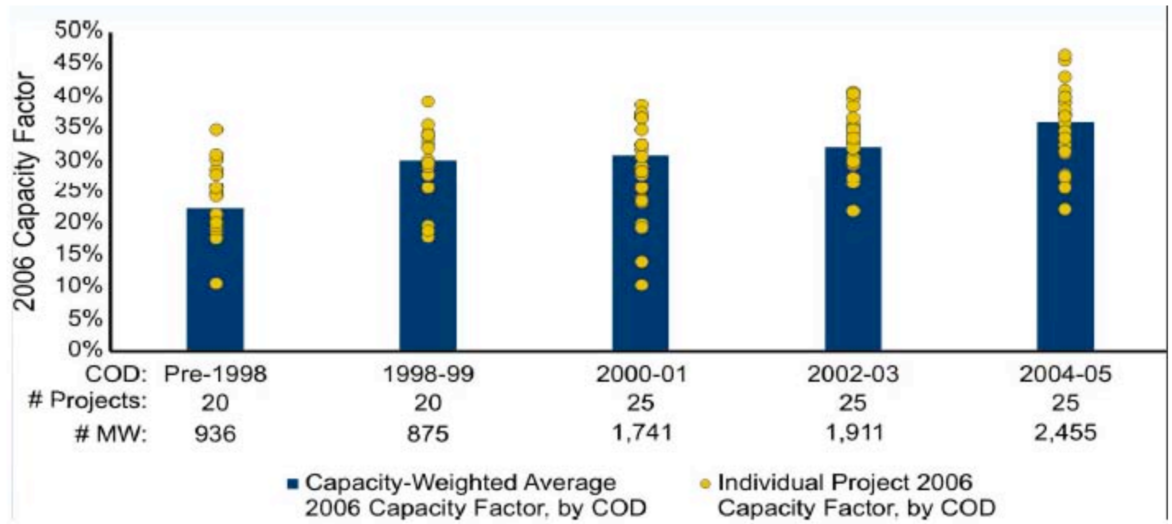

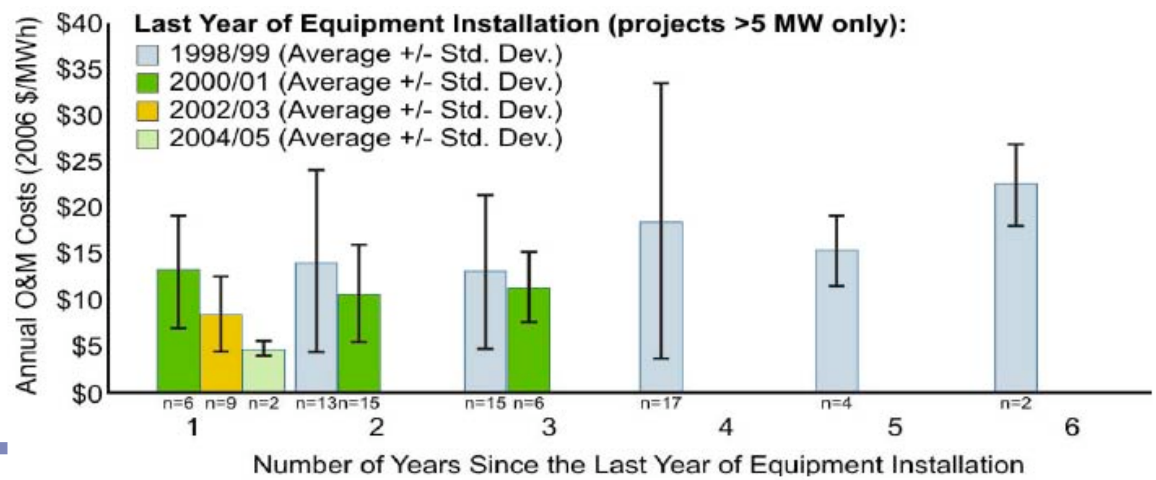

Source: NREL

UC DAVIS

Increased Capacity Factor

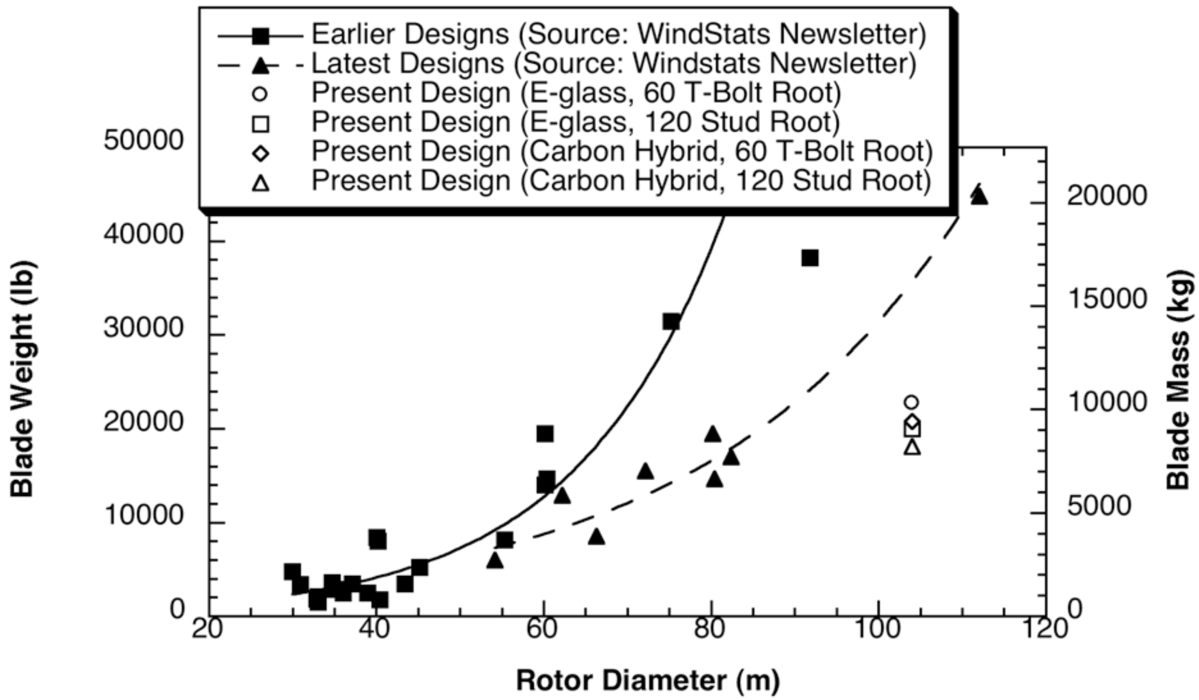

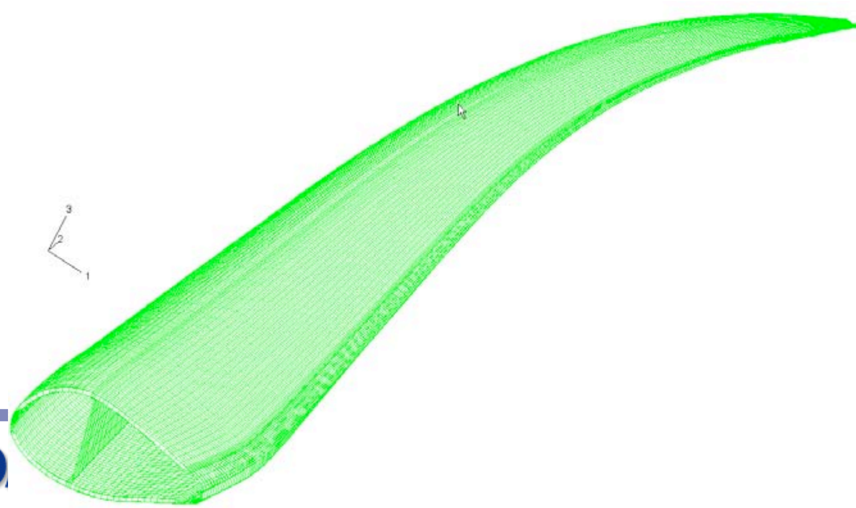

- Larger rotors
  - Increased energy capture
  - Longer, lighter blades
  - Load alleviation (passive, active)
- Taller towers
  - Higher wind speeds
  - Innovative towers, erection methods
- Reduced losses
  - Improved drivetrains, power electronics
  - Wake losses

Innovations in Utility Scale Wind Turbines

Advanced Drive Trains

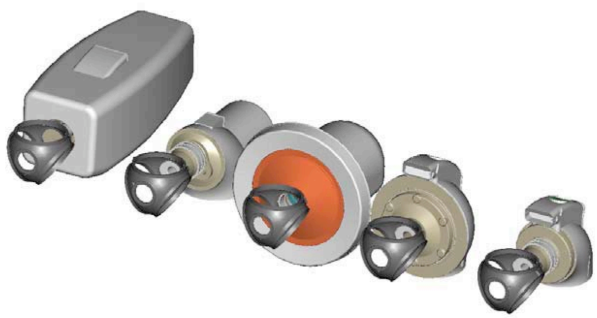

Advanced Blades

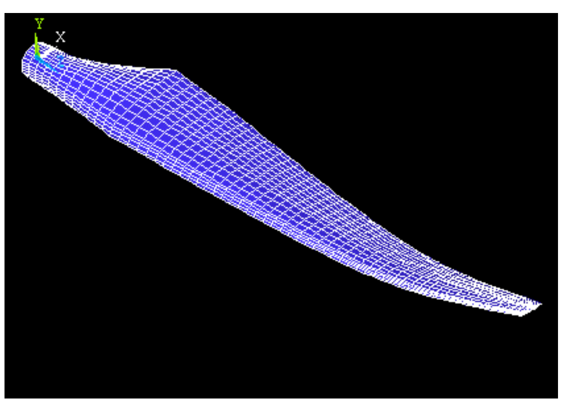

Advanced Tower Designs

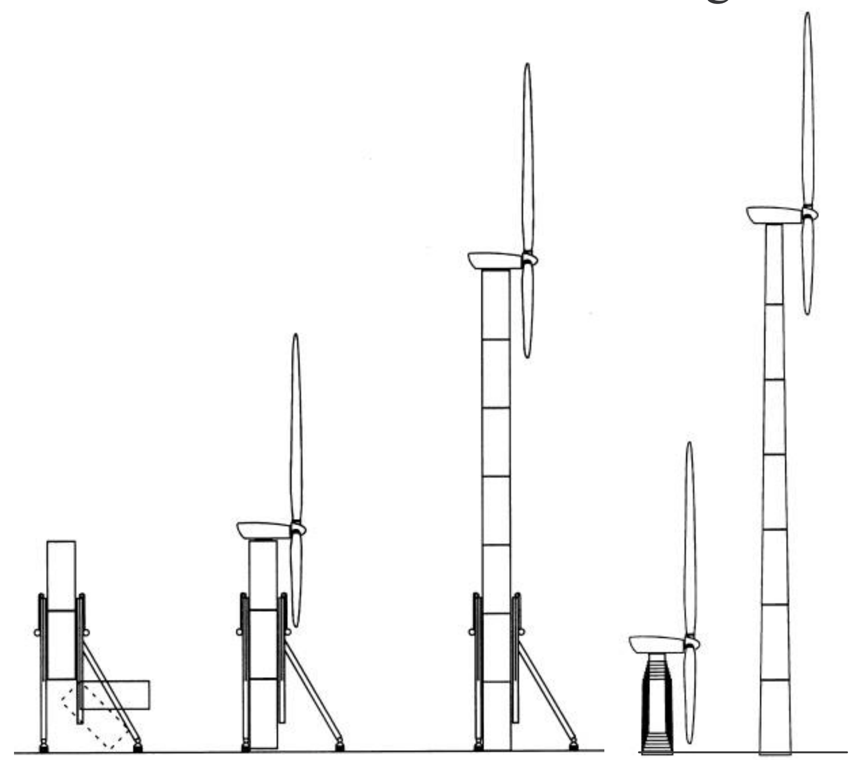

Jack-up concept

Telescoping concept

Utility Scale COE Reduction Potential

Source: Thresher, NREL

Technology	Est. COE Reduction
Larger wind turbines (2-5 MW)	**0% ± 5%**
Advanced rotors and controls	**-15% ± 7%**
Flexible, more slender, higher tip speed, hybrid carbon-glass, active control, etc.	
Advanced drive train concepts	**-10% ± 7%**
Hybrid drive trains with low-speed PM generators, reduced cost PE, etc.	
New tower concepts	**-2% ± 5%**
Taller, modular, field assembled, load feedback control	
Improved availability and reduced losses	**-5% ± 3%**
Better controls, siting and improved availability	
Manufacturing improvements	**-7% ± 3%**
New manufacturing methods, volume production and learning effects	
Region and site tailored designs	**-5% ± 2%**
Tailoring of larger 100 MW wind plant turbine designs to unique sites	

Impact of Advanced Rotors on COE

- Baseline turbine
  - 2.0 MW with 90 m rotor
  - Annual average wind speed at hub height = 6.5 m/s
  - Capacity Factor = 0.327
  - COE = $0.085 /kWh
- Turbine with advanced rotor (blade loads unchanged from baseline)
  - 2.0 MW with 100 m rotor
  - Annual average wind speed at hub height = 6.5 m/s
  - Capacity Factor = 0.370
  - Increased cost for advanced blades (passive and/or active load control)
  - COE = $0.077 - 0.080 /kWh
- Estimated improvement in COE = 6 - 9.5 %

Blade System Design Study (BSDS)

Blade System Design Study (BSDS)

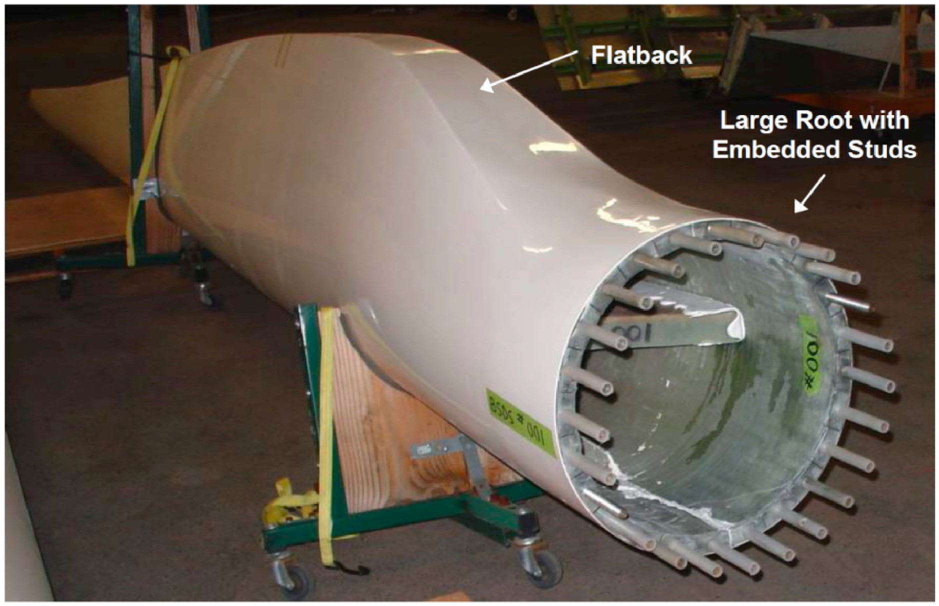

- Multi-phase study with goal to investigate and evaluate design and manufacturing issues for wind turbine blades in the one to ten megawatt size range
- DOE WindPACT award to TPI Composites
- Phase I resulted in preliminary design of 50 m blade
- Phase II focus was to validate gains identified in Phase I preliminary design by:
  - Building, testing, and flying scaled (9 m) prototype blades
  - Conducting more detailed aerodynamic evaluation

Parametric Scaling Results - Blade Thickness

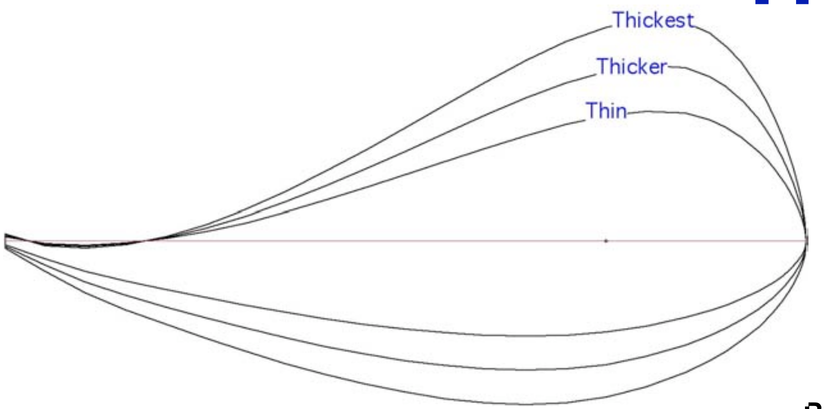

Section shapes at 25% span for 30m blade

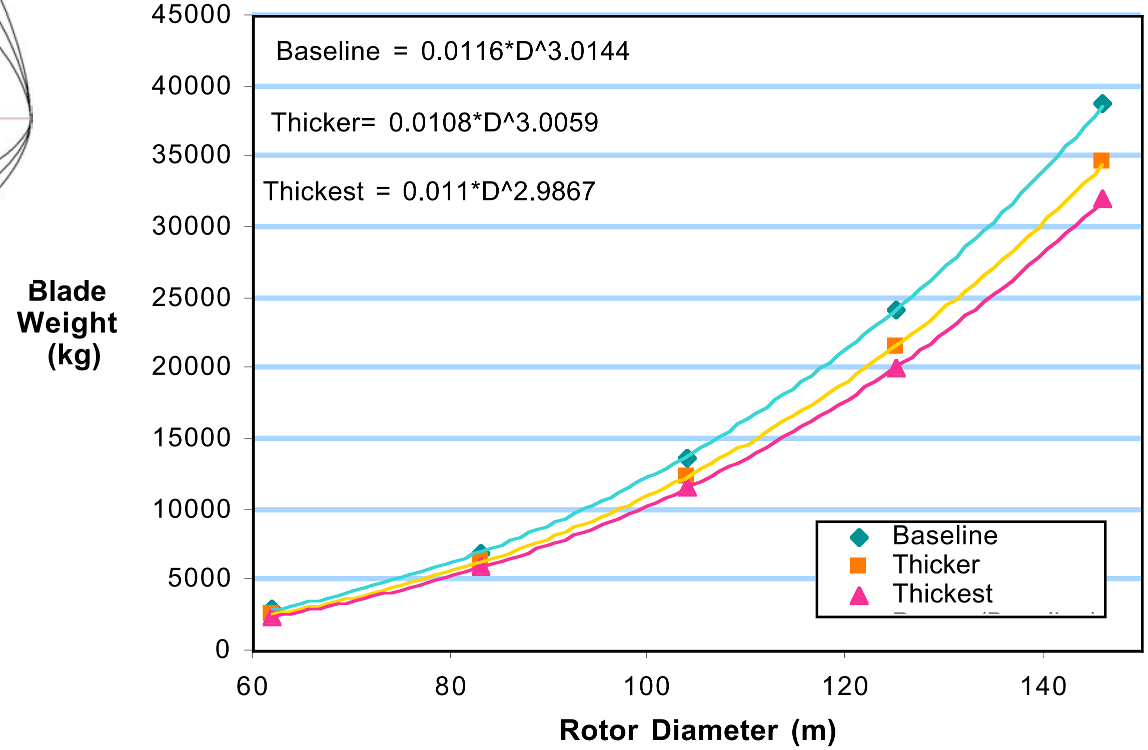

Blade laminate mass as a function of rotor diameter

Effect of Leading Edge Roughness on Sectional Lift

DU97-300mod, t/c = 0.30, Freudenreich (2004)

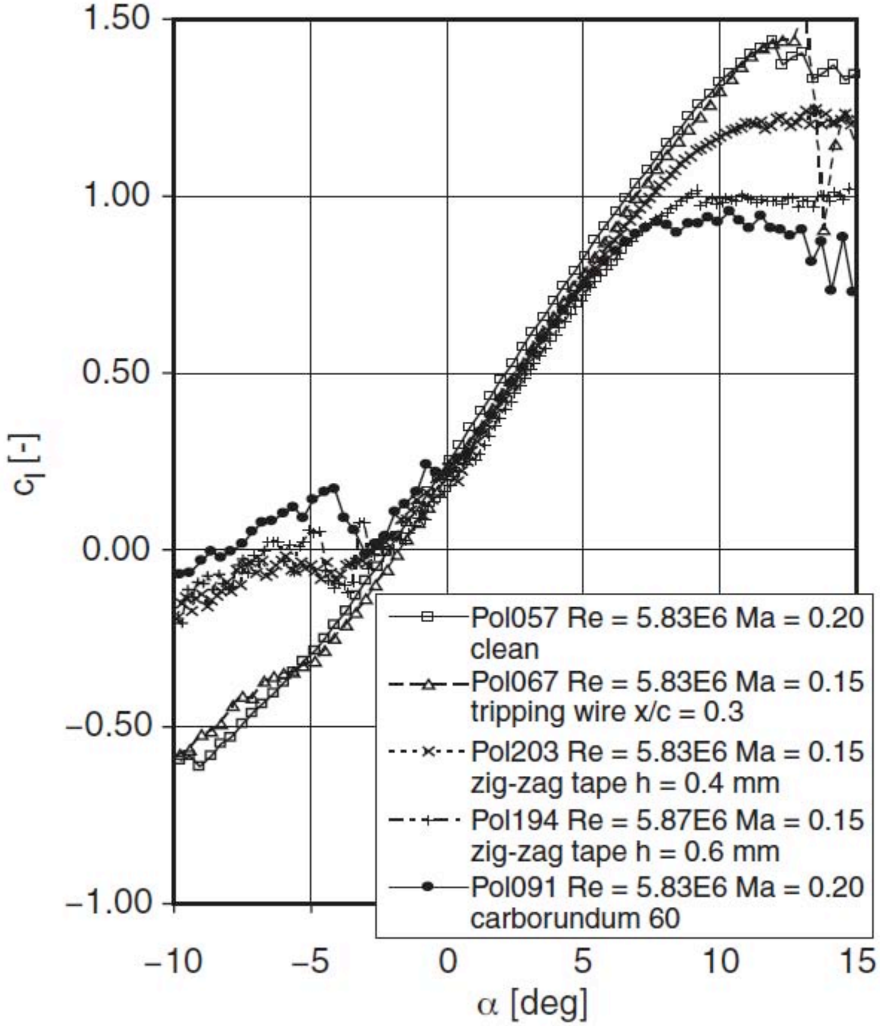

Innovative Design Approaches

- Flatback airfoil development
  - Structural / aerodynamic optimization
- Structurally optimized design
  - Thick airfoils – constant spar cap width / thickness
- Blade material evaluation
  - E-glass
  - Carbon / E-glass hybrid
  - S-glass
  - Carbon / wood / E-glass hybrid (Zebrawood)

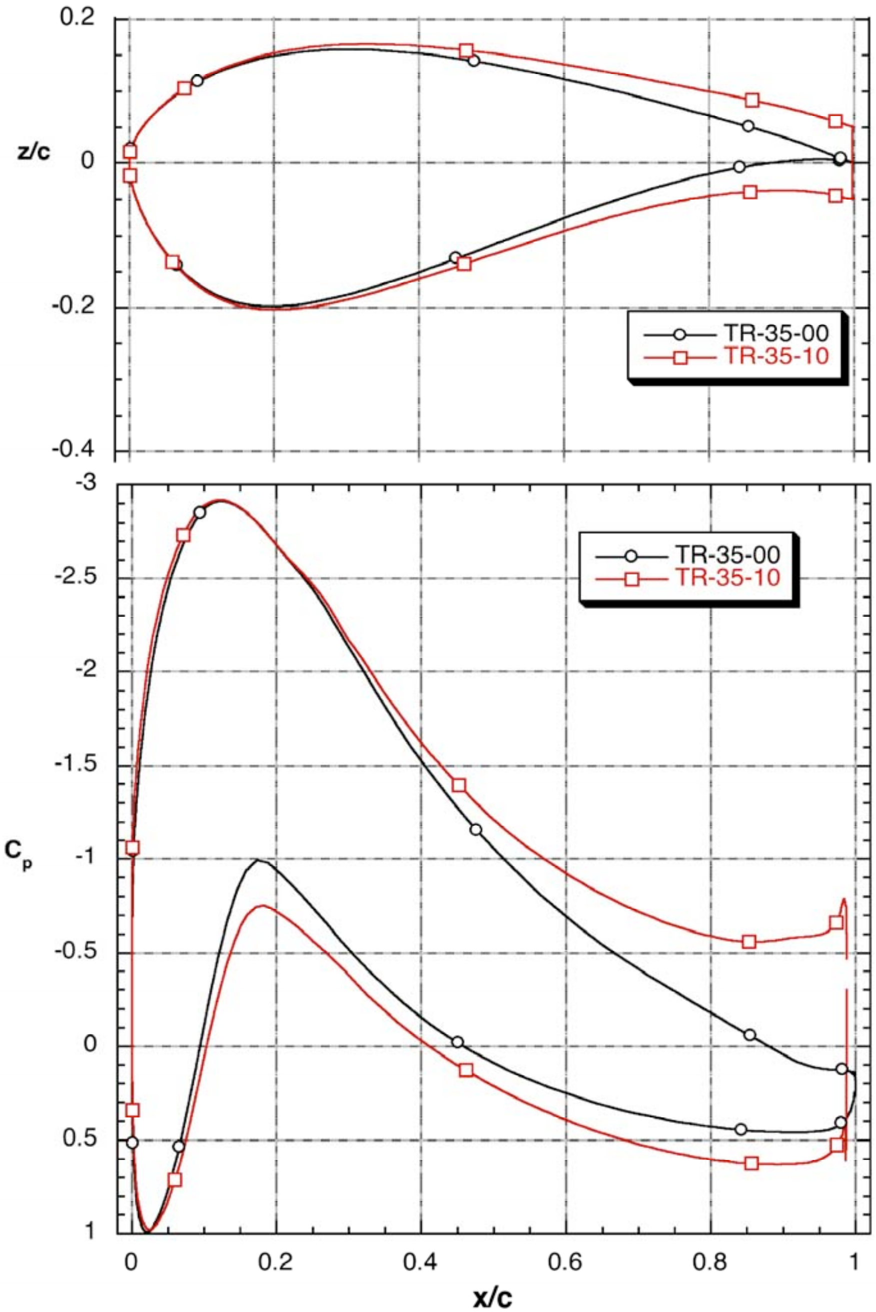

Blunt Trailing Edge or Flatback Airfoils

- Time-averaged pressure distributions of the TR-35 and TR-35-10 airfoils at $\alpha = 8^{\circ}$, Re = 4.5 million, free transition
- Blunt trailing edge reduces the adverse pressure gradient on the upper surface by utilizing the wake for off-surface pressure recovery
- The reduced pressure gradient mitigates flow separation thereby providing enhanced aerodynamic performance
- Note that airfoil is not truncated (this affects airfoil camber distributions) but thickness distribution is modified to provide blunt trailing edge

BSDS Airfoils

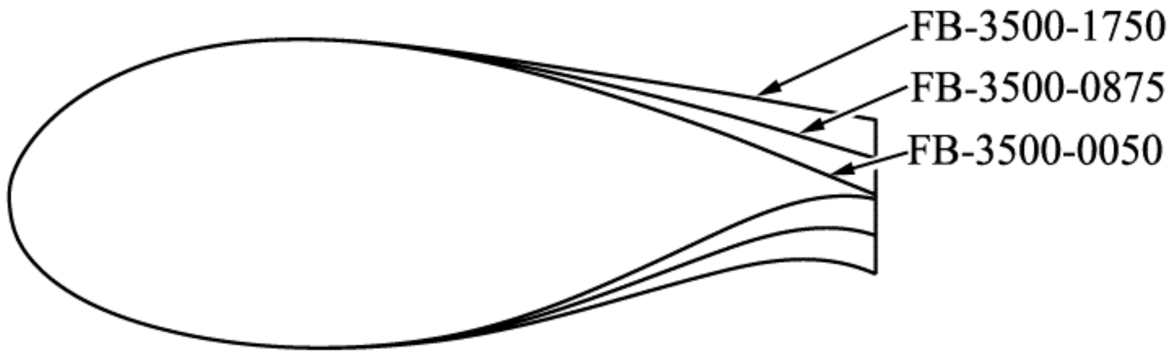

- FB Airfoil Series (FB-XXXX-YYYY)
  - Presented in BSDS Phase I final report
  - XXXX = % maximum thickness to chord ratio × 100, e.g. 3500 → 35% t/c
  - YYYY = % trailing edge thickness to chord ratio × 100, e.g. 0875 → 8.75% t_{te}/c
- Flatback generated by symmetrically adding thickness about the camber line
- Present study investigates FB-3500 airfoil series
  - FB-3500-0050 (nominally sharp trailing edge)
  - FB-3500-0875
  - FB-3500-1750

UCDAVIS

Experimental Results : FB-3500-0050

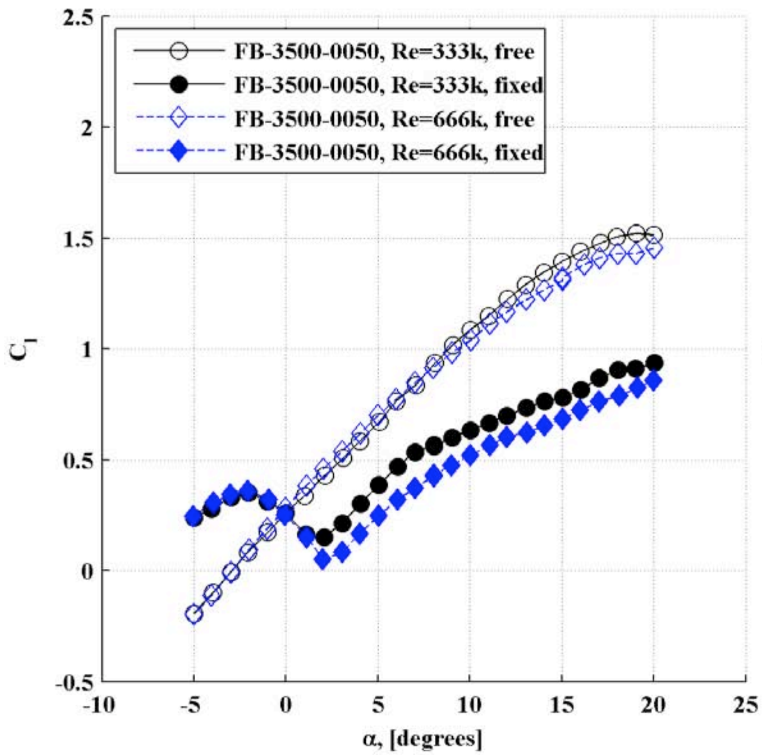

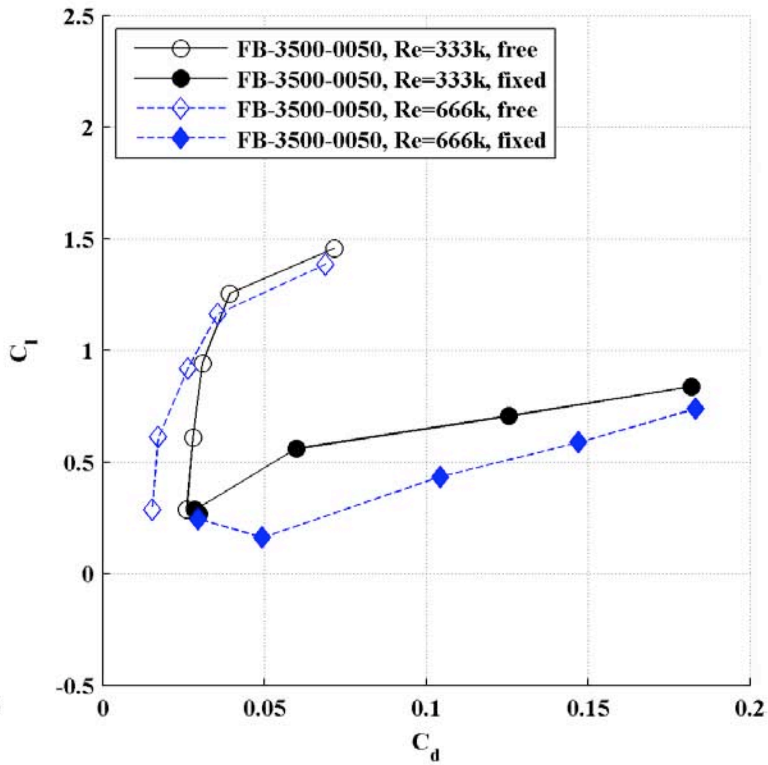

- Leading edge transition sensitivity clearly shown
- Free transition stall occurs near 19° with maximum C_l near 1.5
- Fixed transition stall near 2°, lift continues to increase post stall but airfoil still stalled as shown by dramatic drag increase
- Minimal Reynolds number effects

Experimental Results : FB-3500-0875

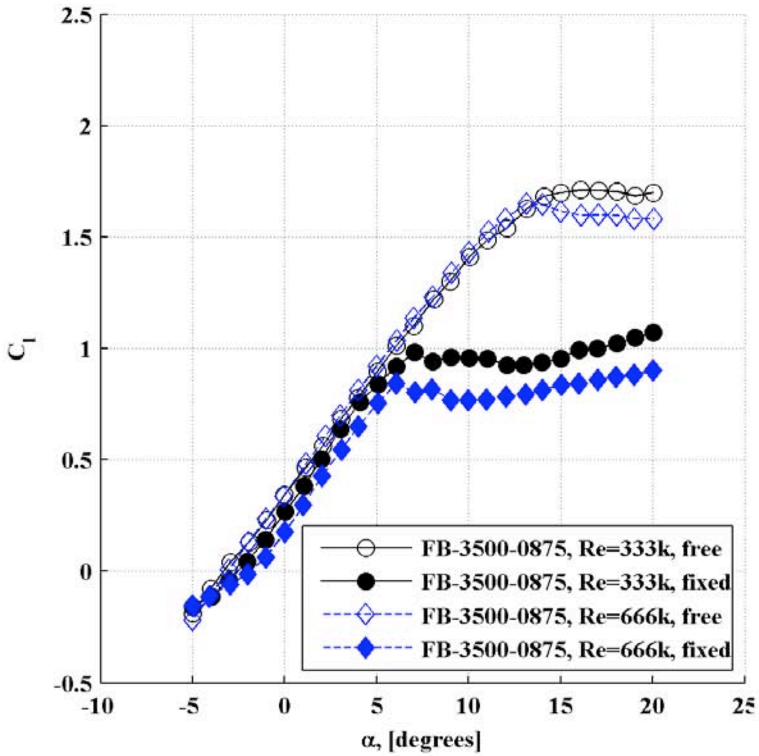

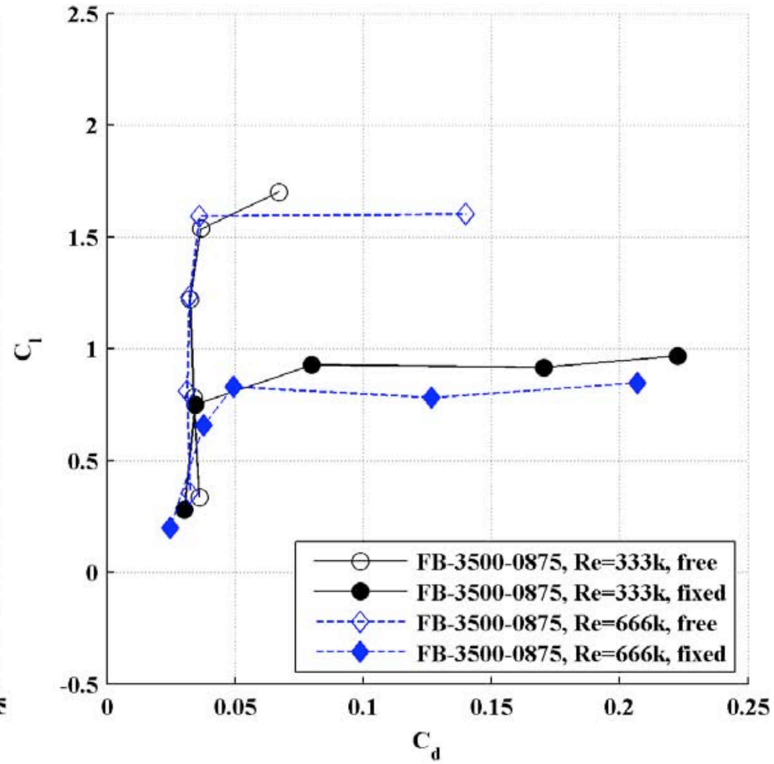

- Reduced in leading edge transition sensitivity
- Maximum C_l approx. 1.65 and 0.9 for free and fixed, respectively
- Lift curve slopes similar for fixed and free transition
- For free transition, increased minimum drag compared to sharp trailing edge airfoil

Experimental Results : FB-3500-1750

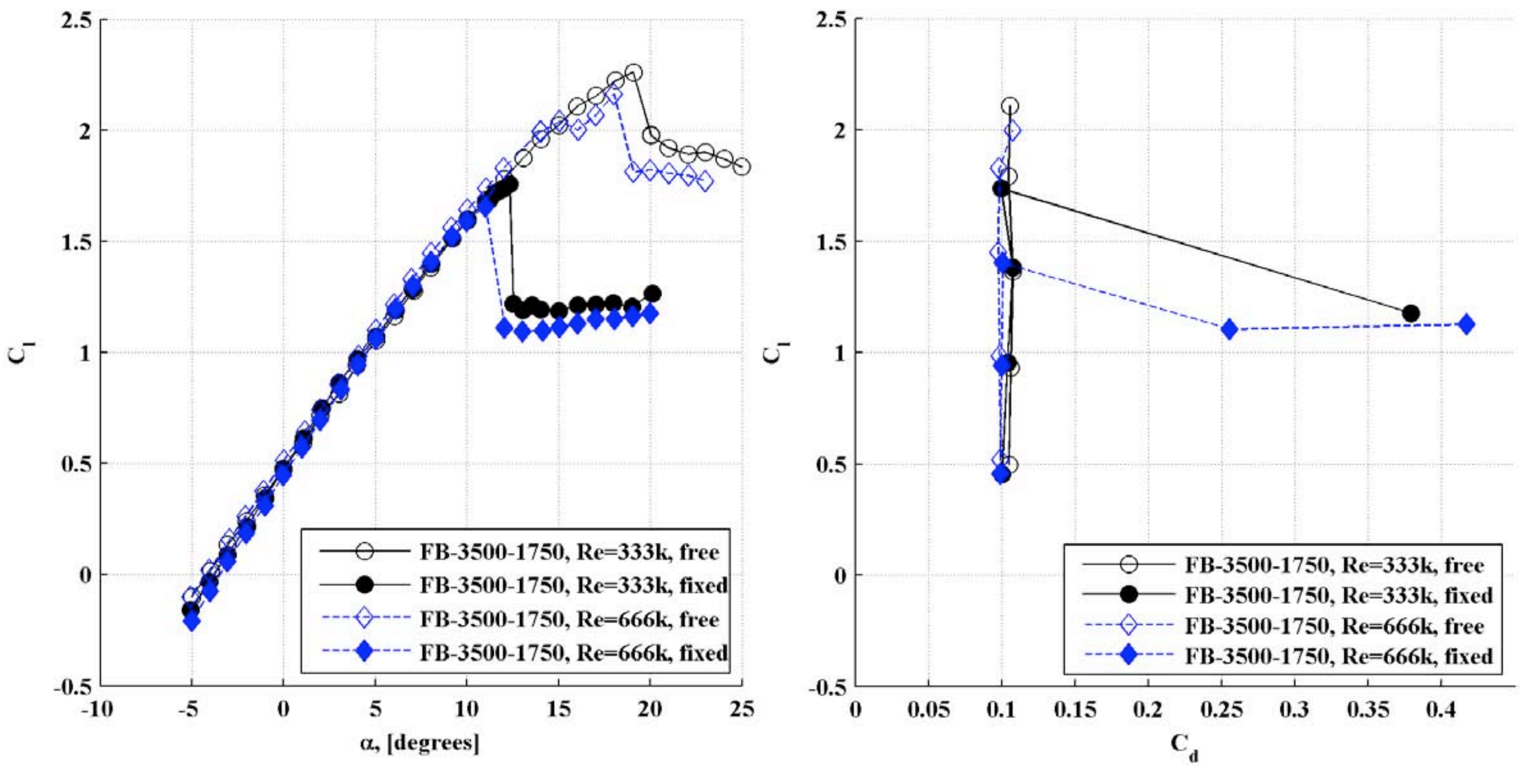

- Further reduction of leading edge sensitivity
- Maximum C_l near 2.2 (free) and 1.7 (fixed)
- Lift curve slope in excellent agreement
- Sharp stall behavior for fixed transition
- Nearly four-fold increase in minimum drag compared to free transition FB-3500-0050

UCDAVIS

Experimental Results: L/D Comparison

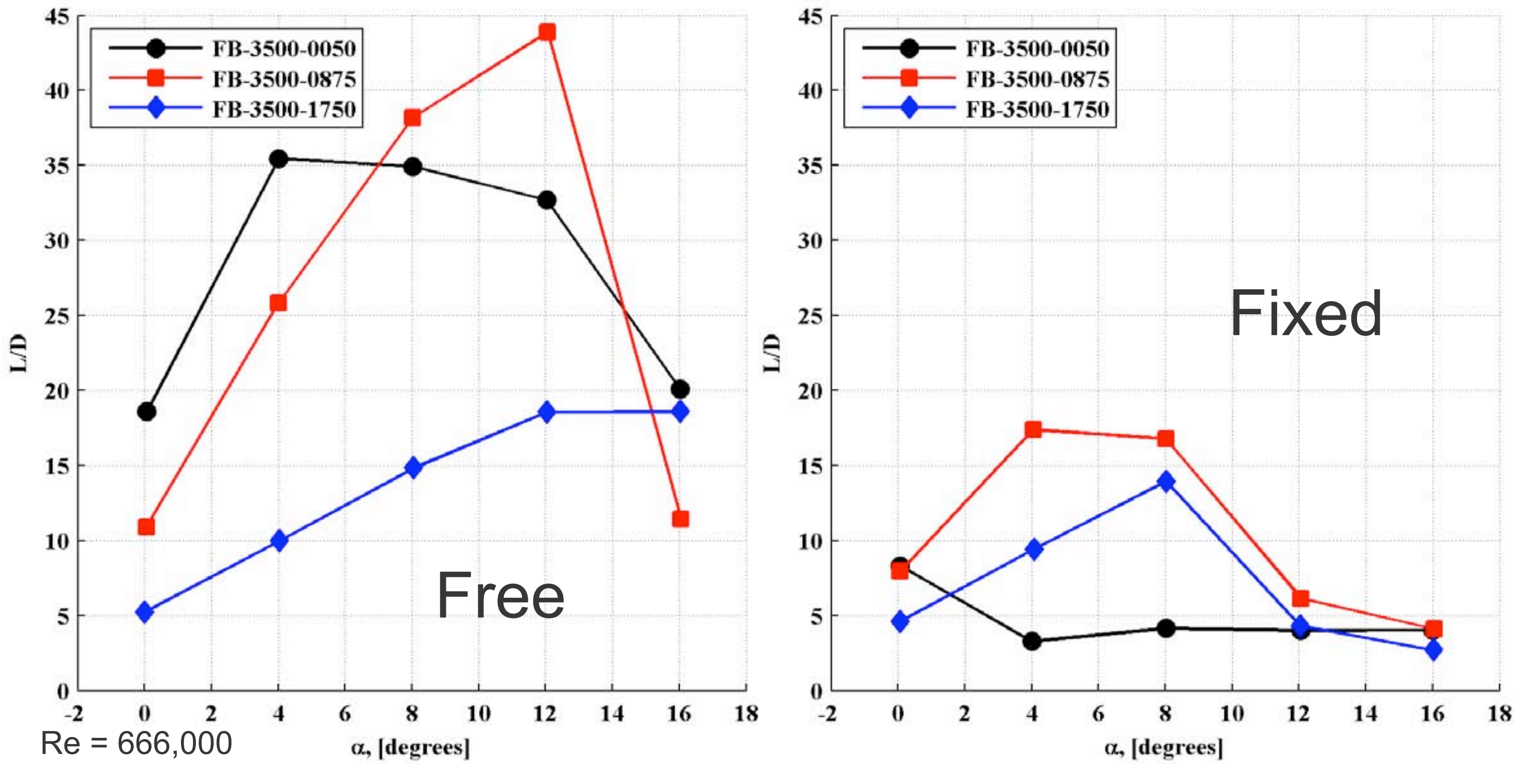

- Re = 666,000
- Free transition
  - FB-3500-0050 does well at low angles of attack, $(L/D)_{max} = 35.5$
  - FB-3500-0875 produces $(L/D)_{max} = 44$
- Fixed transition
  - Flatback airfoils outperform sharp trailing edge airfoil
  - FB-3500-0875 produces $(L/D)_{max} = 17.5$
- Bluff-body drag reduction techniques could be used to further improve performance

Blade Planform and Geometric Data

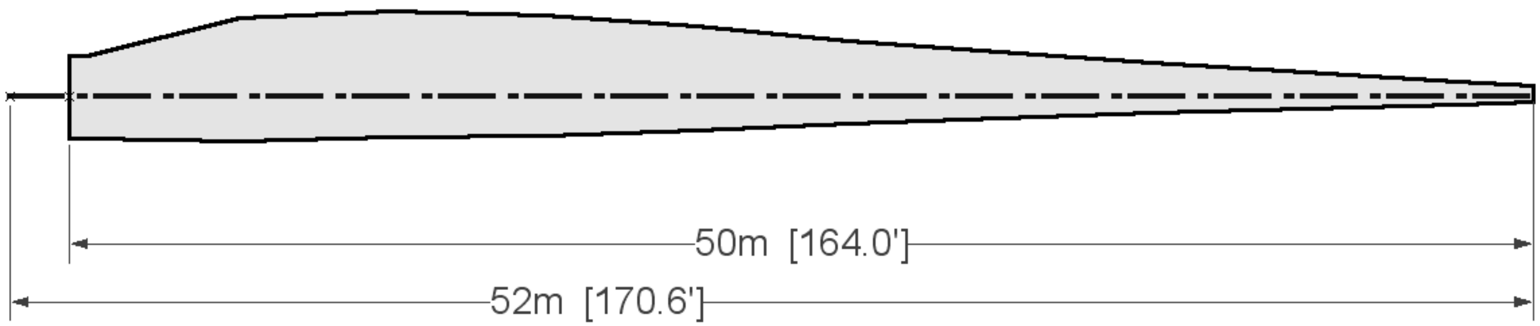

Station Number	Radius Ratio	Twist (deg)	Chord (m)	Thickness (mm)	Thickness Ratio	Airfoil Type	Reynolds Number
1	5%	29.5	2.798	2798	100.00%	Circle	2.00E+06
2	15%	19.5	4.191	2640	63.00%	FB 6300-1800	3.86E+06
3	25%	13.0	4.267	2341	54.87%	FB 5487-1216	5.26E+06
4	35%	8.8	4.097	1756	42.86%	FB 4286-0802	6.51E+06
5	45%	6.2	3.518	1204	34.23%	FB 3423-0596	6.92E+06
6	55%	4.4	2.762	746	27.00%	FB 2700-0230	6.51E+06
7	65%	3.1	2.218	532	24.00%		6.50E+06
8	75%	1.9	1.675	352	21.00%	S830	5.28E+06
9	85%	0.8	1.232	234	19.00%		4.57E+06
10	95%	0.0	0.789	142	18.00%	S831	3.12E+06

Comparative Weight and Strength 9m BSDS blade

Comparison of CX-100 and BSDS Blade Properties and Testing Results

Property	CX-100	BSDS
Weight (lb)	383	289
% of Design Load at Failure	115%	310%
Root Failure Moment (kN-m)	128.6	203.9
Max. Carbon Tensile Strain at Failure (%)	0.31%	0.81%
Max. Carbon Compressive Strain at Failure (%)	0.30%	0.87%
Maximum Tip Displacement (m)	1.05	2.79

Historical Comparison of 9 m Blade Weights and Strengths

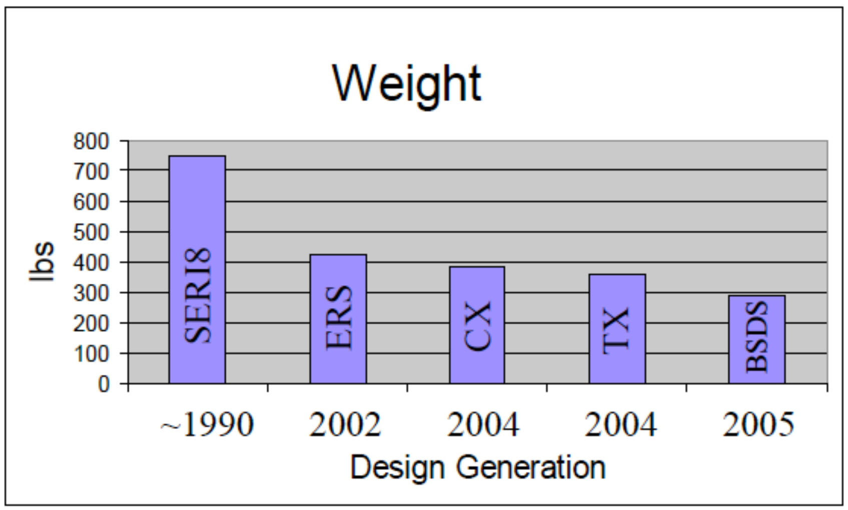

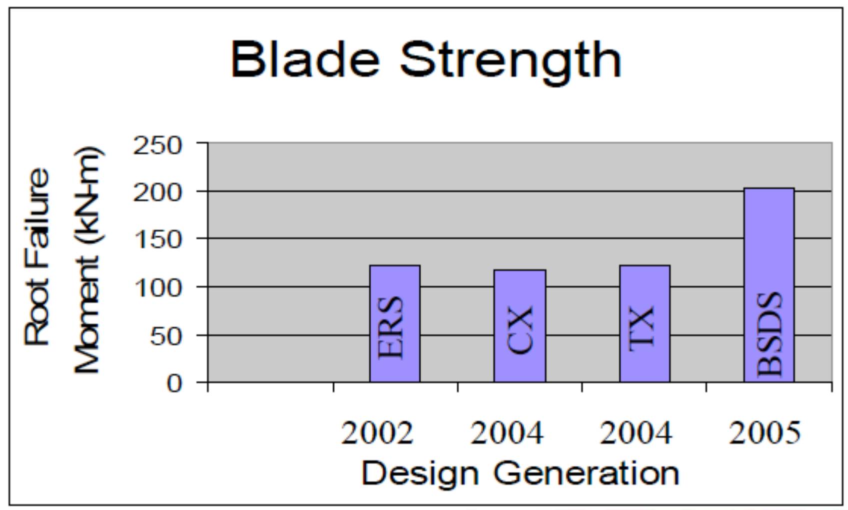

Source: Paquette & Veers, SNL

Issues Encountered in BSDS Study

- Transition has a dominant effect on flow characteristics of thick lifting surfaces but transition model missing in most CFD methods
- Blunt trailing edge airfoils have high levels of base drag negatively affecting their lift-to-drag ratios

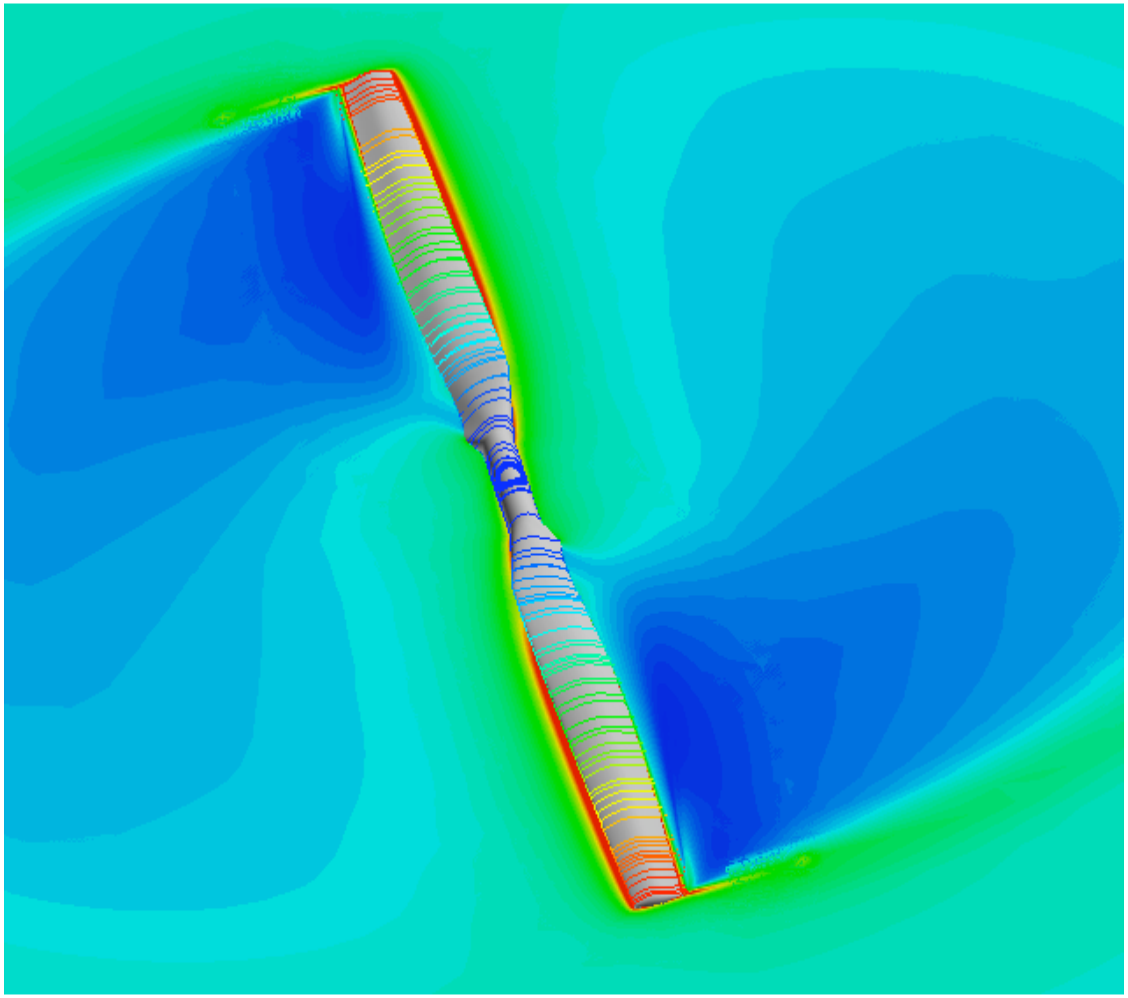

Database e^N Transition Model

$$\frac{A}{A_0} = \exp\left[\int_{x_i}^{x_{tr}} (-\alpha_i)dx\right] \approx e^{N_{crit}}$$

- $-\alpha_i$ is a function of M_e, Re_{δ^*}, H_k and F
- LASTRAC was used to generate a database of $-\alpha_i$ values over a wide range of input values
  - Near-similarity attached velocity profiles
  - Non-similar separated velocity profiles
- $-\alpha_i$ values retrieved from database at run time using multidimensional interpolation
- Database characterizes the stability solver (high computational cost) with interpolation (low cost)

Database Storage

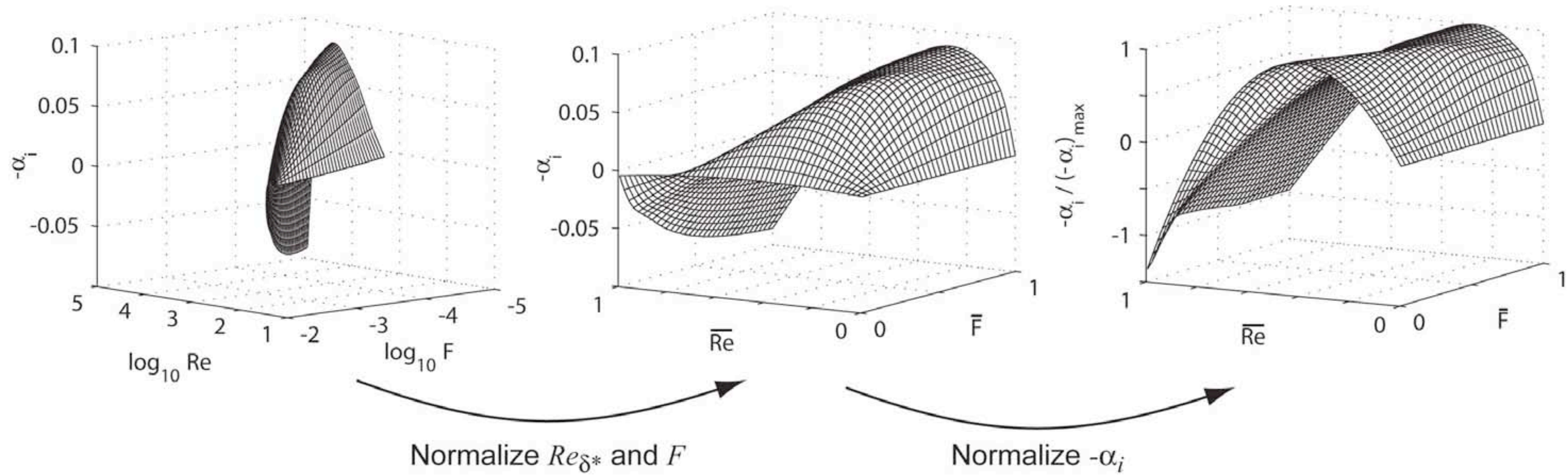

- Normalized structured topology is most efficient for storage and interpolation
- Interpolation / extrapolation is accomplished with n^{th}-order Lagrangian interpolating polynomials

FB-3500-0050 Performance

Re_c = 666,000
M = 0.3, 0.13 (ARC2D, Exp.)
$(x/c)_{trip,upper}$ = 0.02
$(x/c)_{trip,upper}$ = 0.05

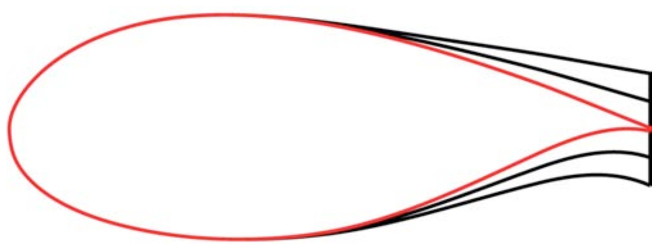

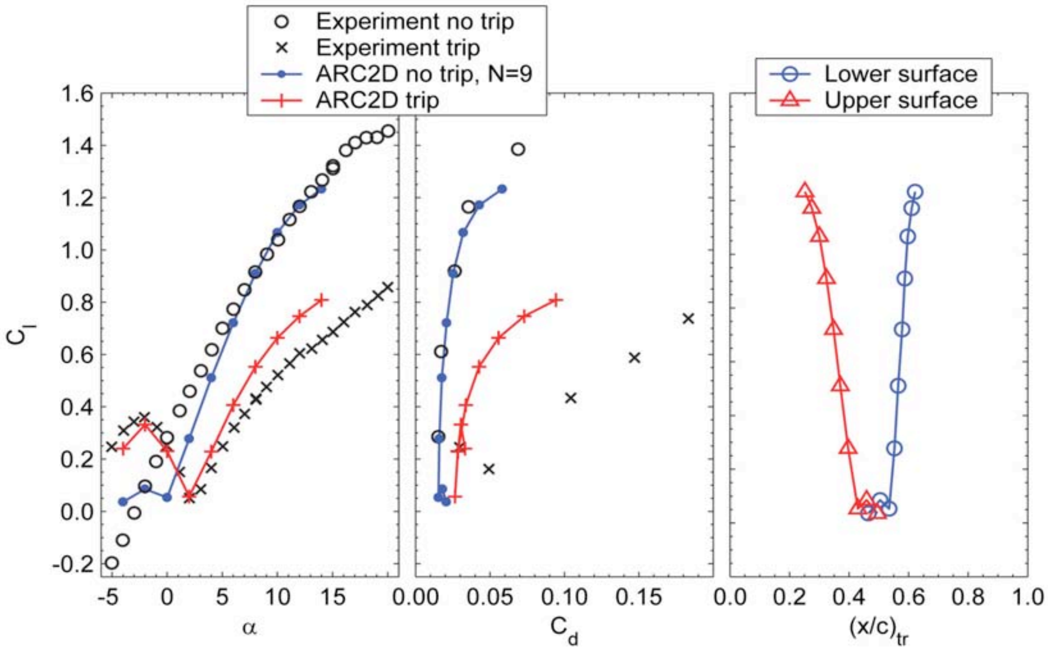

- Lift is very sensitive to surface soiling
- Premature boundary layer separation causes large drag forces

FB-3500-0875 Performance

Re_c = 666,000
M = 0.3, 0.13 (ARC2D, Exp.)
$(x/c)_{trip,upper}$ = 0.02
$(x/c)_{trip,upper}$ = 0.05

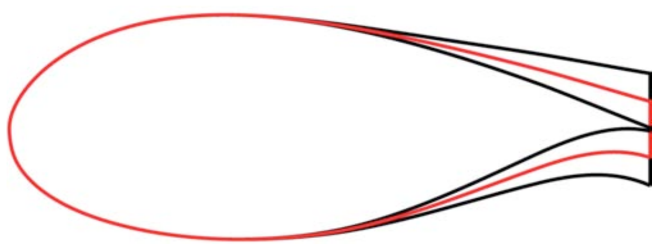

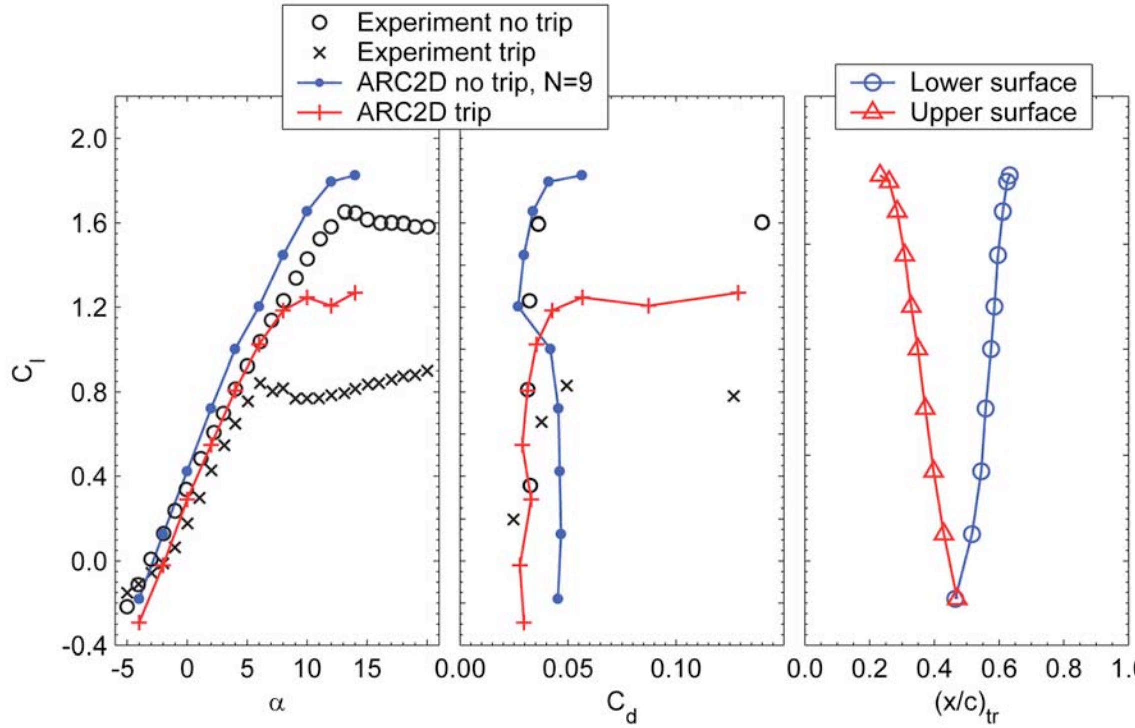

- Reduced sensitivity to surface soiling
- Only a modest drag penalty compared to the FB-3500-0050

FB-3500-1750 Performance

Re_c = 666,000
M = 0.3, 0.13 (ARC2D, Exp.)
$(x/c)_{trip,upper}$ = 0.02
$(x/c)_{trip,upper}$ = 0.05

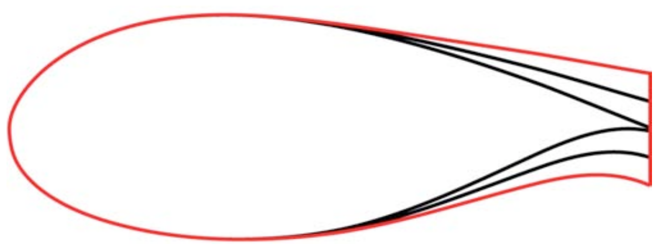

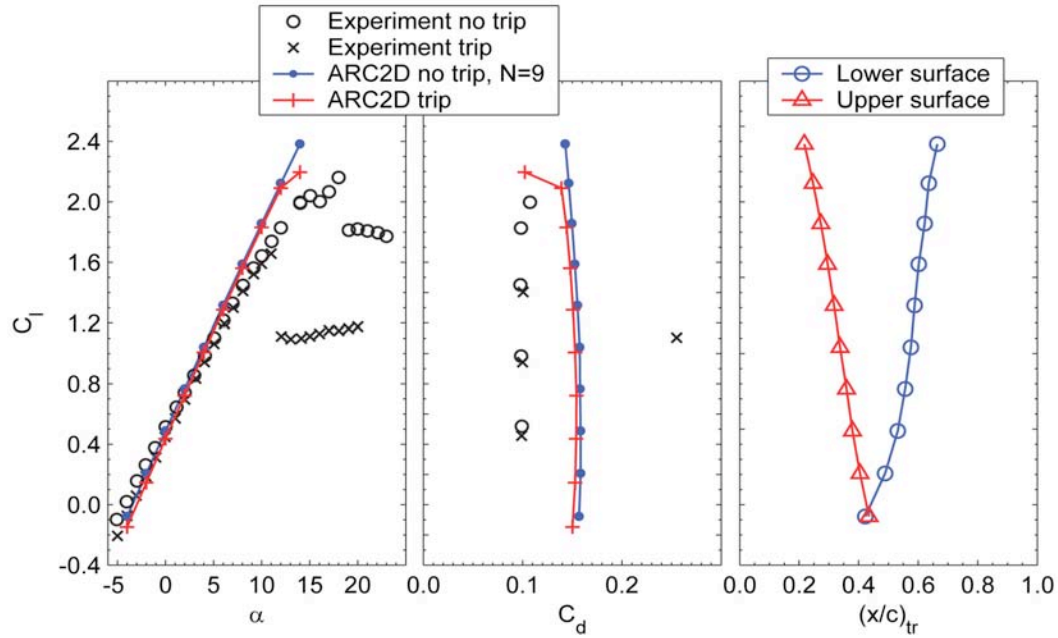

- Sensitivity to surface soiling greatly reduced
- Large (3x) drag penalty due to base drag
  - Baker is studying methods for drag reduction

Blunt Trailing Edge Airfoil Drag Reduction

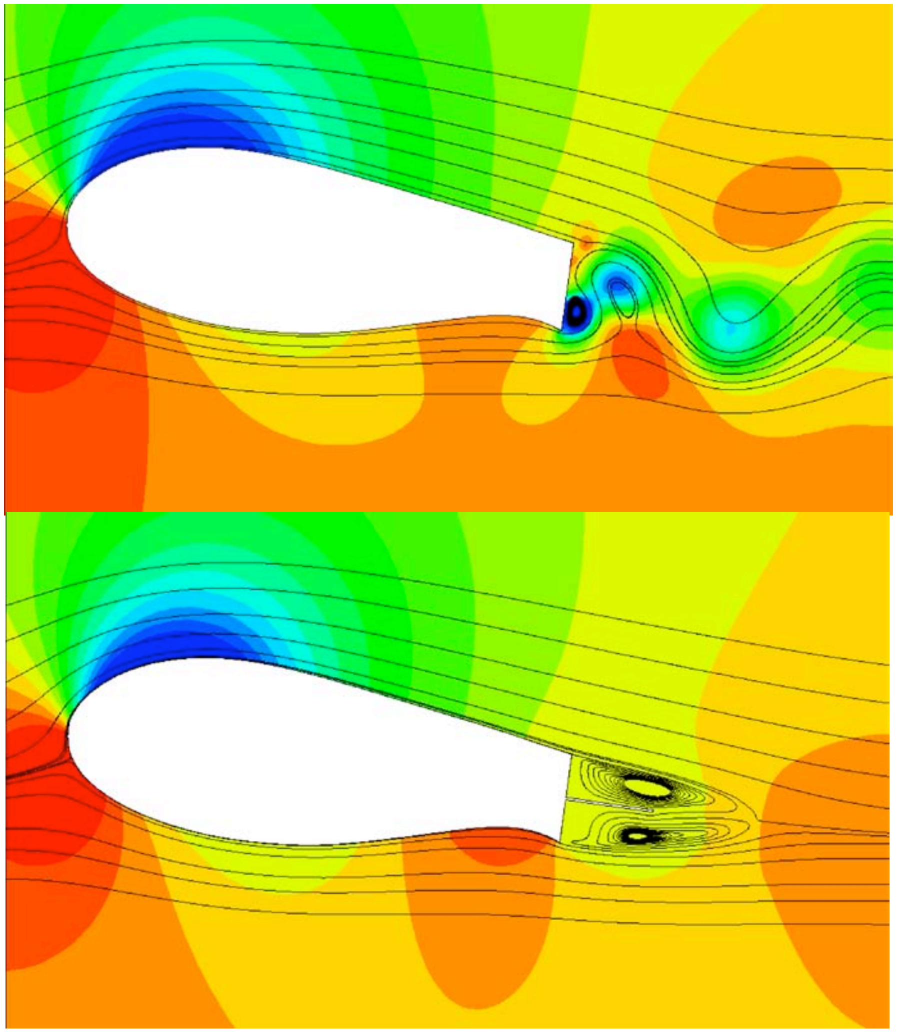

- Baseline
  - Large vortical wake structure
  - Vortex street
  - Computations may overpredict vortex strength due to 2D flow restriction
- Splitter
  - Twin, stable vortical structures surround plate

Simple Splitter Plate

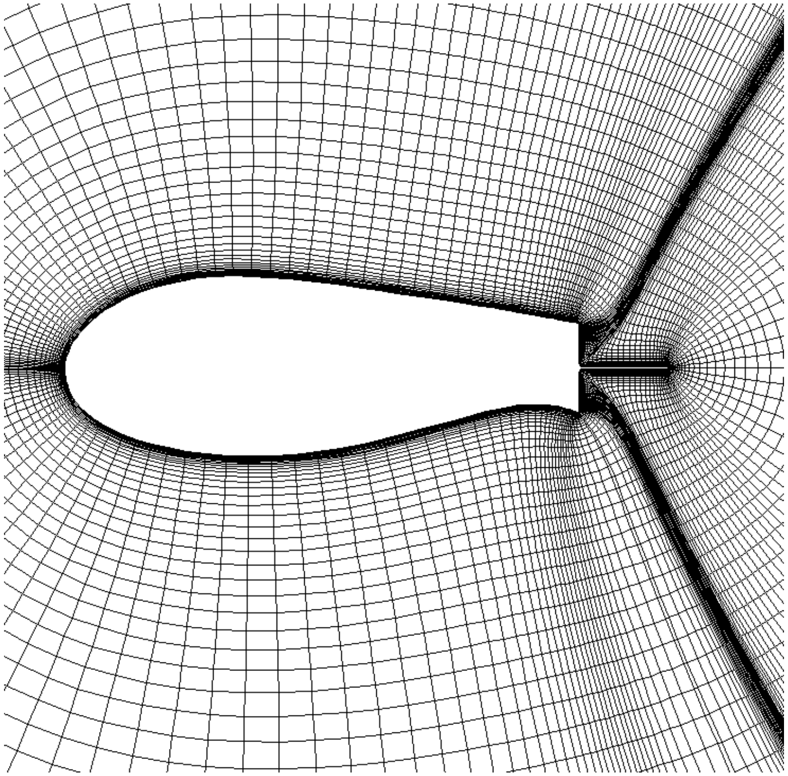

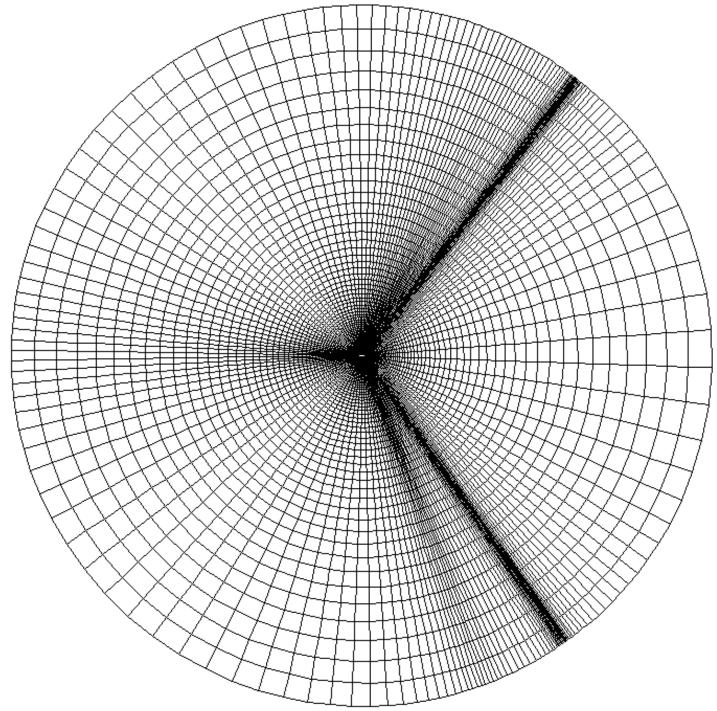

- Nearfield
  - Splitter plate
  - O-grid topology
  - Note grid shock
- Farfield

Splitter Plate Length

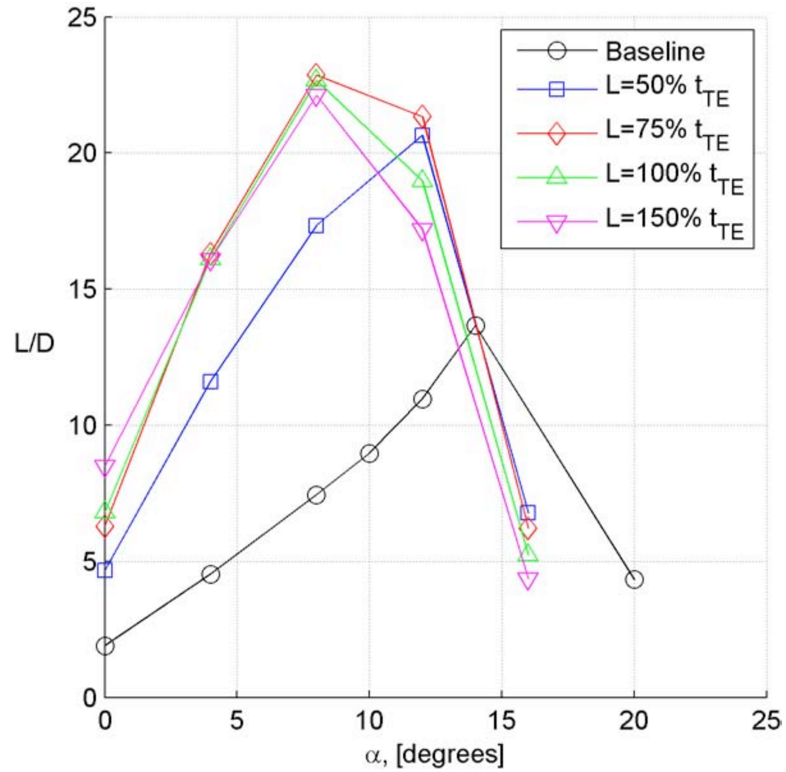

- Best L/D max: 75% t_{TE} length

Offset Trailing Edge Cavity

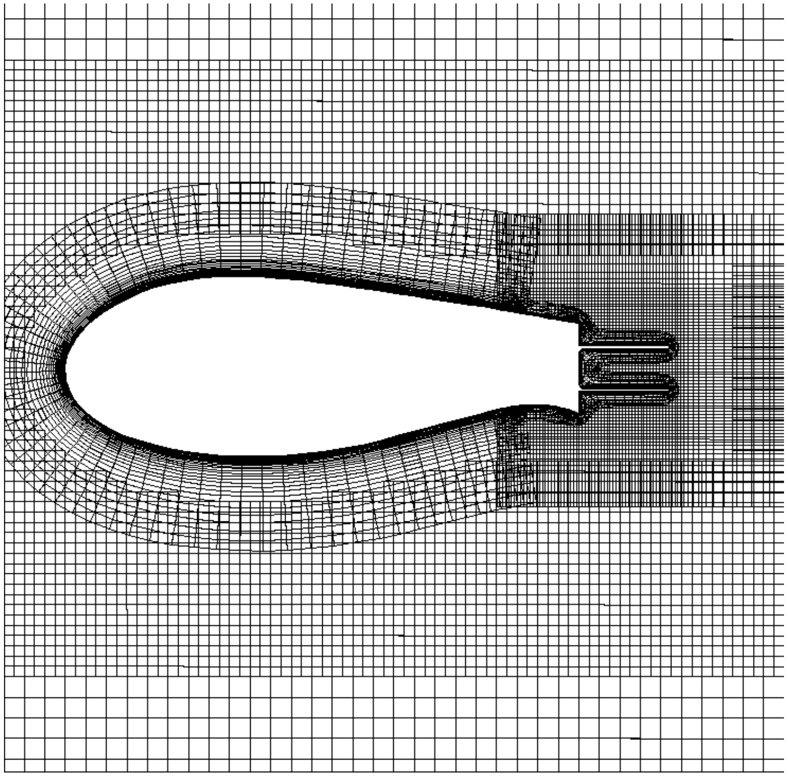

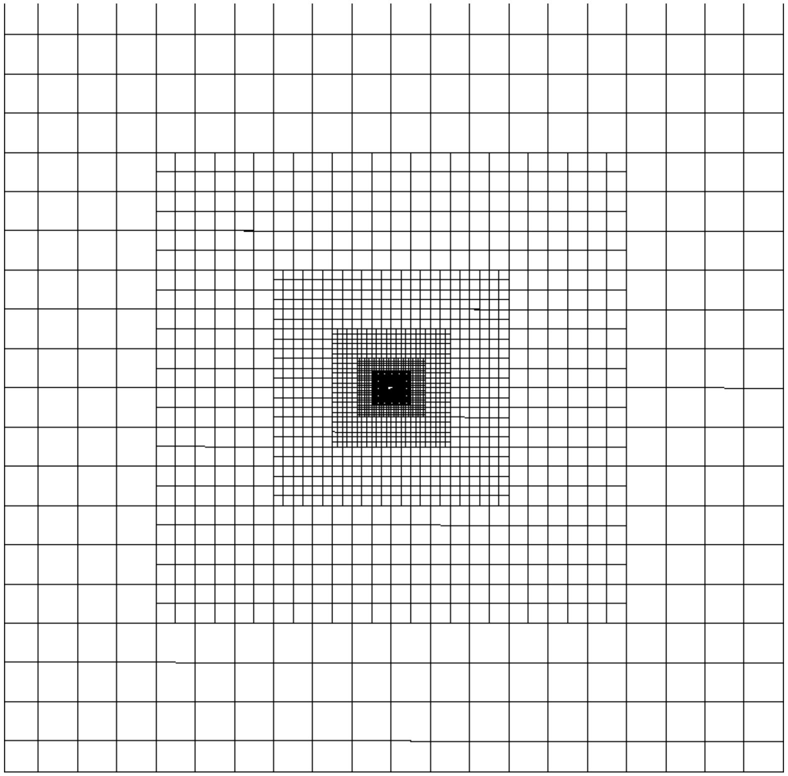

- Nearfield
  - O-grid topology near airfoil
  - Grid cell self-intersection required overset approach
- Farfield
  - Automatically generated “bricks”, cartesian offbody grids

UCDAVIS

Offset Cavity

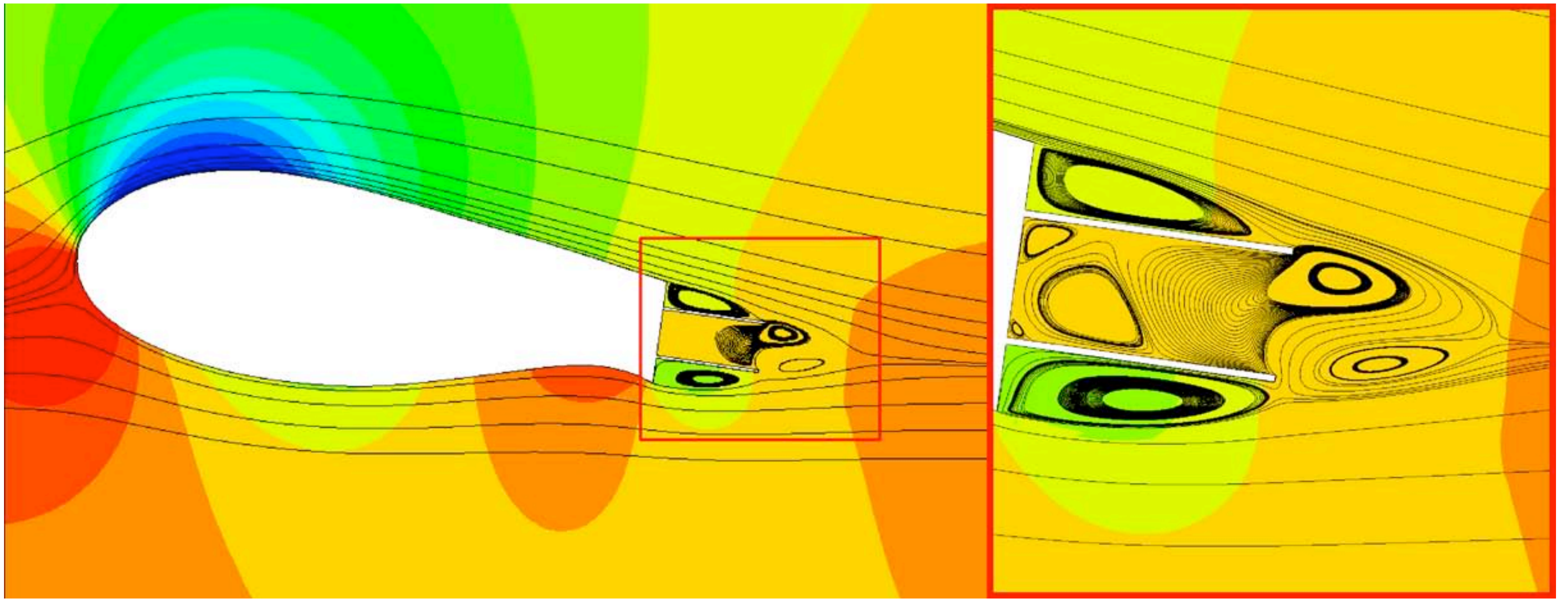

- Loss in lift caused by reduced suction peak, compared to baseline
- Offset cavity resulted in steady flow for all angles prior to stall
- Multiple standing vortices surrounding plates
- Nearly stagnant flow in cavity

Offset Cavity

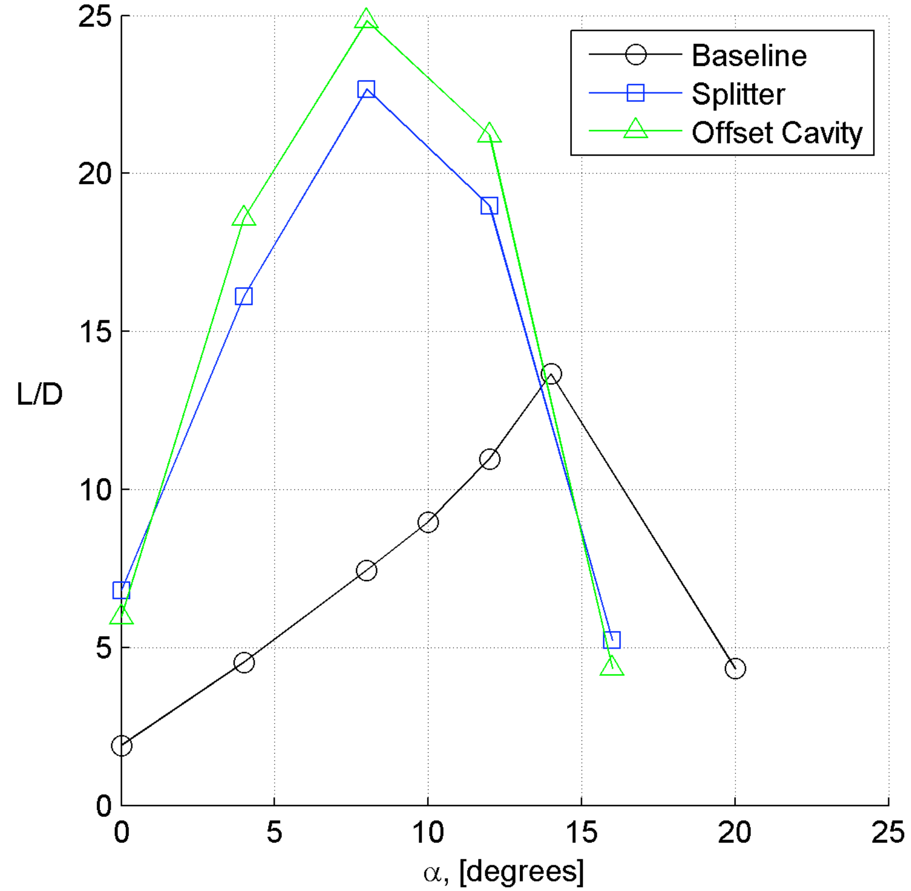

- Improved drag performance of offset cavity overcomes lift reduction for L/D

BSDS Blade

- Increased structural efficiency without loss of aerodynamic performance resulting in a much more cost effective blade
- Concept now adapted by major turbine manufacturers
- Blunt trailing edge airfoil (flatback) concept to improve lift characteristics of thick airfoils was studied and optimized using CFD
- Drag reduction concepts studied using CFD and now validated through wind tunnel and field testing

Sweep-Twist Adaptive Rotor (STAR)

Sweep Twist Adaptive Rotor (STAR)

- 2004 DOE award to Blade Division of Knight & Carver to design, build, and demonstrate a rotor based on the sweep-twist concept
- Rotor designed for testing on a Zond Z48 turbine with 750 kW rating
- Goal to increase annual energy capture of baseline turbine by 5%-10% without exceeding baseline rotor loads
- To achieve this rotor radius was increased from 24 m to 27 m
- Rotor test conducted in 2008
- Program results published in SAND2009-8037

Sweep Twist Passive Load Control Concept

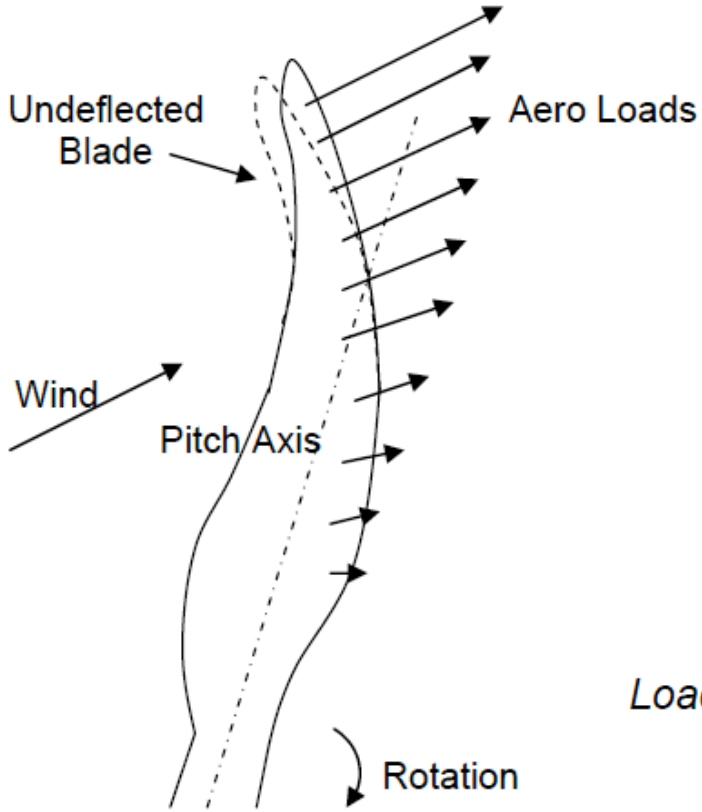

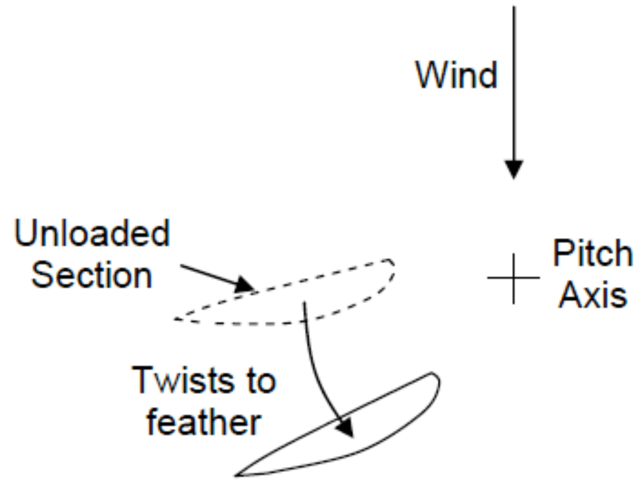

Tip View

Load Control through passive means utilizing blade geometry

Structured Grid System

Total number of grid points = 3.5 million

Swept rotor

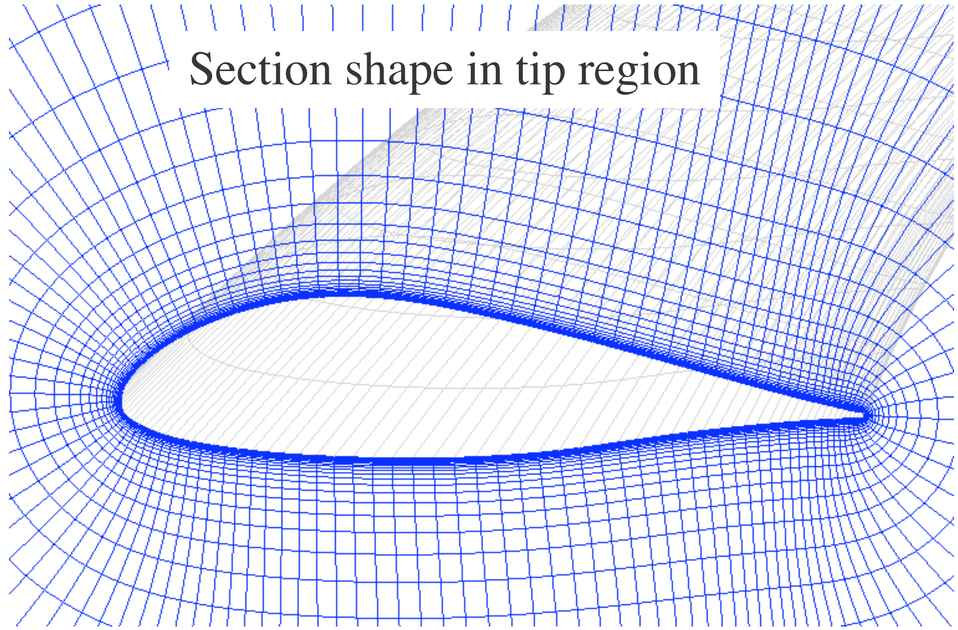

Unswept blade

Swept blade

Conditions

- Rotor RPM = 26.6
- Zero yaw
- Full turbulent flow (SST turbulence model) over blades
- Freestream velocities:
  - 10 m/s
- Solution techniques:
  - Steady - source terms with low-Mach preconditioning, actual velocity and rpm

CFD vs. BEM Blade Spanwise Loads

Swept blade, V_{wind} = 10 m/s, RPM = 26.6

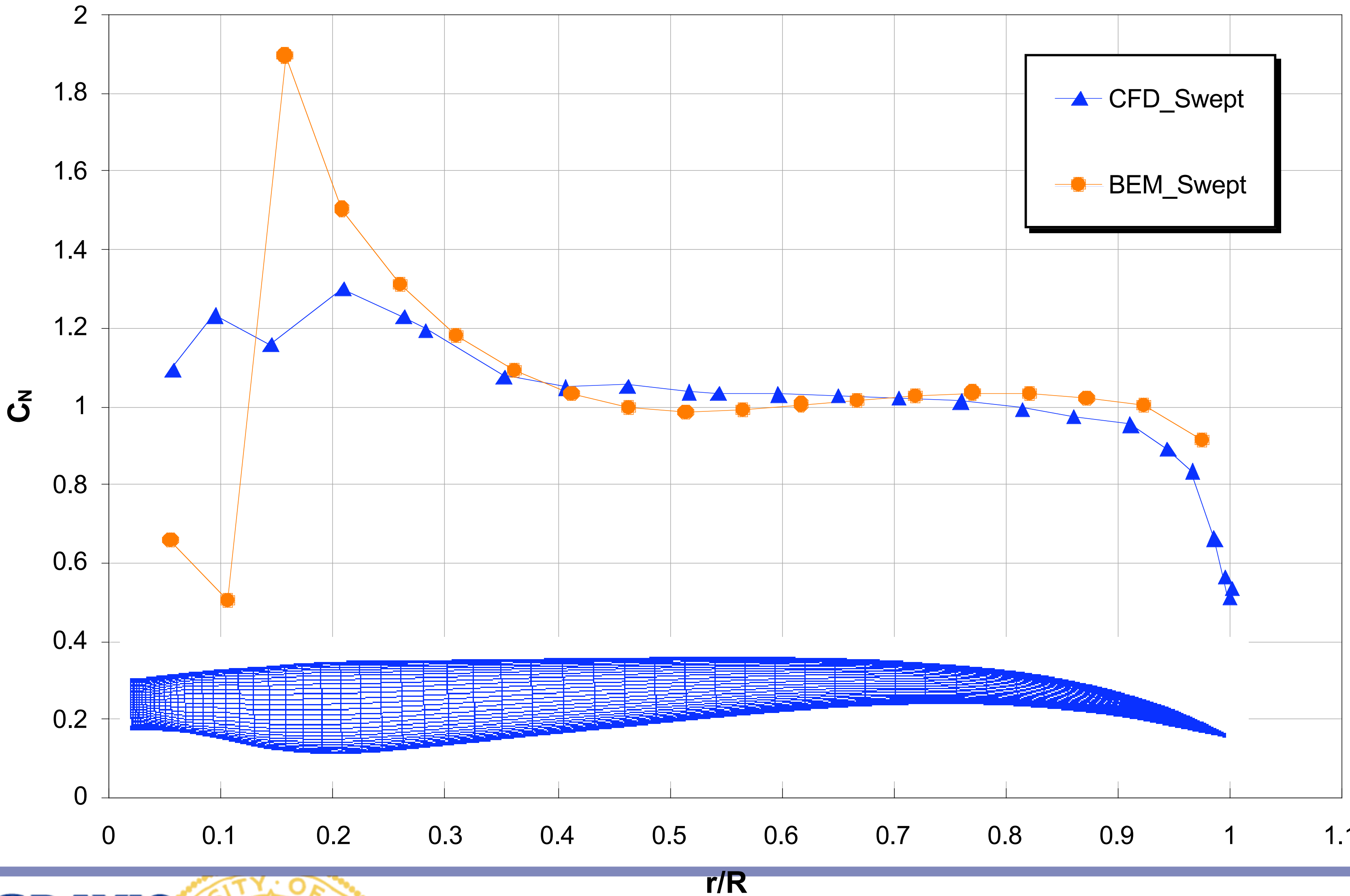

UCDAVIS

Effect of Blade Sweep on Spanwise Loads

CFD, V_{wind} = 10 m/s, RPM = 26.6

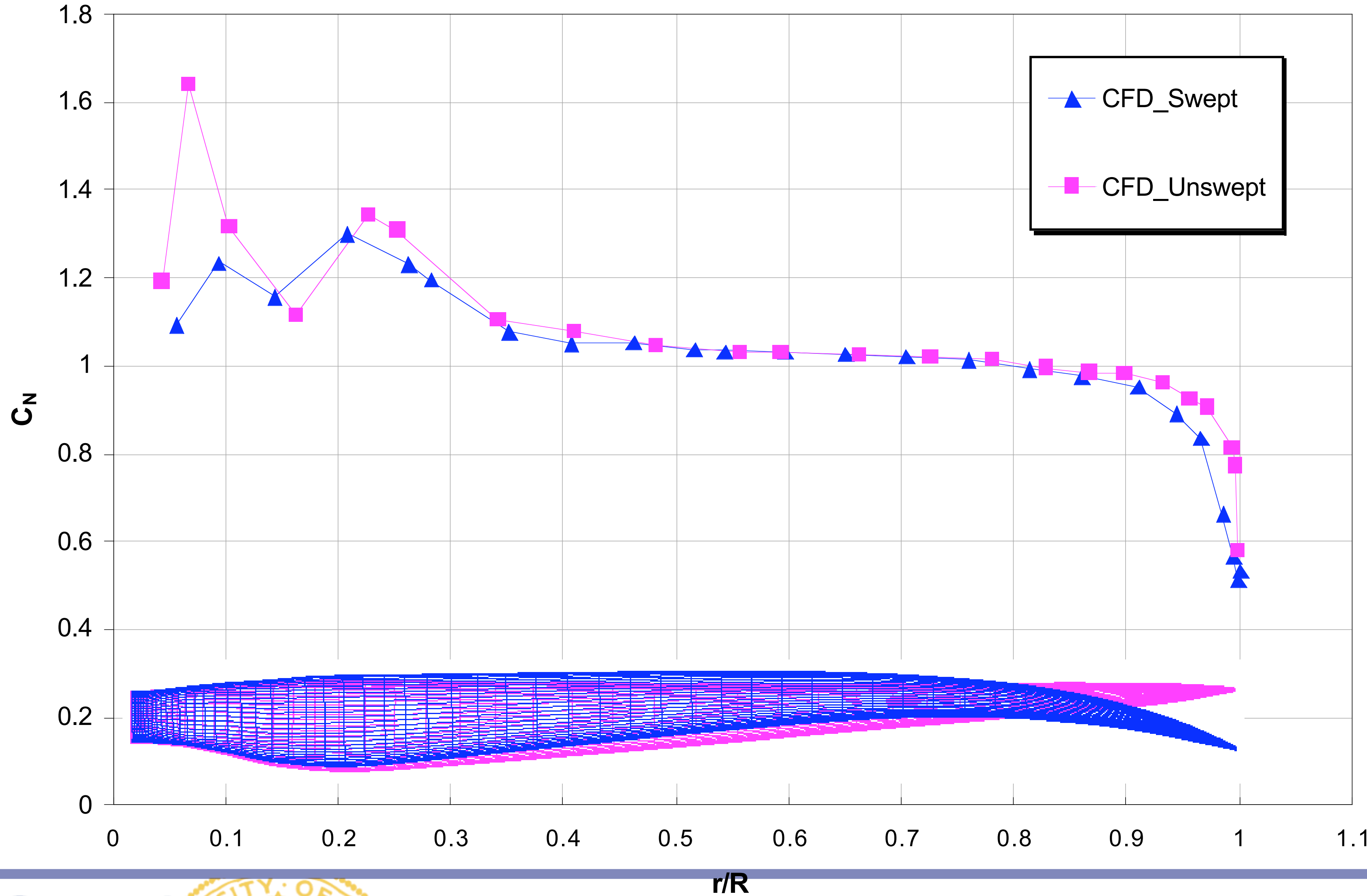

Comparison of Power and Thrust Predictions

V_{wind} = 10 m/s, RPM = 26.6

	Unswept Blades		Swept Blades	
	CFD	BEM	CFD	BEM
Power [kW]	734	733	729	725
Thrust [kN]	114.6	114.2	113.4	112.5

- Good agreement between BEM and CFD predictions
- Currently no experimental data available to compare against

Effect of Blade Sweep on Blade Pressure

CFD, r/R = 0.99

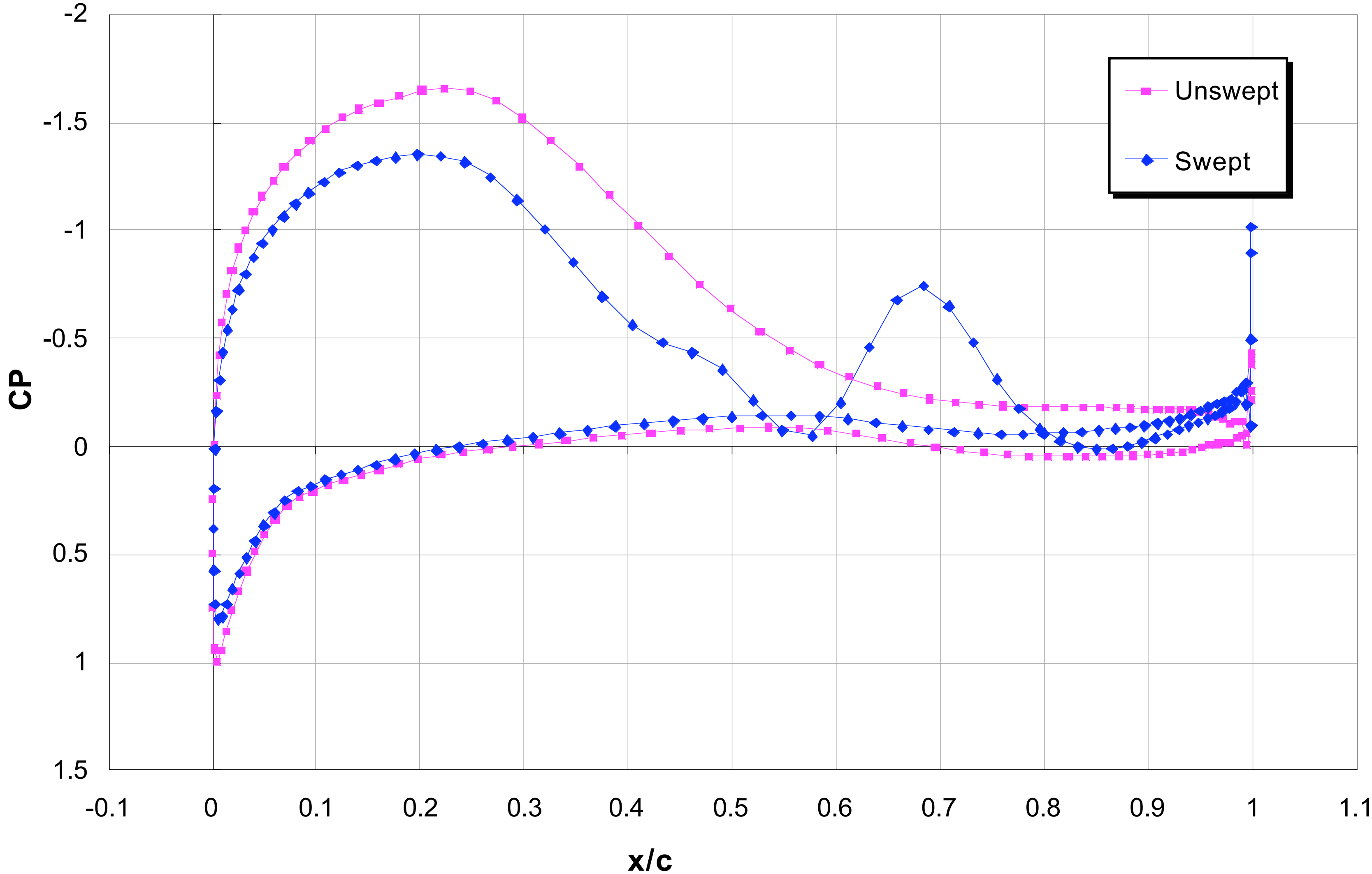

UCDAVIS

Oil Flow Simulations

V_{wind} = 10 m/s, RPM = 26.6, Blade suction side

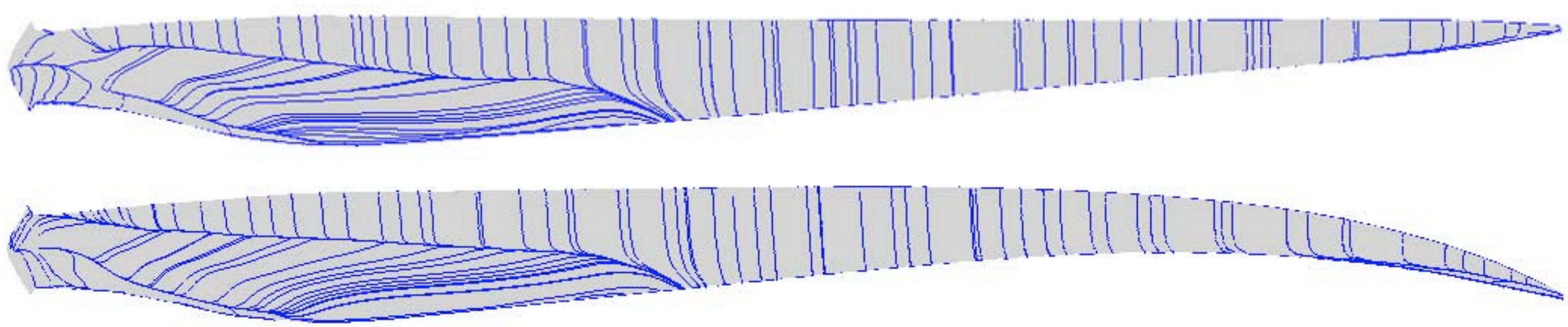

Field Testing

Field Test Site

Tehachapi Wind Resource Area

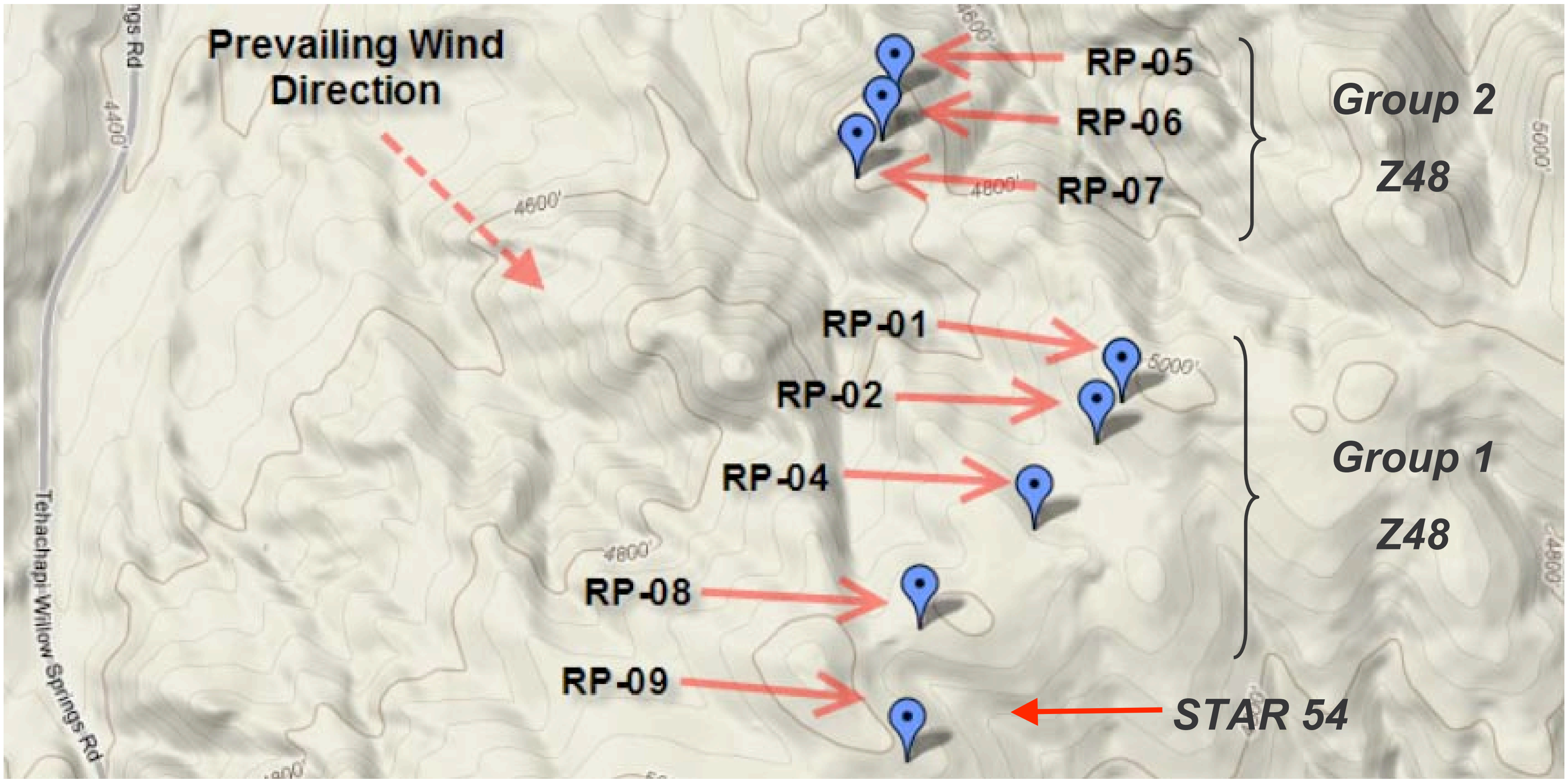

Power Comparison

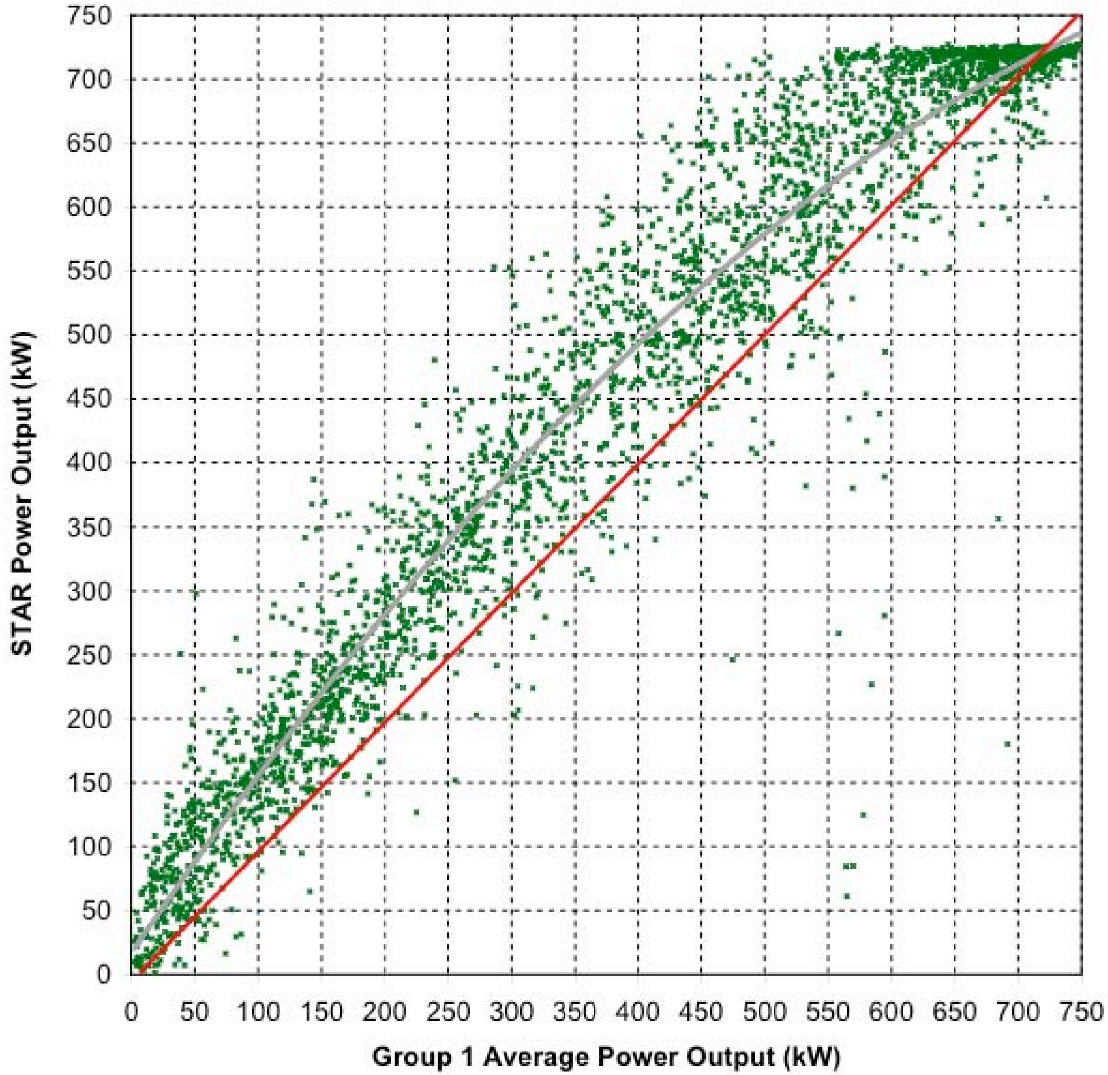

Measured Power Curves

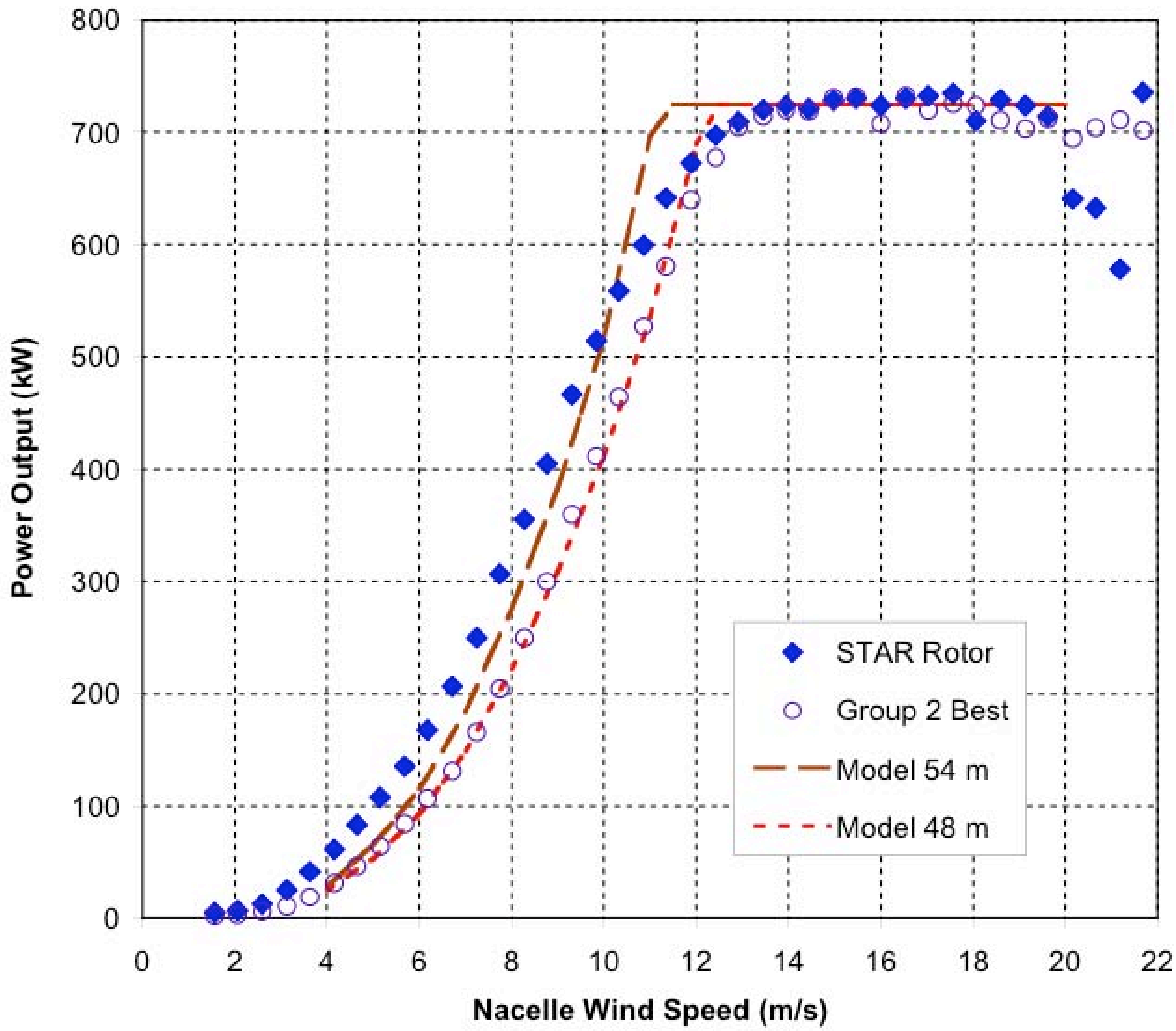

UCDAVIS

Energy Comparison

Turbine Group 1	Energy (kWh)	Compare	Turbine Group 2	Energy (kWh)	Compare
RP-01	243009	101%	RP-05	144456	99%
RP-02	236301	99%	RP-06	145654	100%
RP-04	237148	99%	RP-07	146298	101%
RP-08	242496	101%			
Average	239738	100%	Average	145469	100%
STAR	268711	112%	STAR	197147	136%

UCDAVIS

Flatwise Blade Root Moment Comparison

- STAR rotor loads compared to Z48 data collected at Lake Benton site

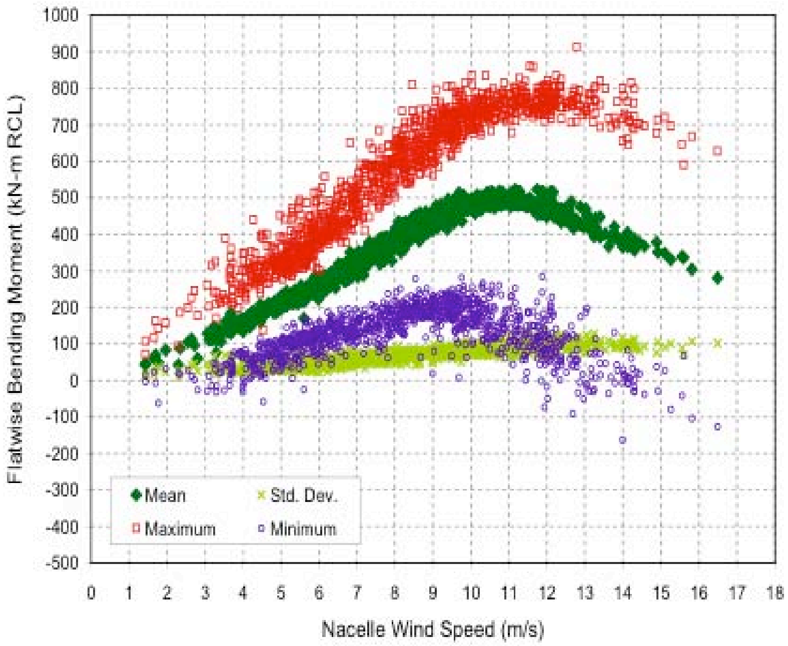

STAR 54

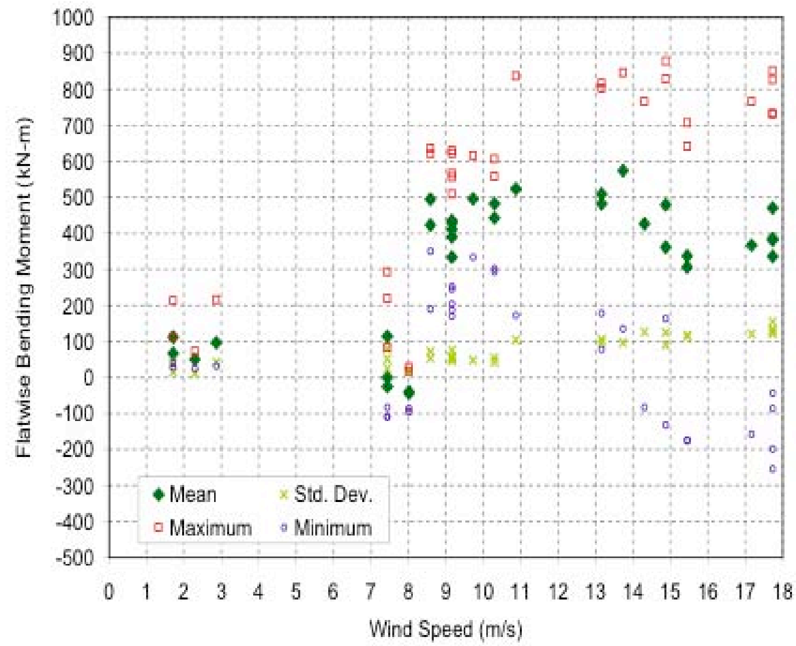

Z48

UCDAVIS

Rank Ordered Blade Flatwise Load Maxima

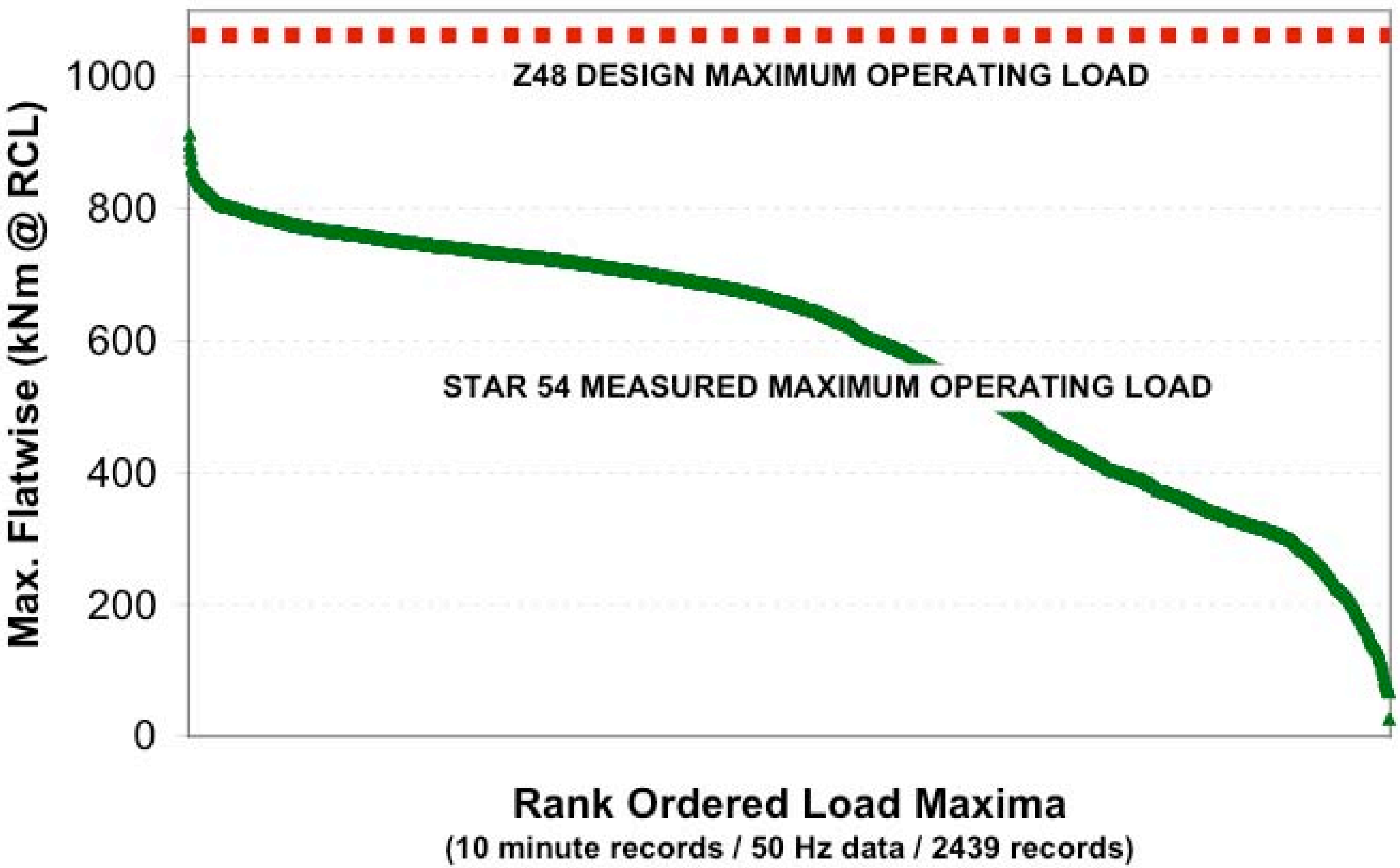

UCDAVIS

STAR Blade

- Increased rotor energy capture through aeroelastically tailored blade design is feasible.
- STAR-54 captured 12% more energy over baseline Z48 turbines without increasing blade loads.
- Effectiveness of concept is demonstrated by fact that prototype STAR-54 is operating without any issues more than 2 years after installation and it remains the highest grossing “Z48” in Tehachapi.
- CFD was key to validate aerodynamic performance and loads of swept blade rotor

Active Aerodynamic Load Control (AALC)

Active Load Control

- With wind turbines blades getting larger and heavier, can the rotor weight be reduced by adding active devices?
- Can active control be used to reduce fatigue loads?
- Can energy capture in low wind conditions be improved?
- Goal is to understand the implications and benefits of embedded active blade control, used to alleviate high frequency dynamics

Blade Load Control Techniques

- Techniques to control blade loads and rotor performance:
    - Blade size (variable blade length)
    - Incidence angle (variable pitch, variable twist)
    - Airspeed (variable speed)
    - Section aerodynamic characteristics
- In future consider the control of all of these simultaneously

$$L = \int_{r=0}^{R} \left[C_L \, \tfrac{1}{2} \rho \left\{ V_{wind}^{2} + (2\pi n r)^{2} \right\} c \right] dr$$

$$C_{L\,min} \le C_L = C_{L_\alpha} \left(\alpha + \beta - \alpha_o \right) \le C_{L\,max}$$

- Focus is on small fast-acting systems that change sectional aerodynamic characteristics to alleviate load spikes due to gusts and to reduce blade tip deflections during high load conditions

UCDAVIS

Rotor Control Strategy Diagram

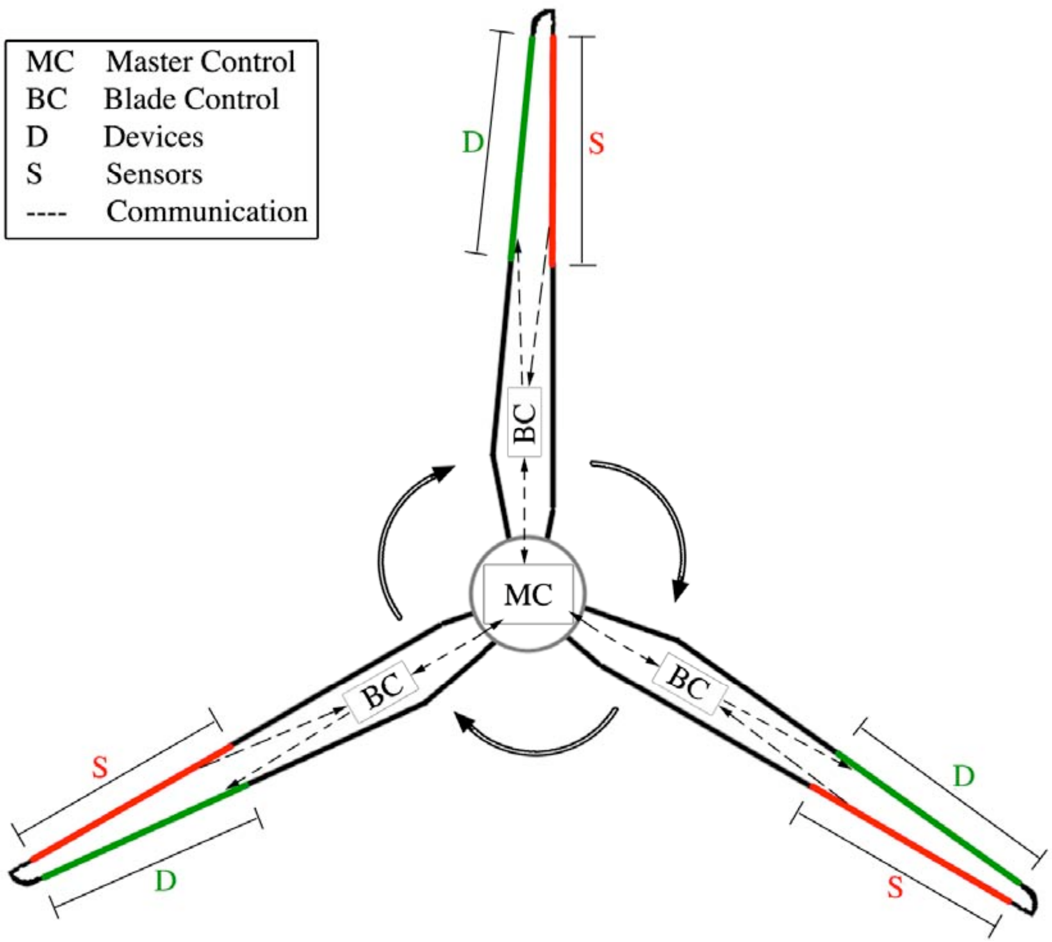

Microtab Concept

- Conceptualized in 1998
- Tabs that deploy (near-)normal to flow direction
- Forward of the trailing edge
  - Upper or lower surface
- Hinge-less device
  - Small actuation forces
- h_{tab} ~ boundary layer thickness
- Trailing-edge flow condition is altered

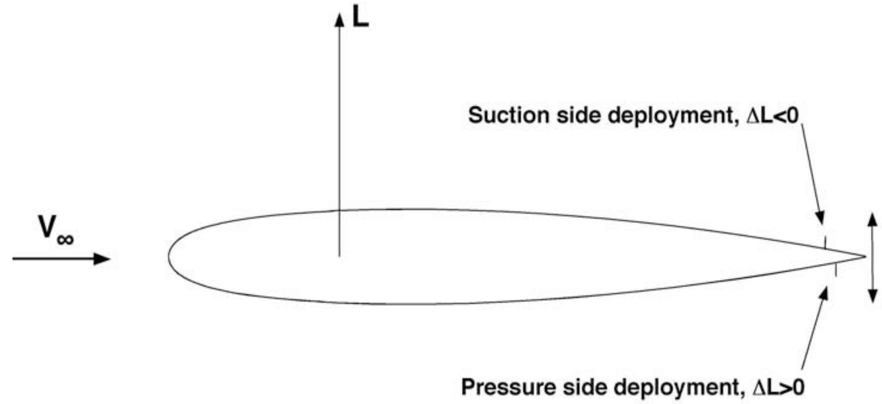

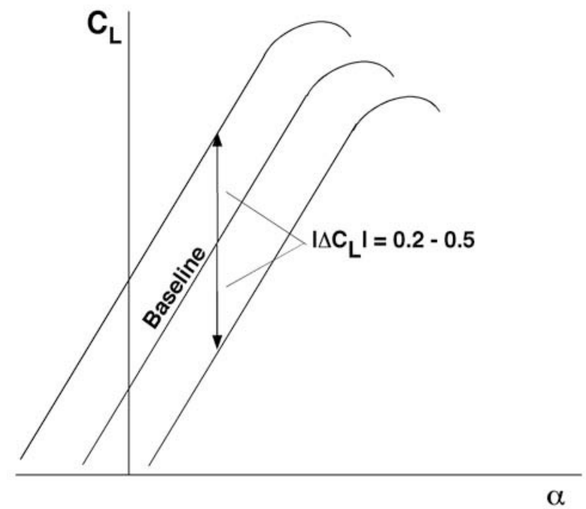

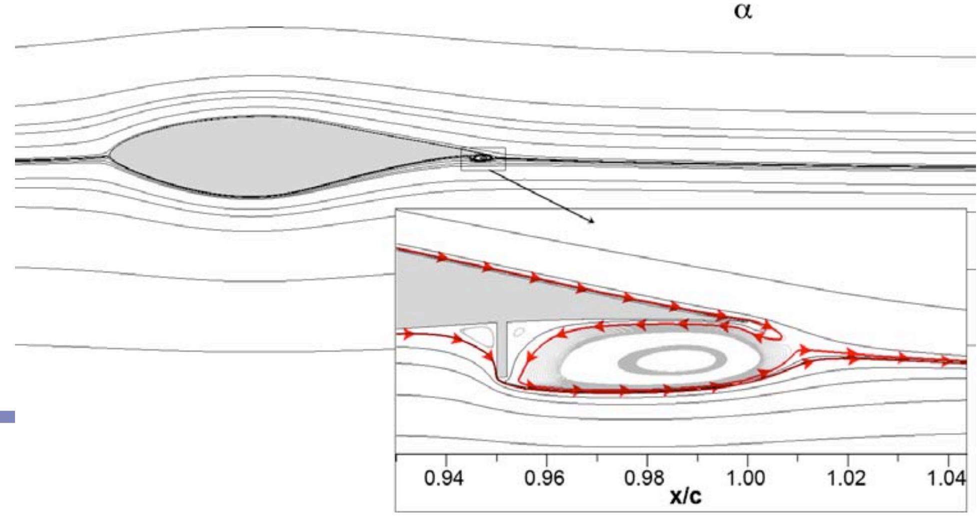

UCDAVIS

Microtab Grids

- Leading edge of the tab placed at 95.0%c of airfoil

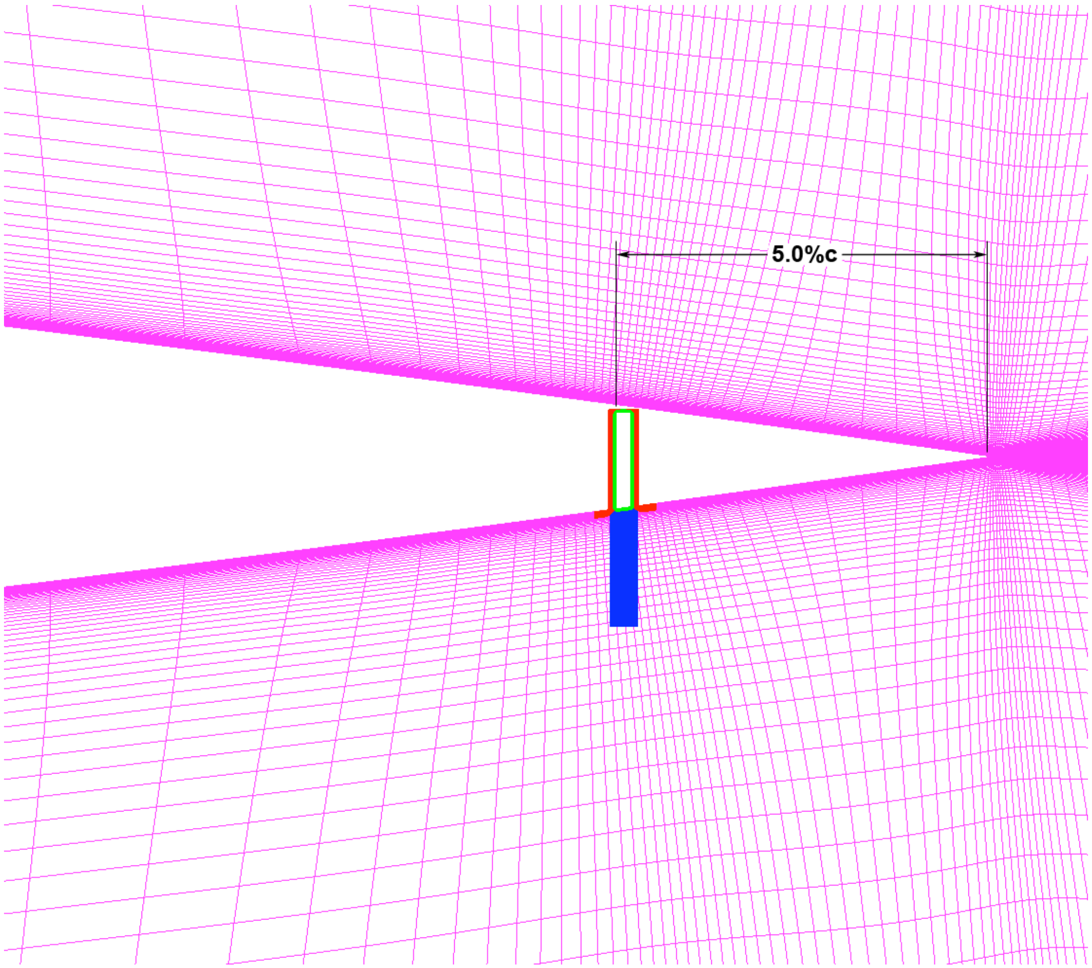

Microtab Grids

- Leading edge of the tab placed at 95.0%c of airfoil
- An additional 183×74 refinement grid is added
- 40,626 grid points

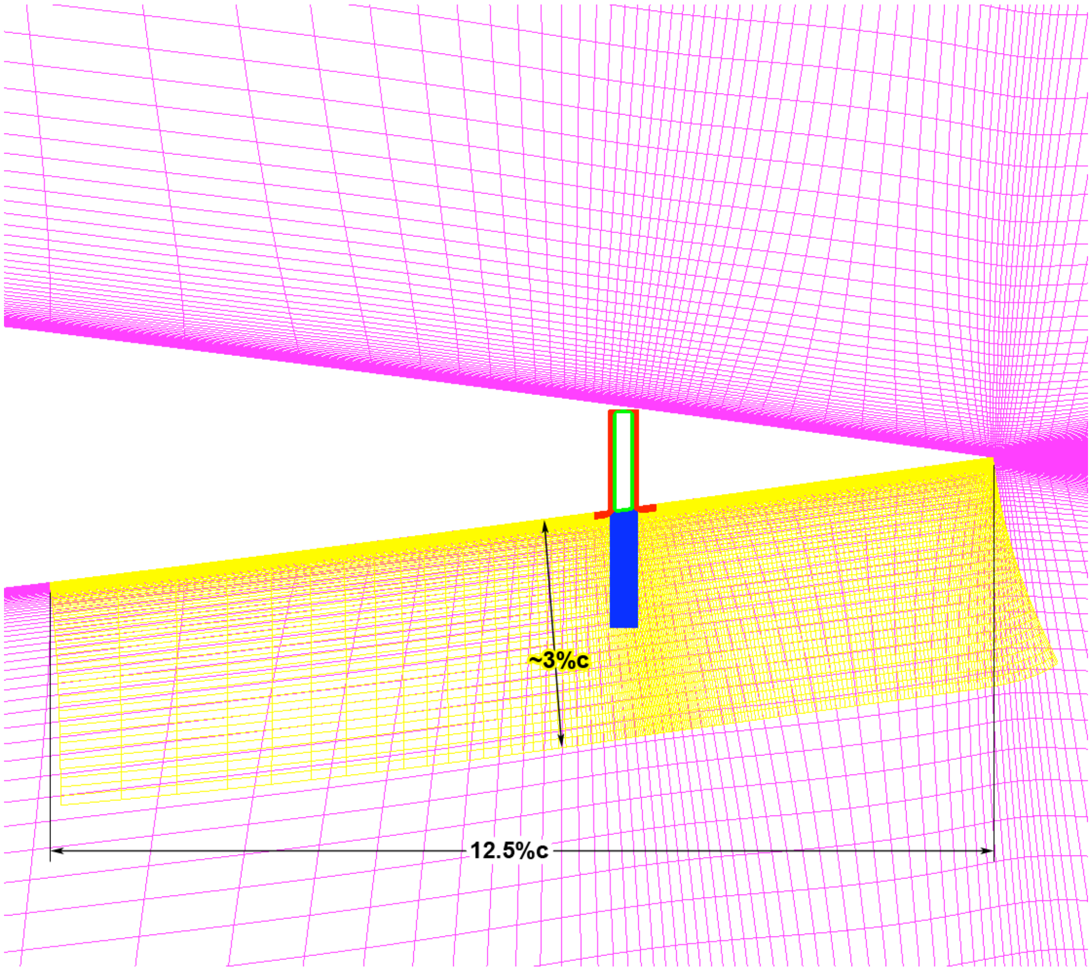

Off-Body Grids

- 35 Cartesian off-body ‘Bricks’
- 8 Levels grid expansion
- Far-field ~50c away
- ~300,000 total grid points in domain

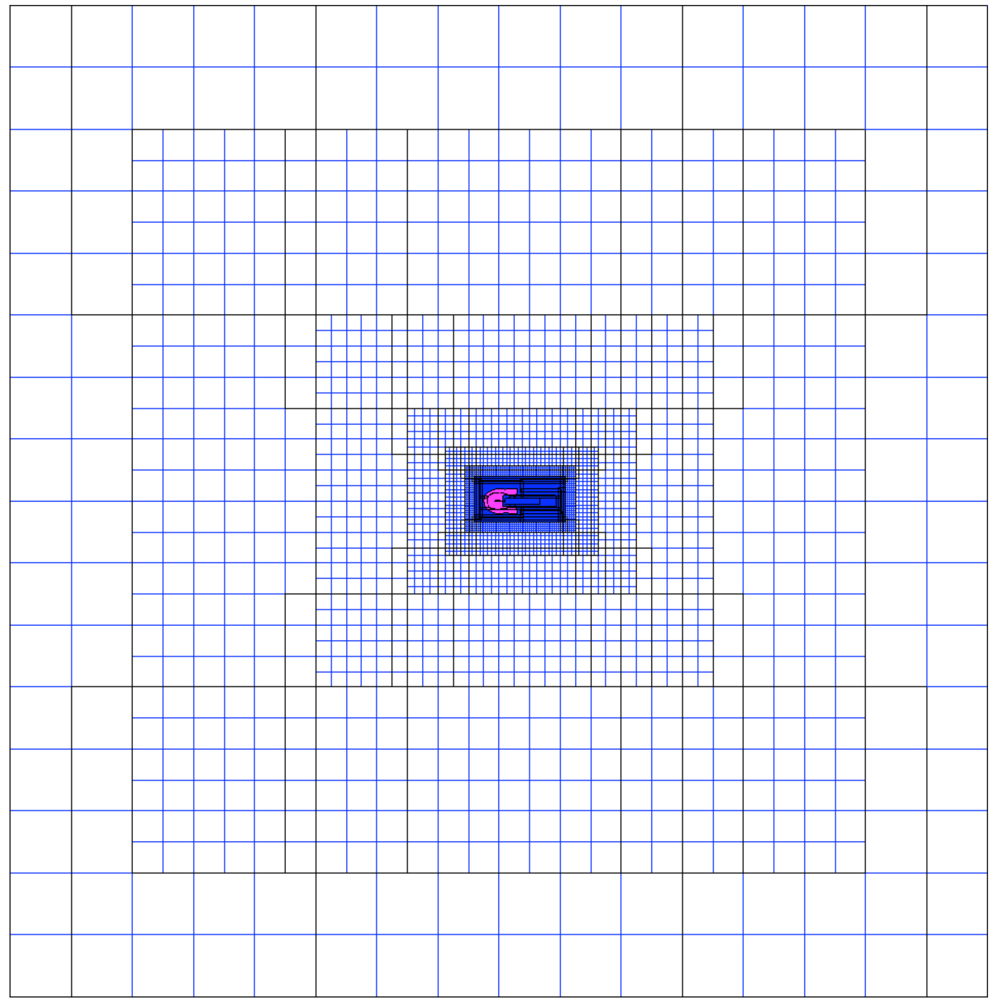

Microtab Deployment

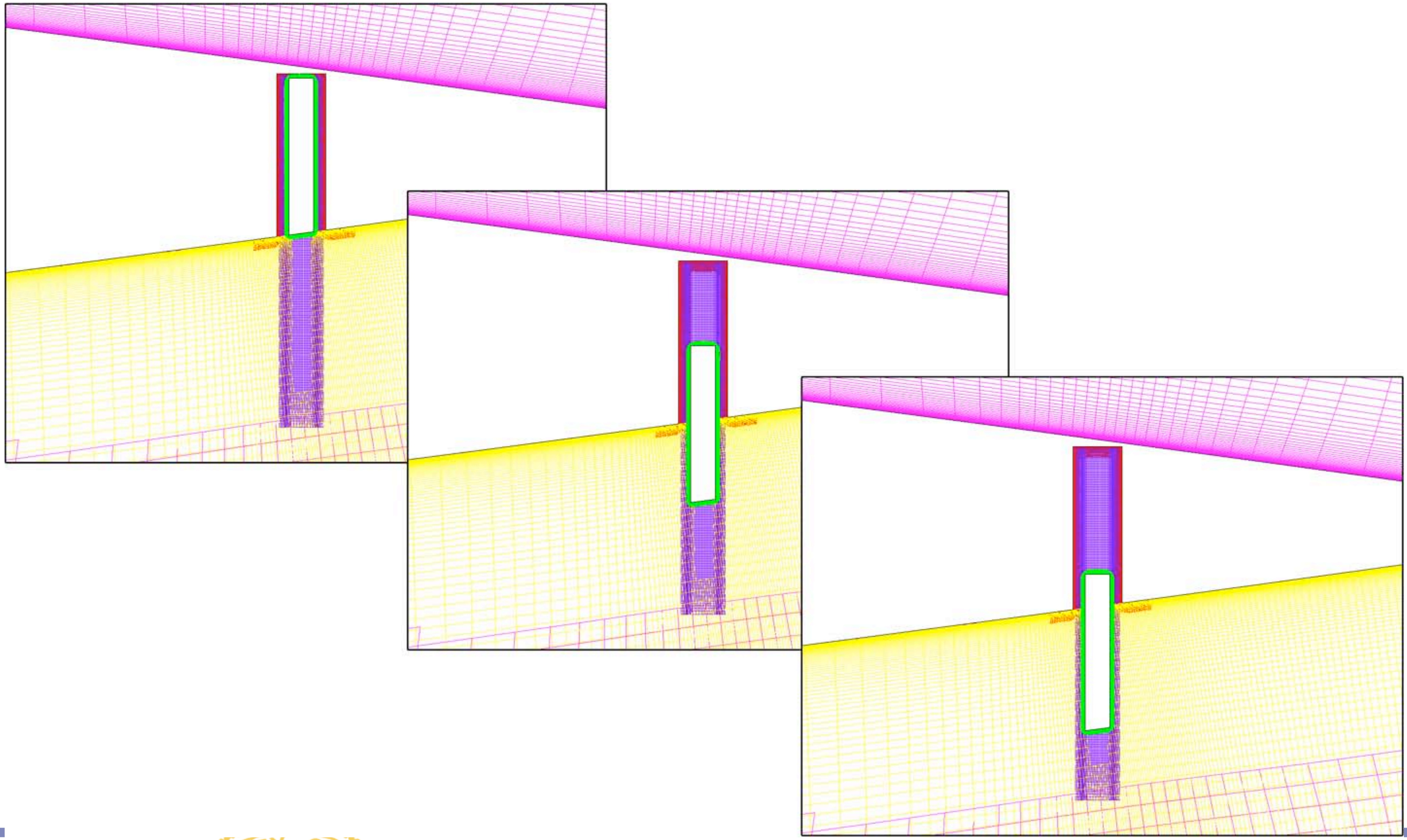

Tab Aerodynamic Response

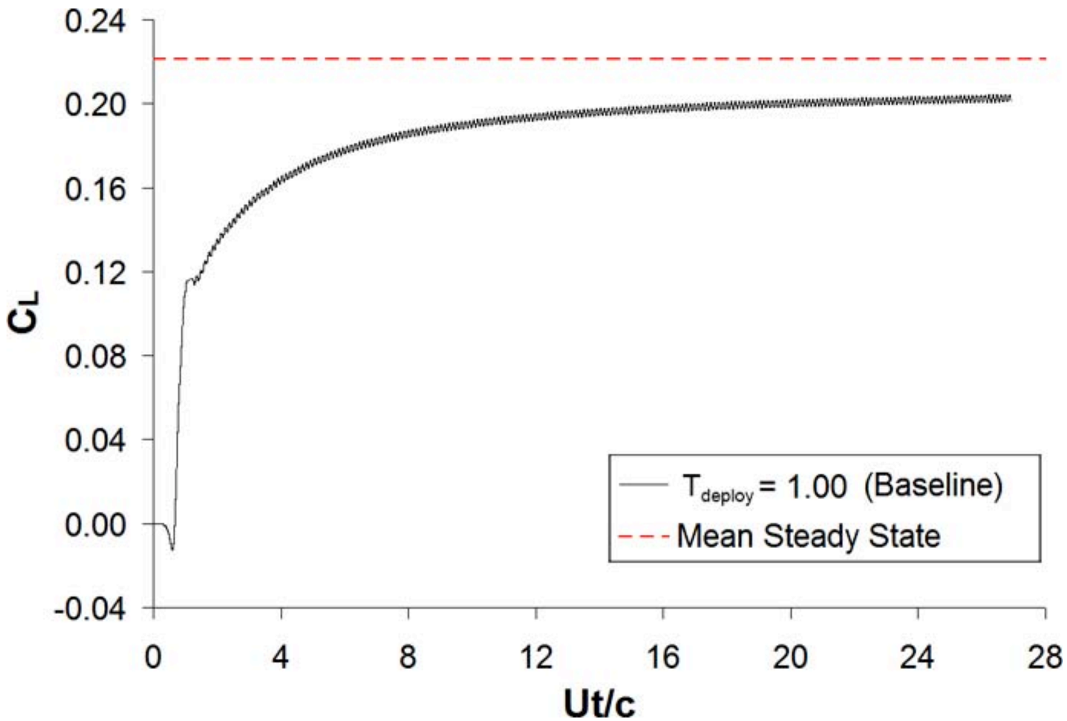

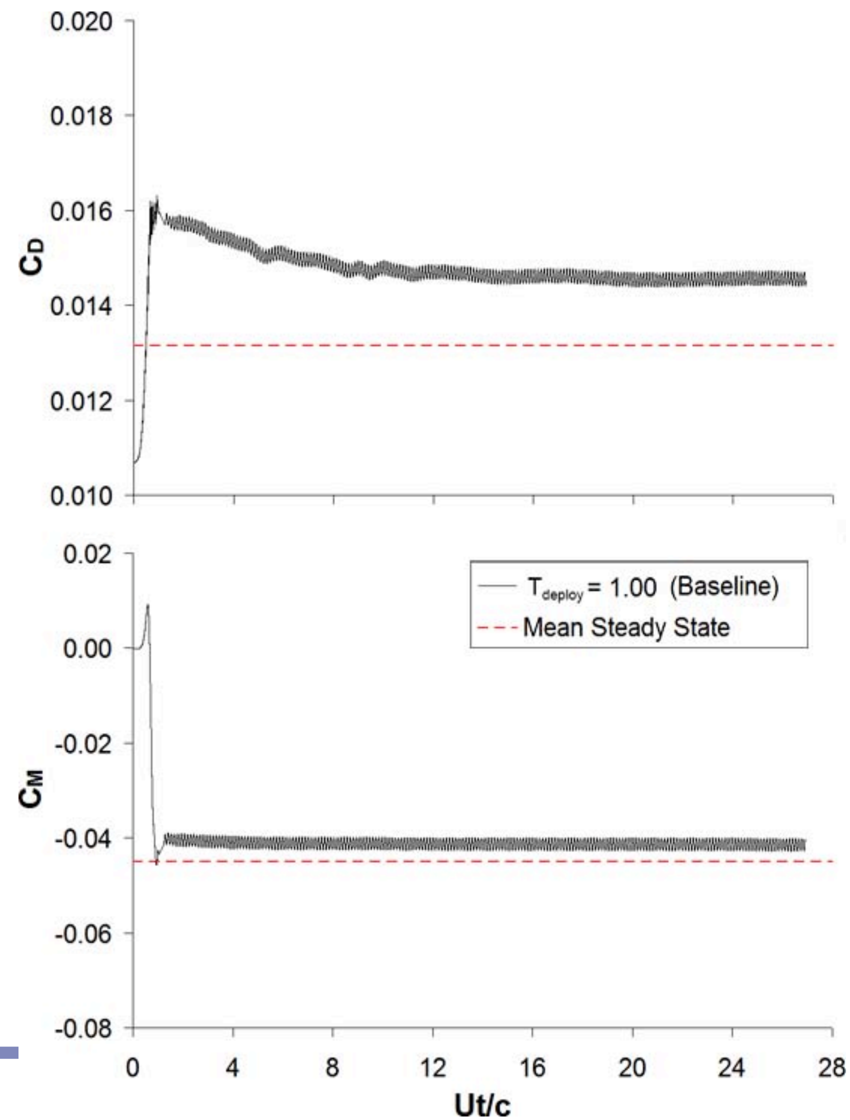

Tab Activation Details

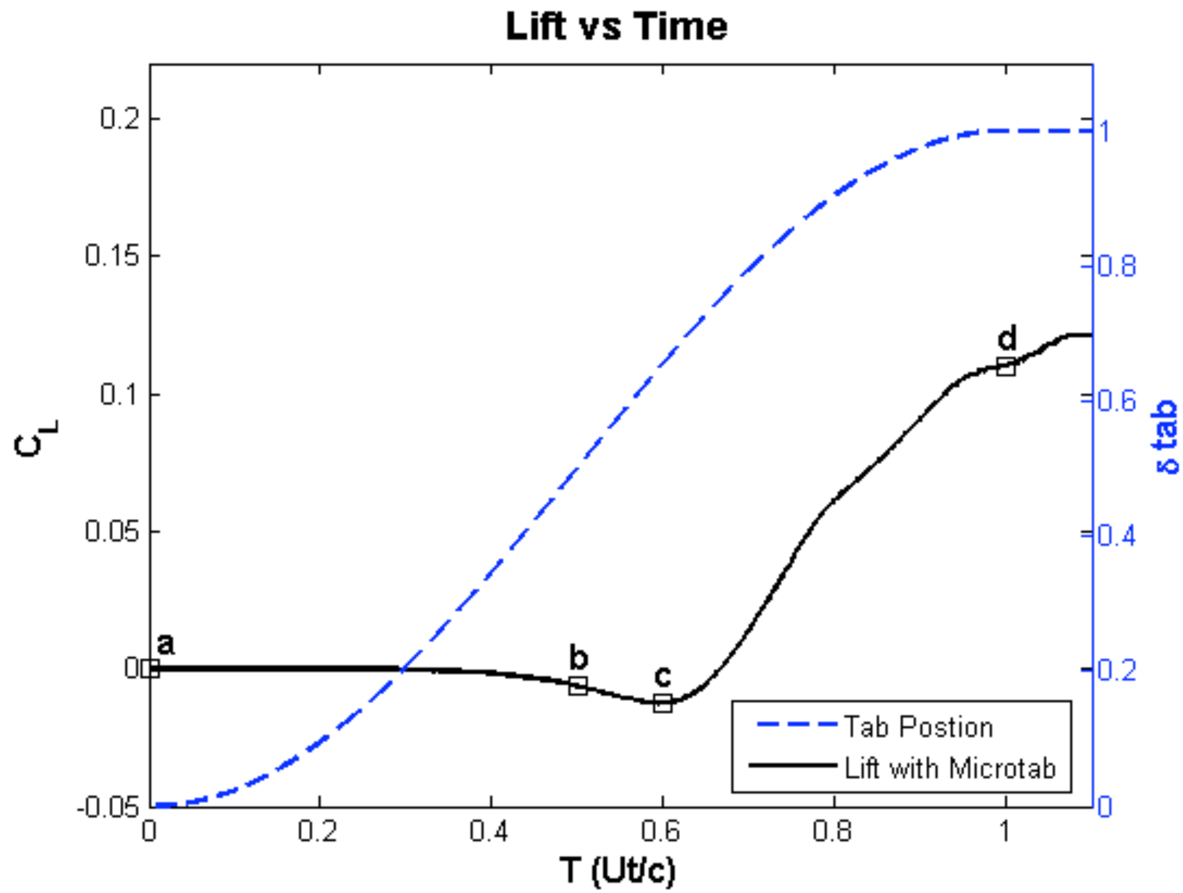

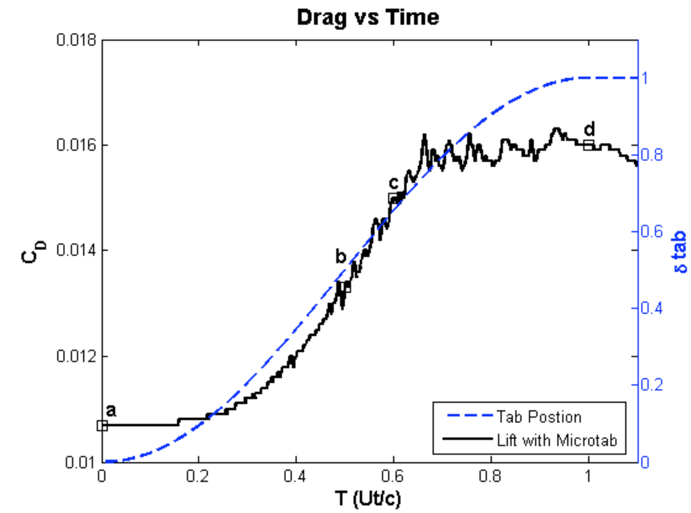

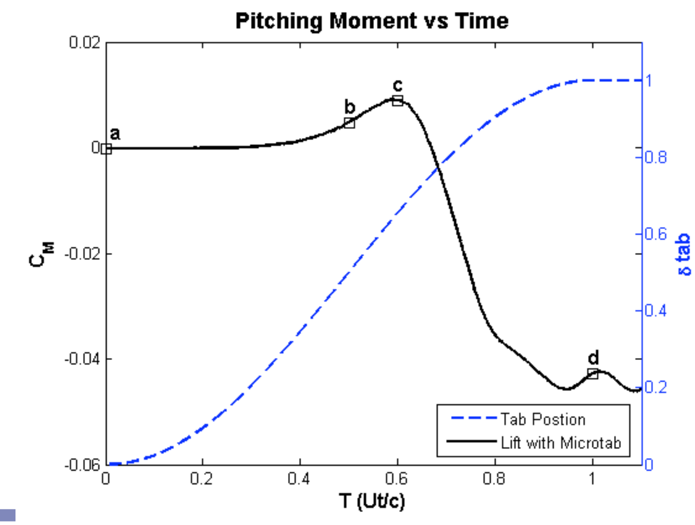

UCDAVIS

NACA 0012, Re=1x10^6, Ma=0.25, T_{act}=1, α=0, h_{tab} = 0.01c

Tab Deployment Details

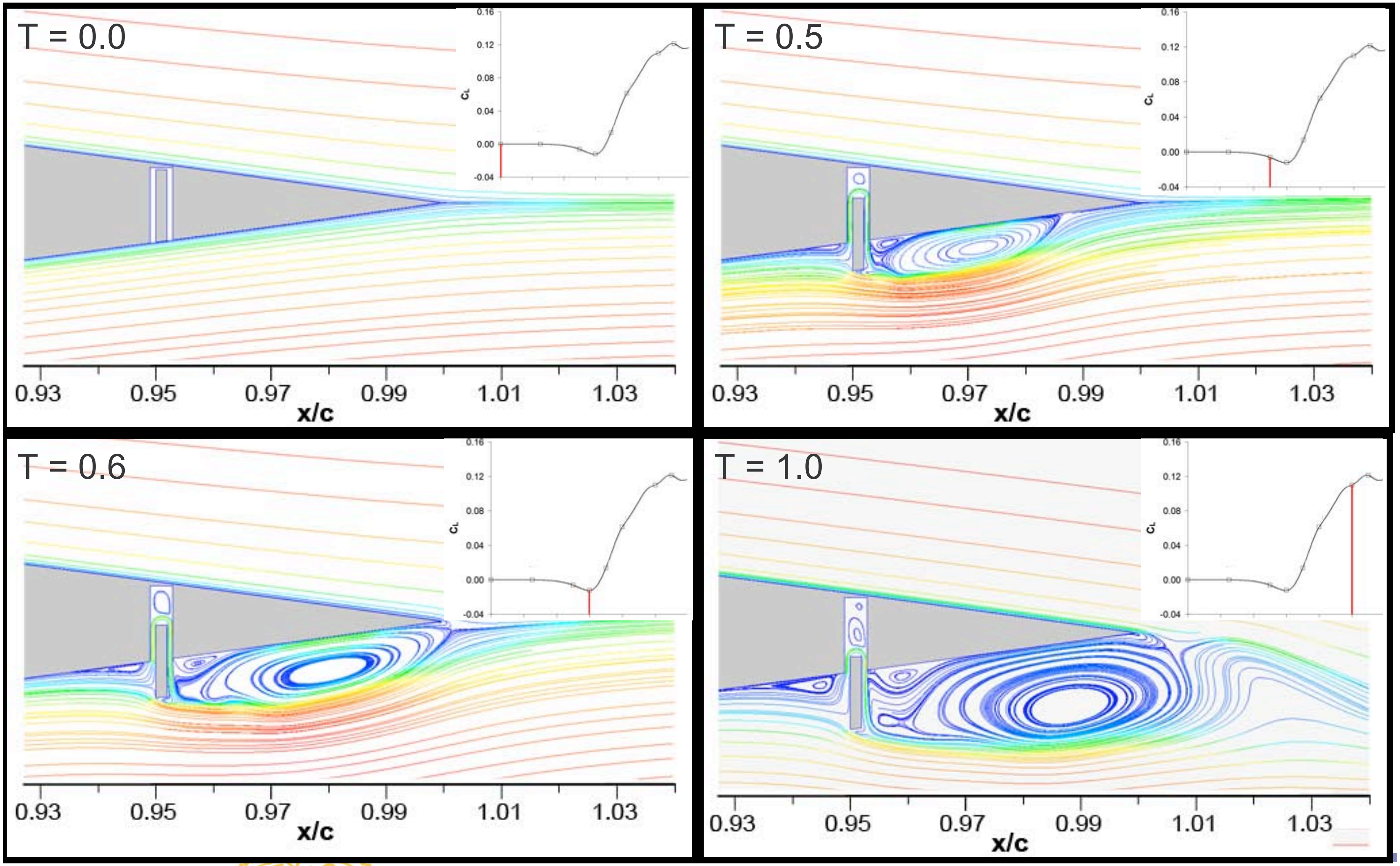

NACA 0012, Re=1x10^6, Ma=0.25, T_{act}=1, α=0, h_{tab} = 0.01c

C_p Contours: T = 0 → 2 c/U

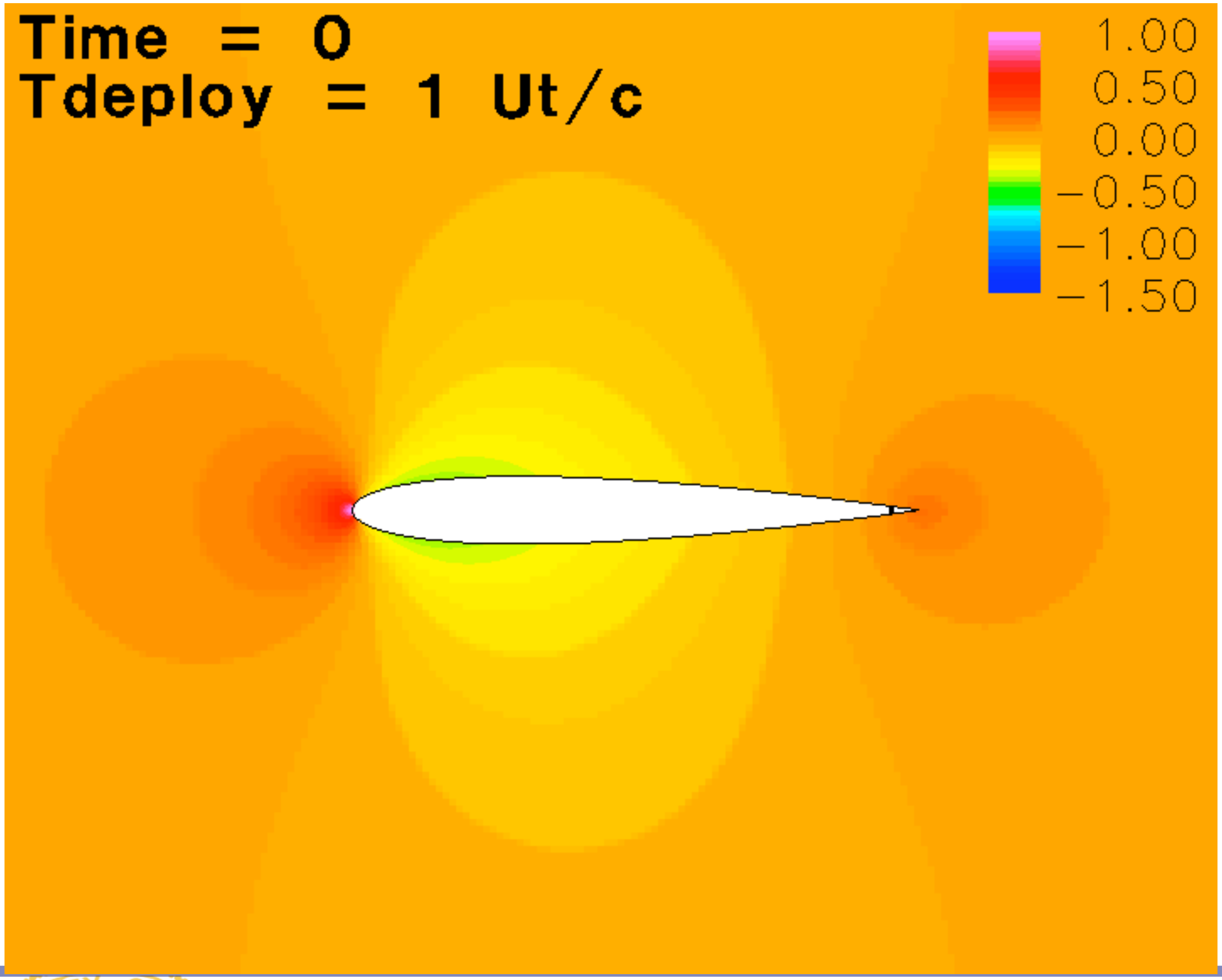

C_p Contours: T = 0 → 2 c/U

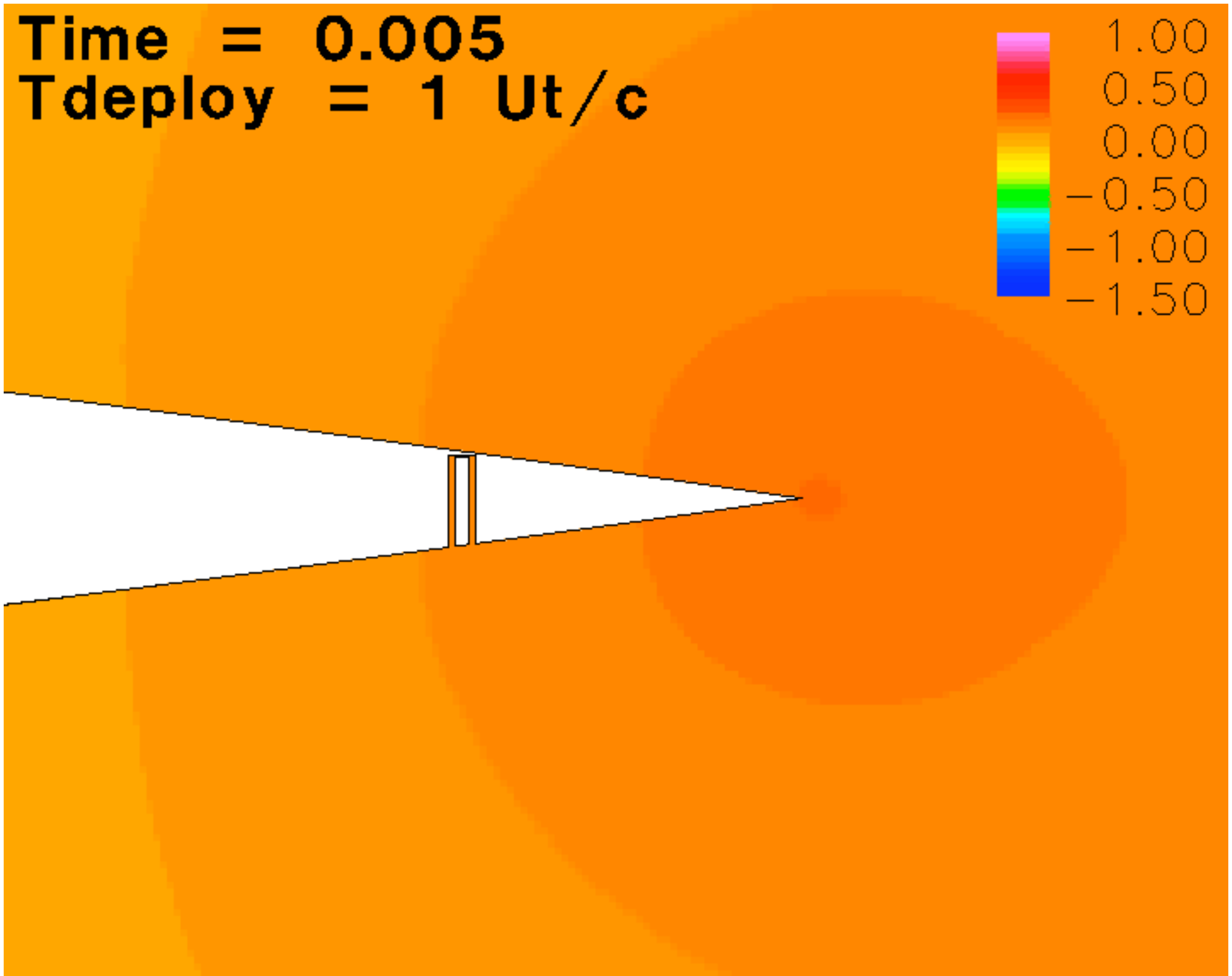

Microjet Concept

- Pneumatic system may be preferred over mechanical system
- Simulation of actively controlled microjet simpler than microtab
- Is effect of physical tab similar to that of jet at same location?

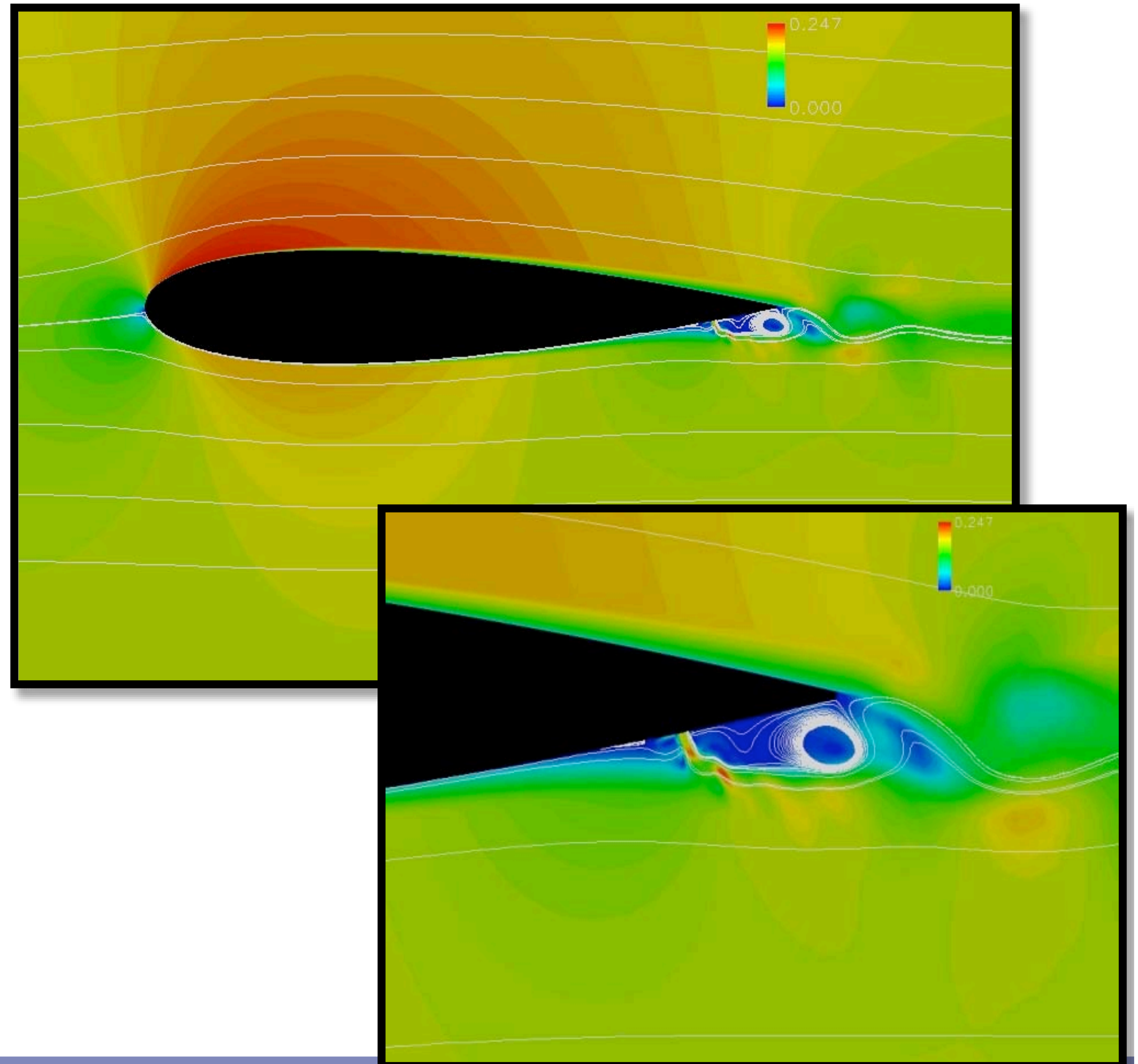

NACA 0018, Re=6.6x10^5, M_∞=0.176, α=0

Jet Activation Details

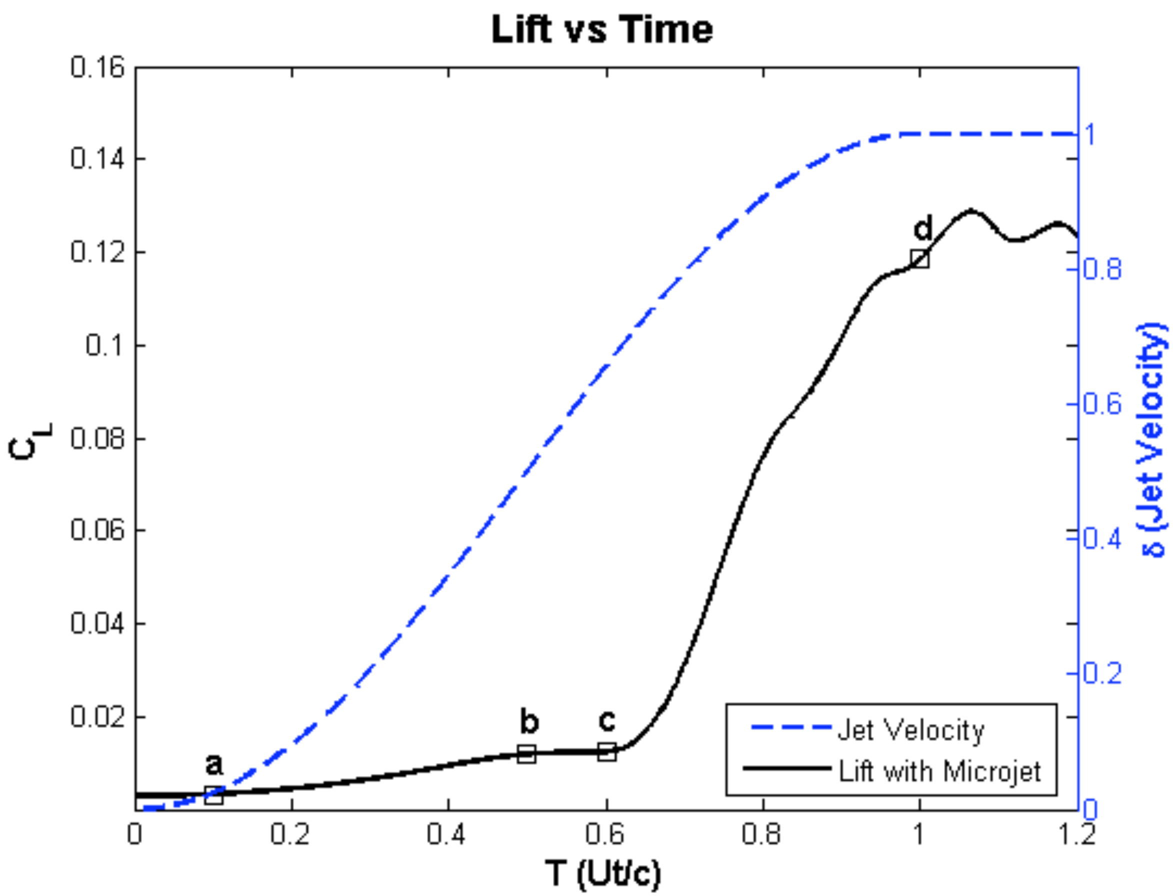

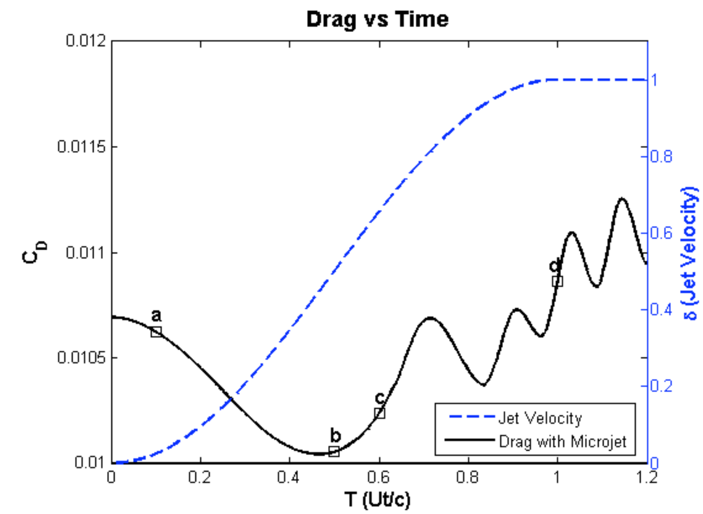

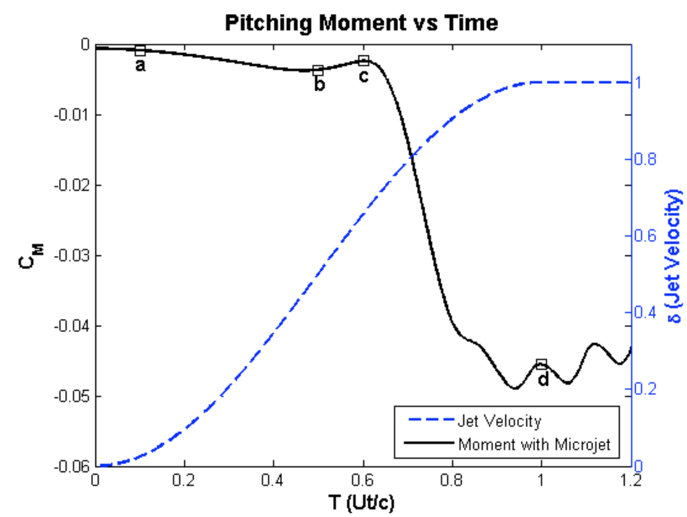

NACA 0012, Re=1x10^6, Ma=0.25, T_{act}=1, α=0, C_μ=0.0029

Jet Activation Details – T=0.1

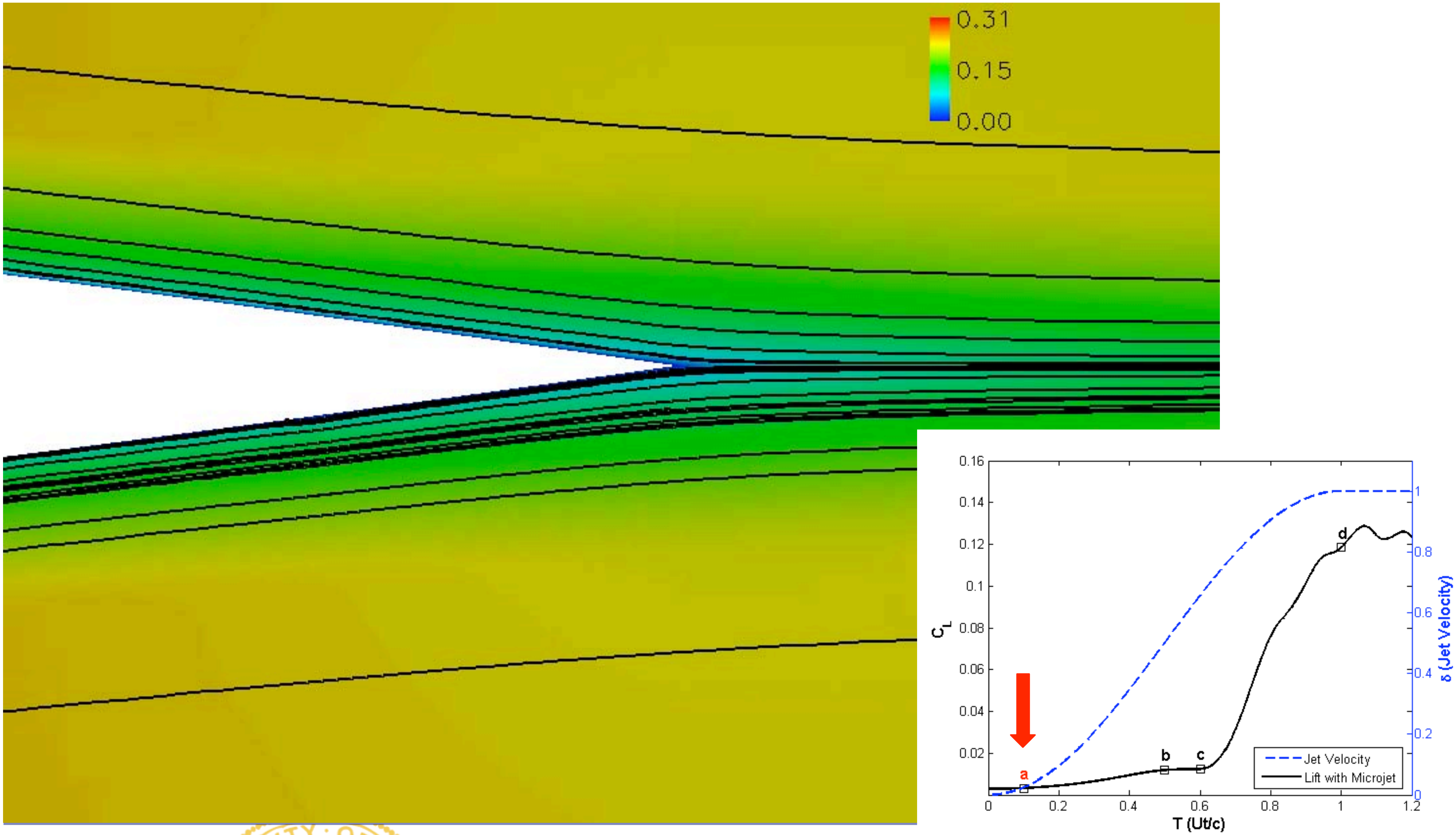

UCDAVIS

NACA 0012, Re=1x10^6, Ma=0.25, T_{act}=1, α=0, C_μ=0.0029

Jet Activation Details –T=0.5

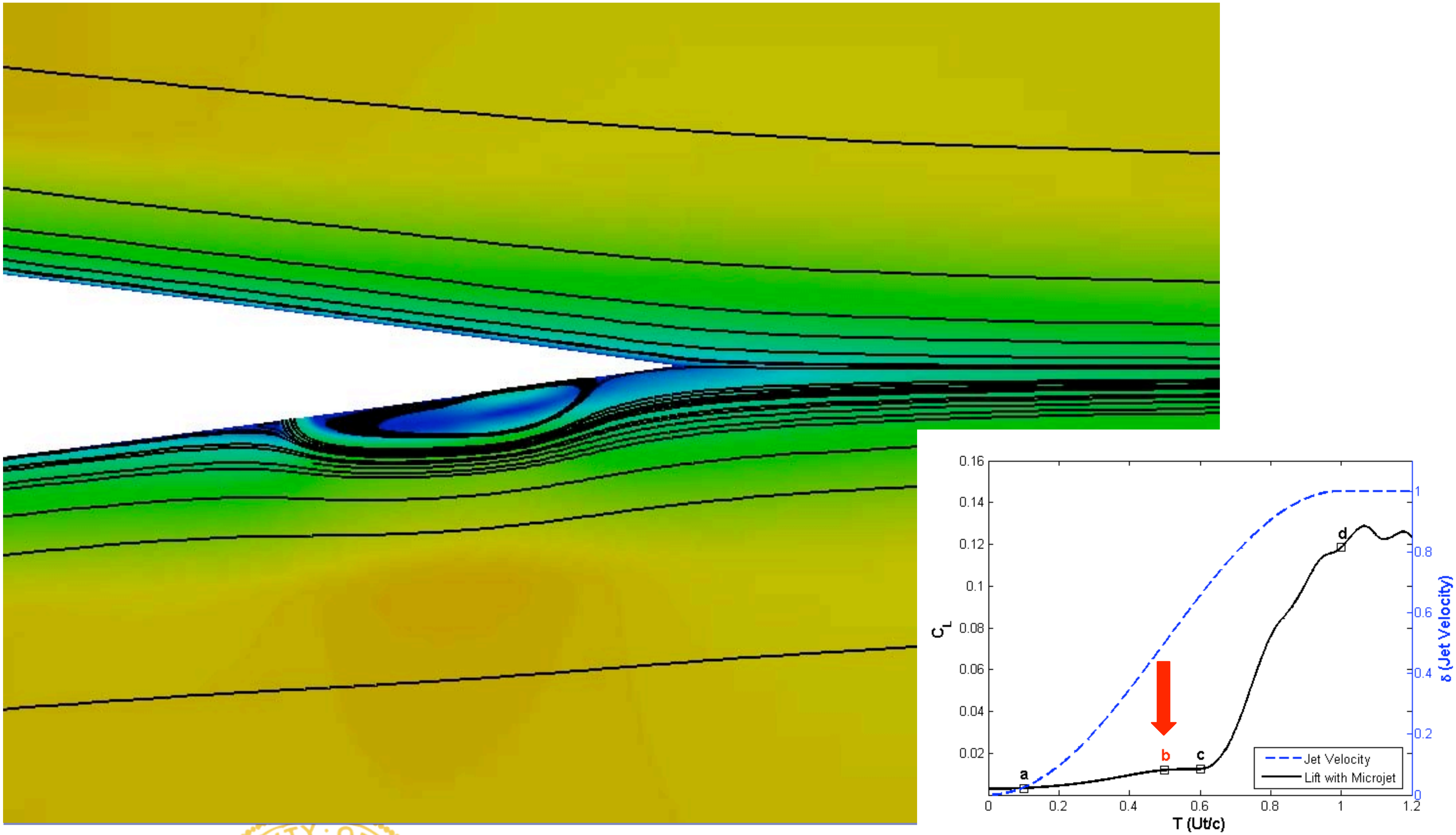

NACA 0012, Re=1x10^6, Ma=0.25, T_{act}=1, α=0, C_μ=0.0029

78

Jet Activation Details – T=0.6

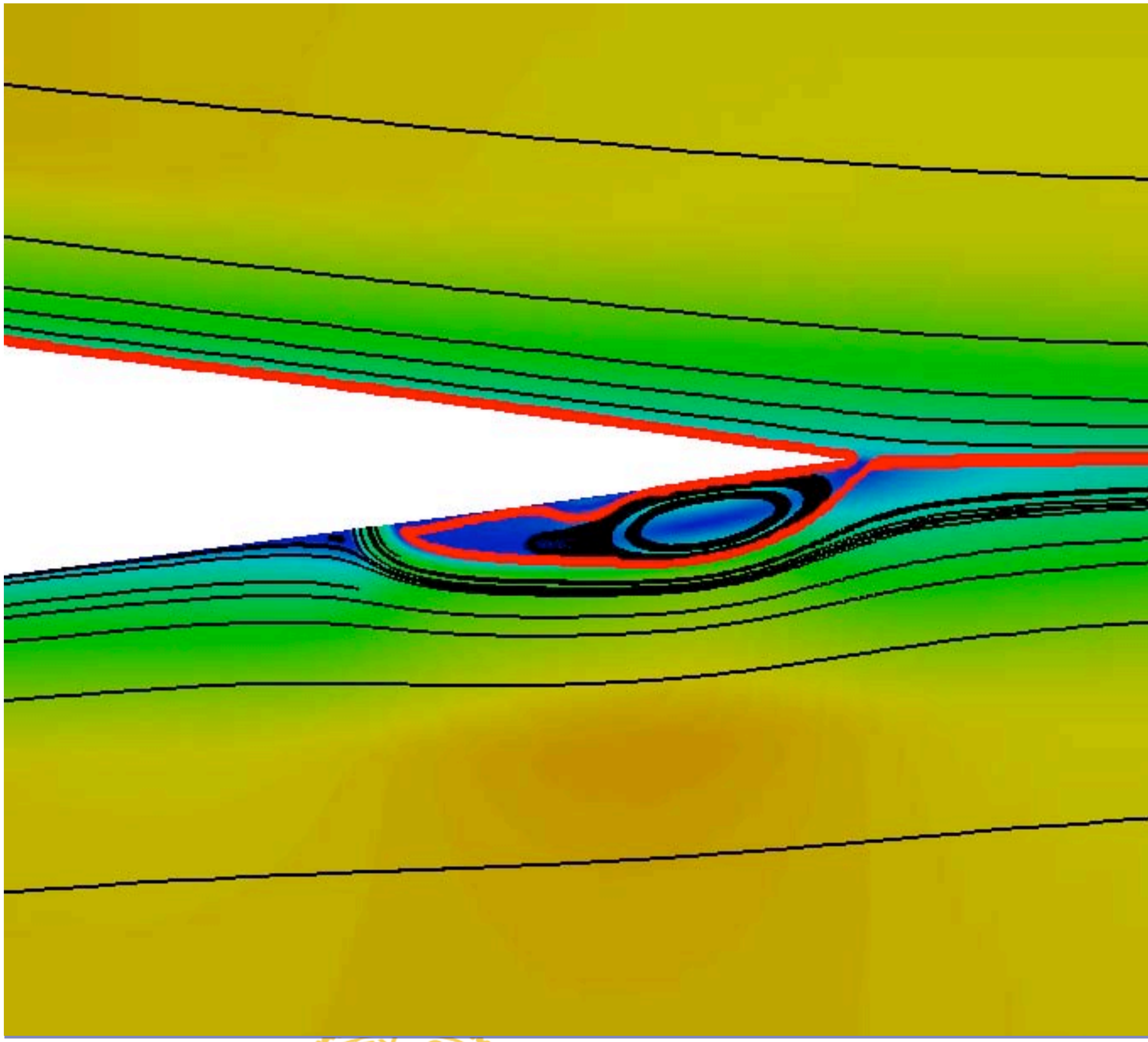

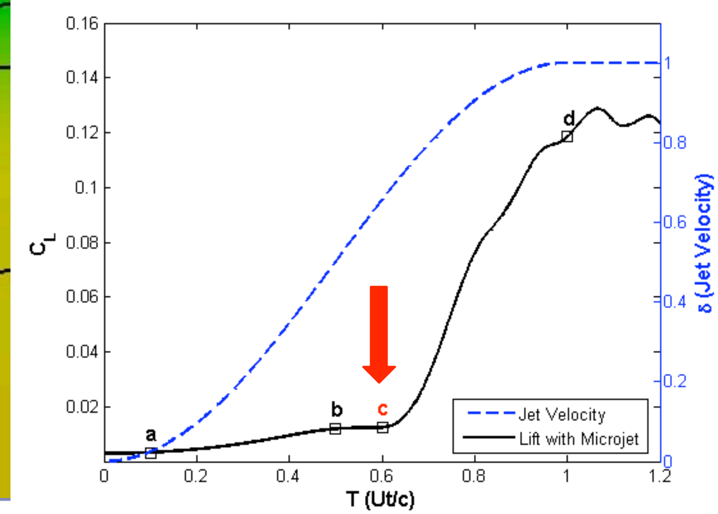

NACA 0012, Re=1x10^6, Ma=0.25, T_{act}=1, α=0, C_μ=0.0029

Jet Activation Details –T=1.0

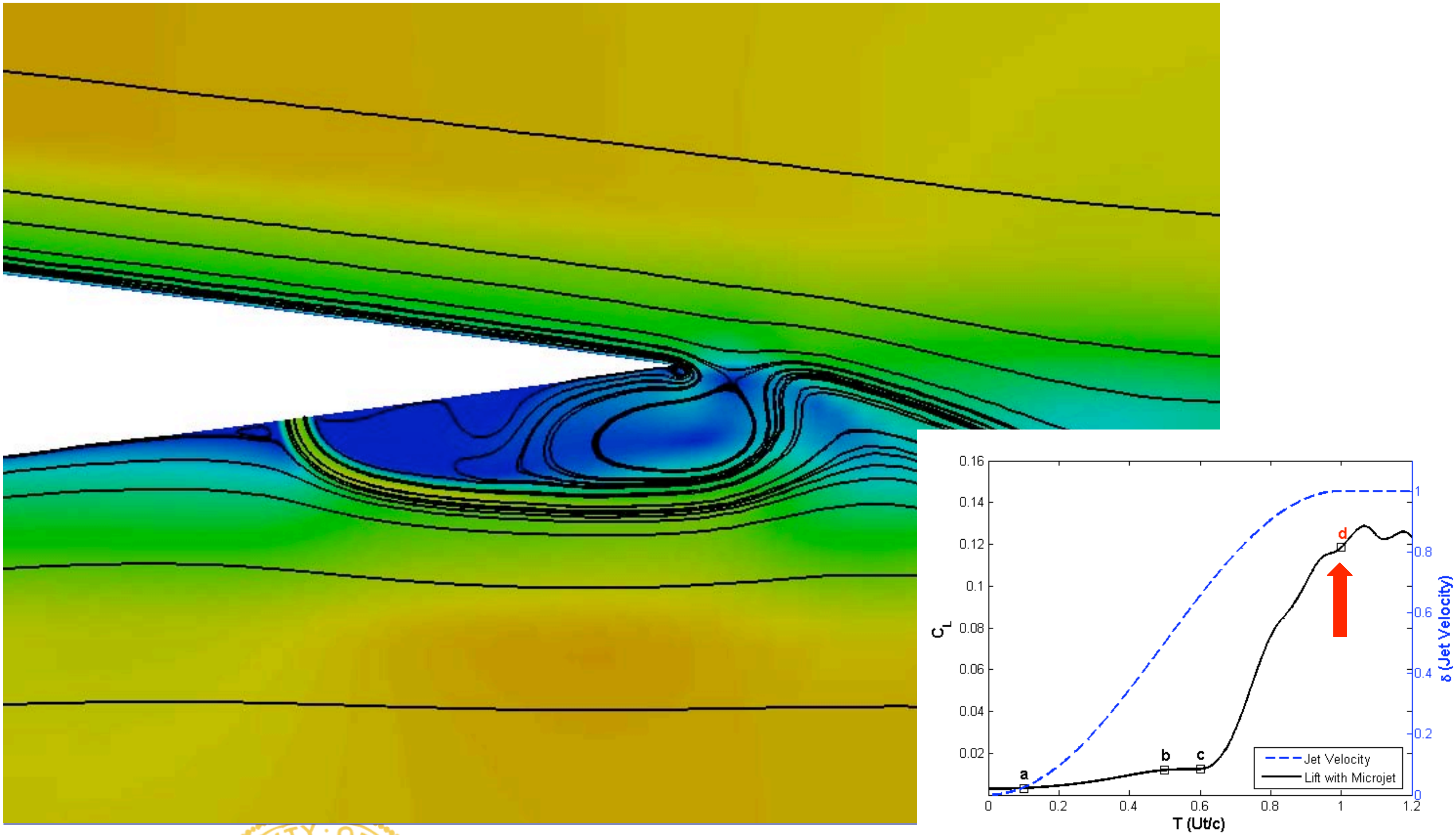

UCDAVIS NACA 0012, $Re=1x10^6$, Ma=0.25, $T_{act}=1$, α=0, $C_\mu=0.0029$

80

Active Aerodynamic Load Control

- CFD was key technology to design and analyze effectiveness of active aerodynamic load control for wind turbine blades.
- Systems must:
  - Be small and scalable
  - Have fast activation speed
  - Have low activation force and power requirements
  - Should be reliable and dependable
- Blade manufacturing and maintenance should be considered when embedding AALC systems
- Driving factor is economics $\Rightarrow$ successful system must reduce COE
- AALC (include tab-based system) is currently being field tested on wind turbines in Europe and USA

Inboard Flow Separation Mitigation

NREL 5-MW Rotor

- Geometry based on 6MW DOWEC rotor
  - Conceptual off-shore turbine design
  - ECN (Energy Research Centre of the Netherlands)
- Rotor diameter truncated and hub diameter reduced

NREL 5-MW Rotor

- 126 m rotor diameter
- 12.1 RPM
- $TSR_{Design} = 8$
- 3 m hub diameter
- 61.5 m blade length
- 4.7 m max chord
- 13.3° inboard twist
- 3 m/s cut-in speed
- 25 m/s cut-out
- 12 m/s rated speed

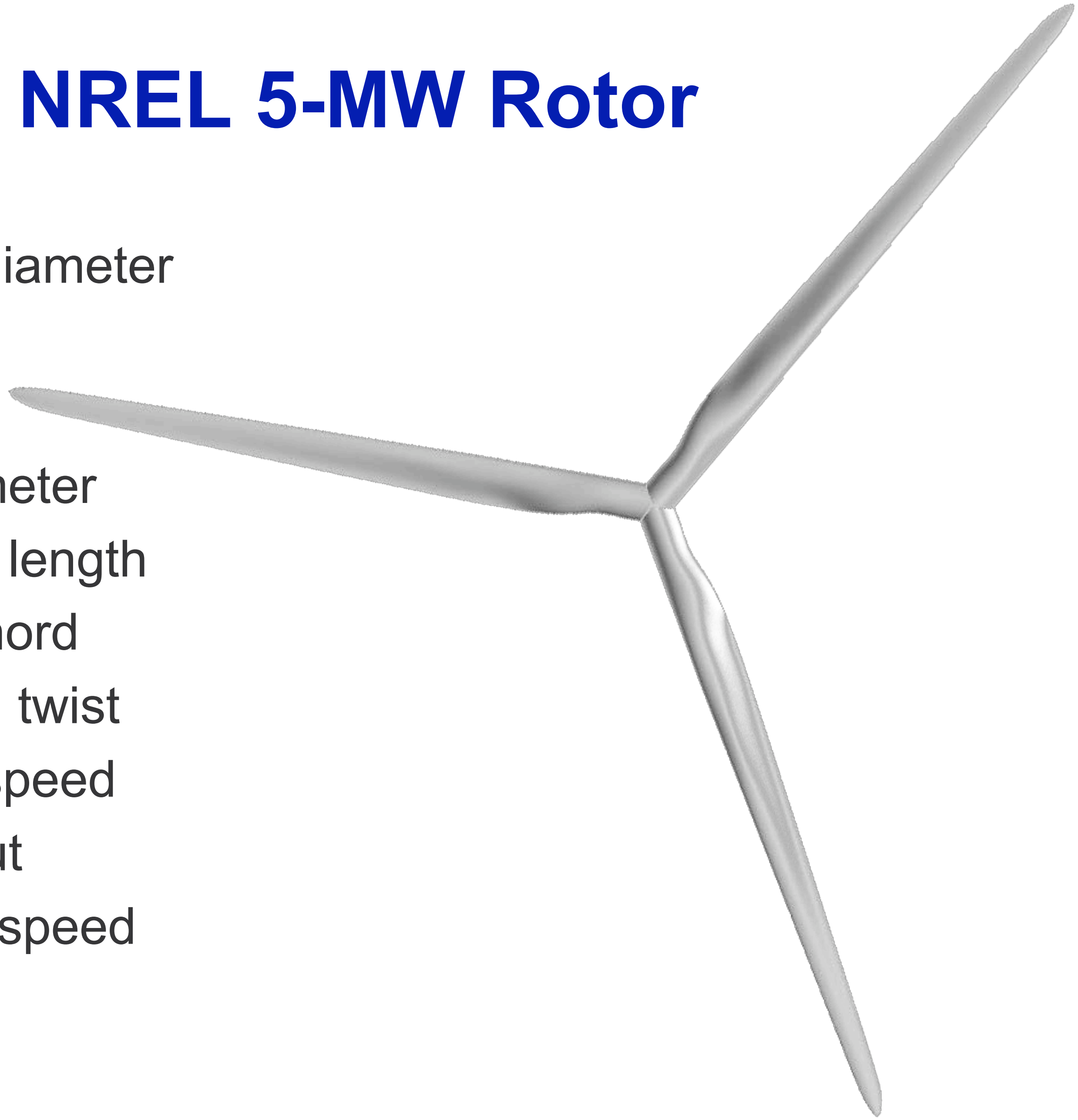

NREL 5-MW – Grid Topology

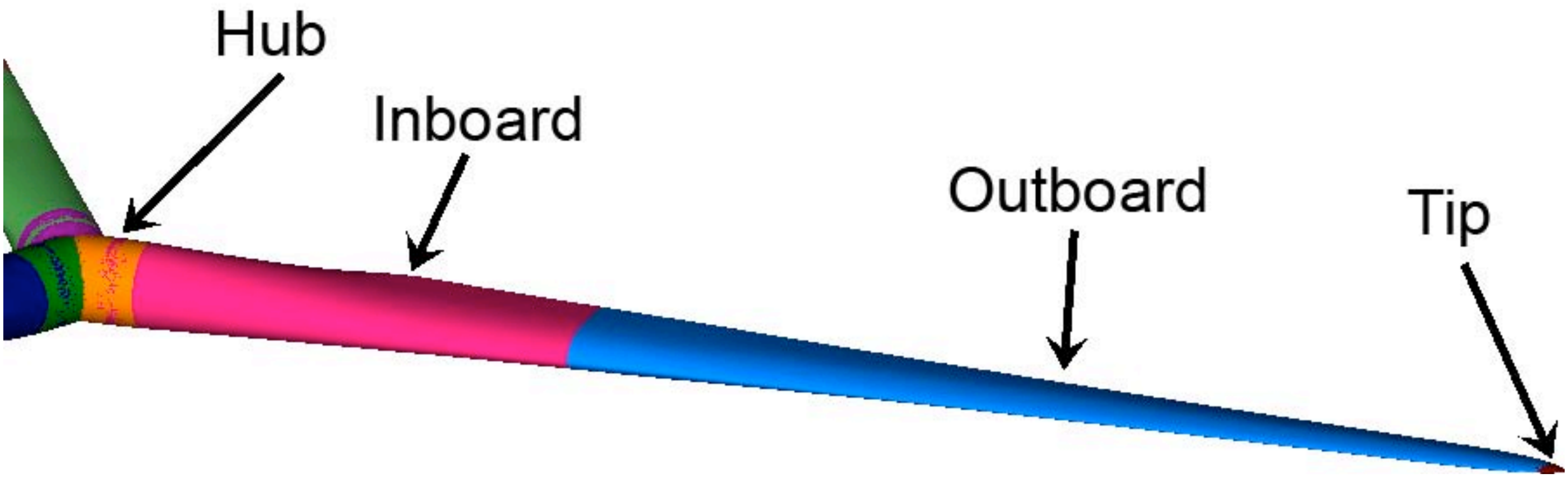

- Grid system designed to take advantage of overset/Chimera topology
- Modifications limited to inboard region

NREL 5-MW – Grid Topology

- Inboard (r < 20 m) blade grid can be modified and replaced
- Surface and volume grids of the outboard and tip regions can be reused
- Geometric modifications can be kept consistent and isolated to inboard region
- Hub geometry can also be examined without affecting remaining grid system

NREL 5-MW – “Baseline” Grid

- Baseline grid
  - Near-body ~10M
- Tip grid: 61×61×81

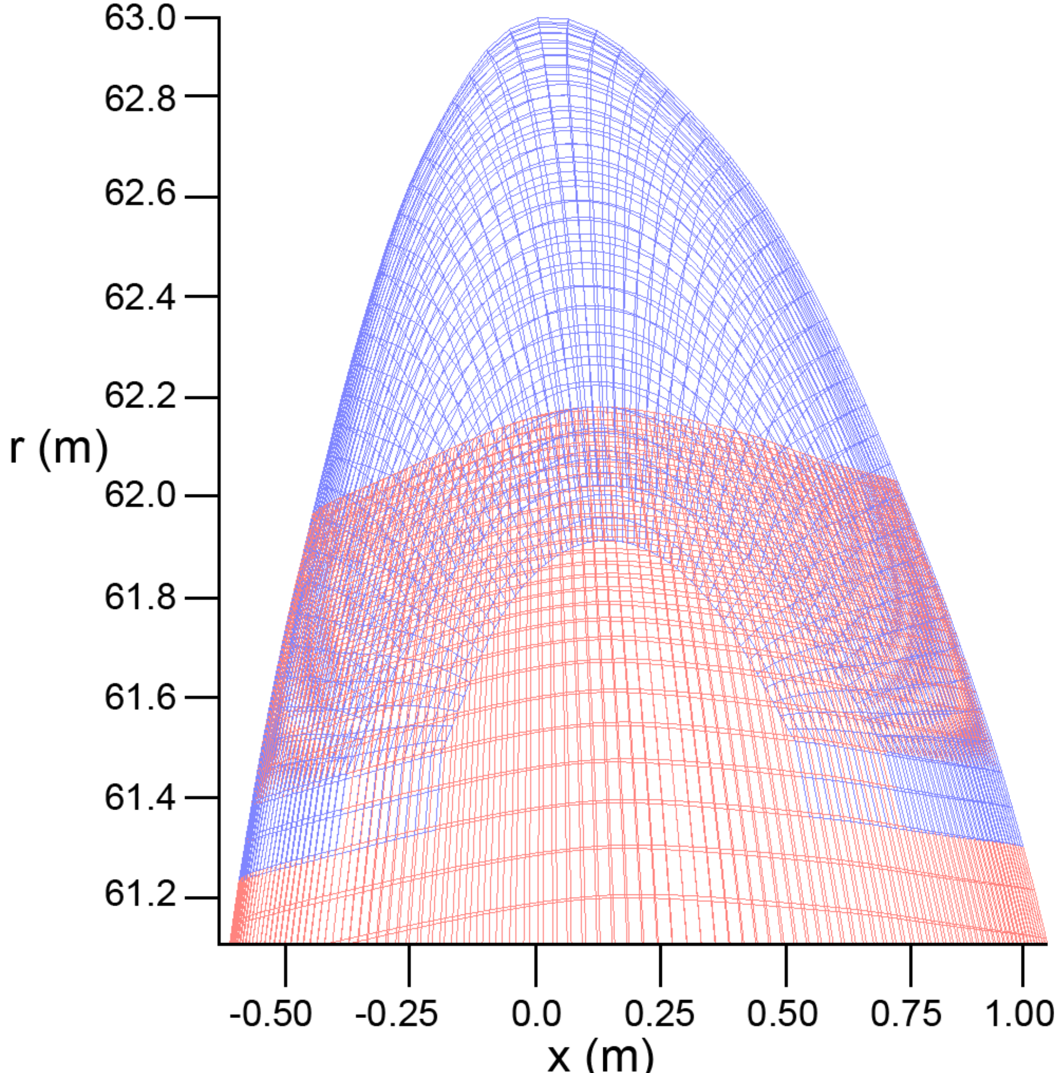

UCDAVIS

NREL 5-MW – "Baseline" Grid

- Baseline grid
  - Near-body ~10M
- Tip grid: 61×61×81
- Outboard: 201×116×81

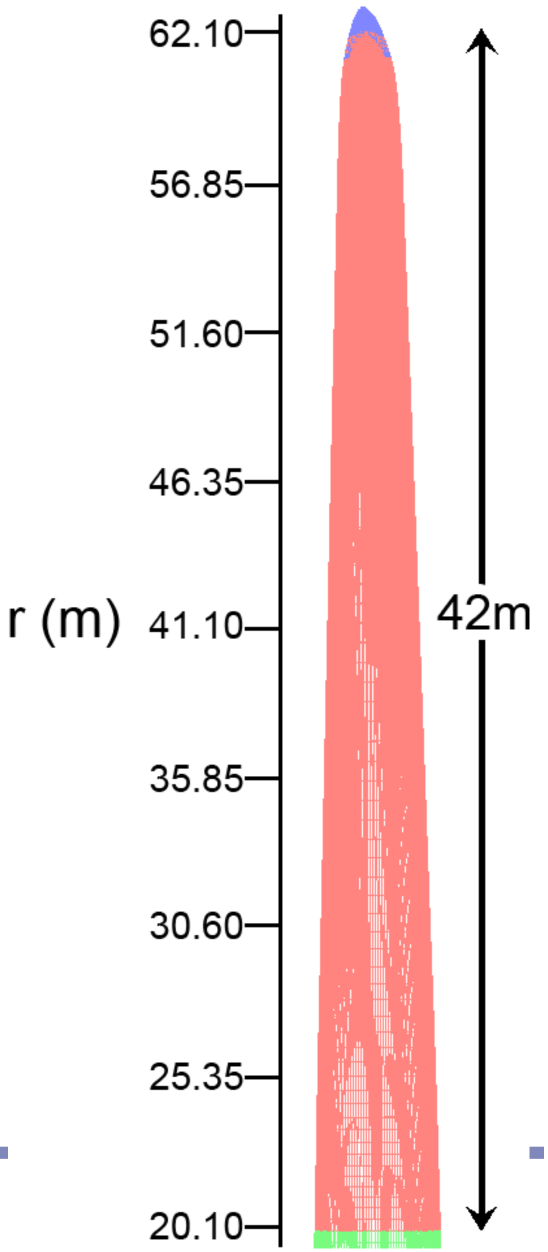

NREL 5-MW – "Baseline" Grid

- Baseline grid
  - Near-body ~10M
- Tip grid: 61×61×81
- Outboard: 201×116×81
- Inboard: 201×43×81

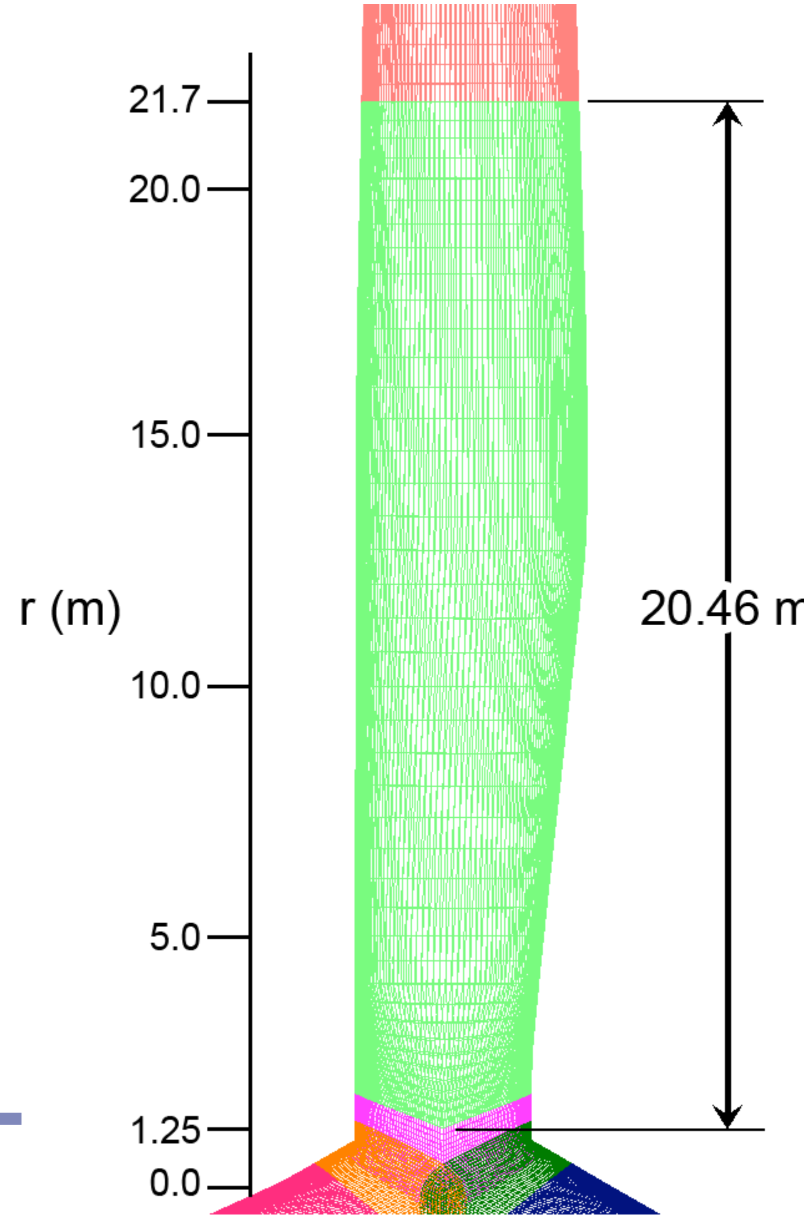

UCDAVIS

NREL 5-MW – “Baseline” Grid

- Baseline grid
  - Near-body ~10M
- Tip grid: 61×61×81
- Outboard: 201×116×81
- Inboard: 201×43×81
- Hub: 201×26×81

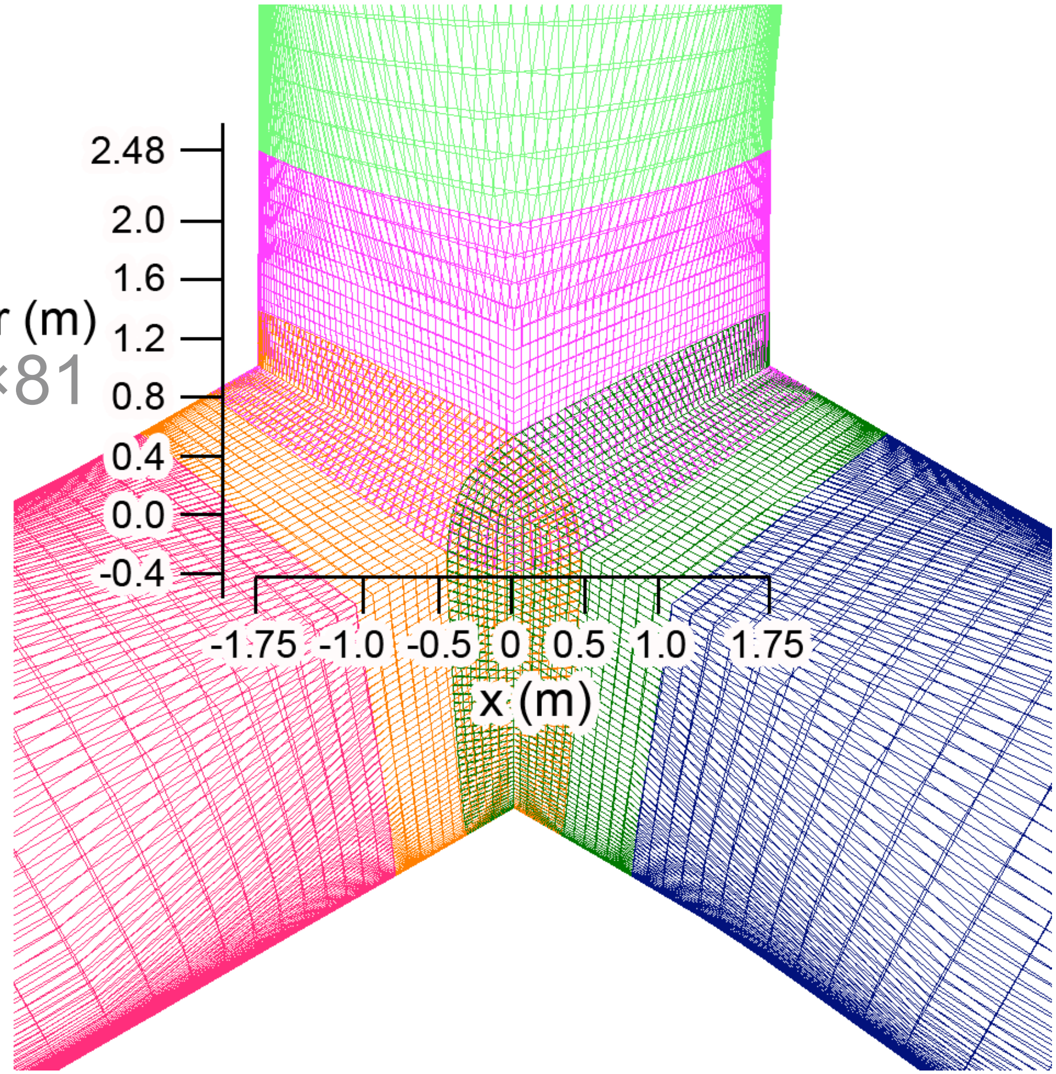

NREL 5-MW – Baseline Grid Domain

- Top view of domain
- 9 layers of BRICKS
- Each layer doubles cell dimension, ie:
  - DS_{inner} = 0.5 n
  - DS_{outer} = 128 m

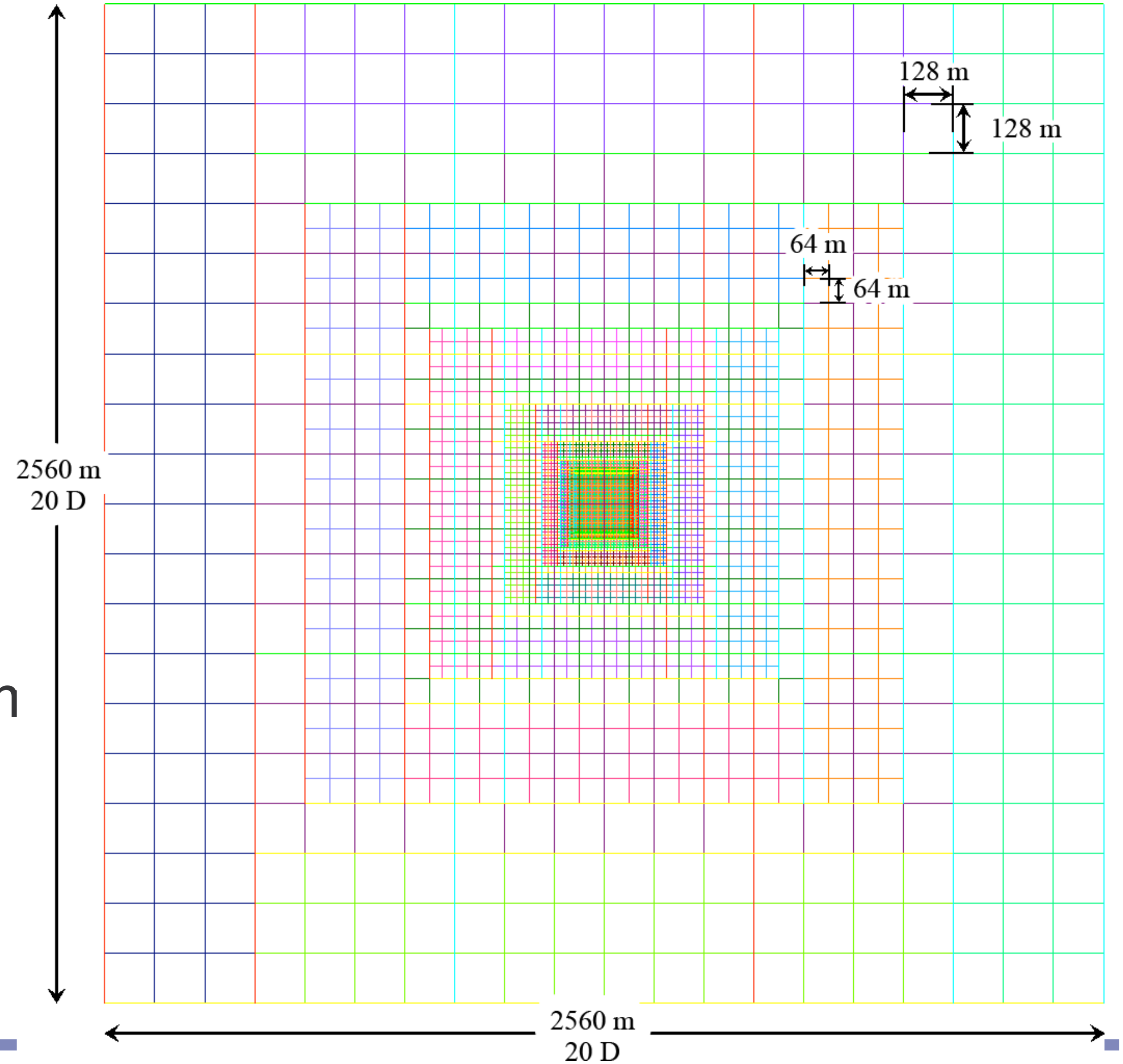

UCDAVIS

NREL 5-MW – Initial Off-Body Grid

- Side view

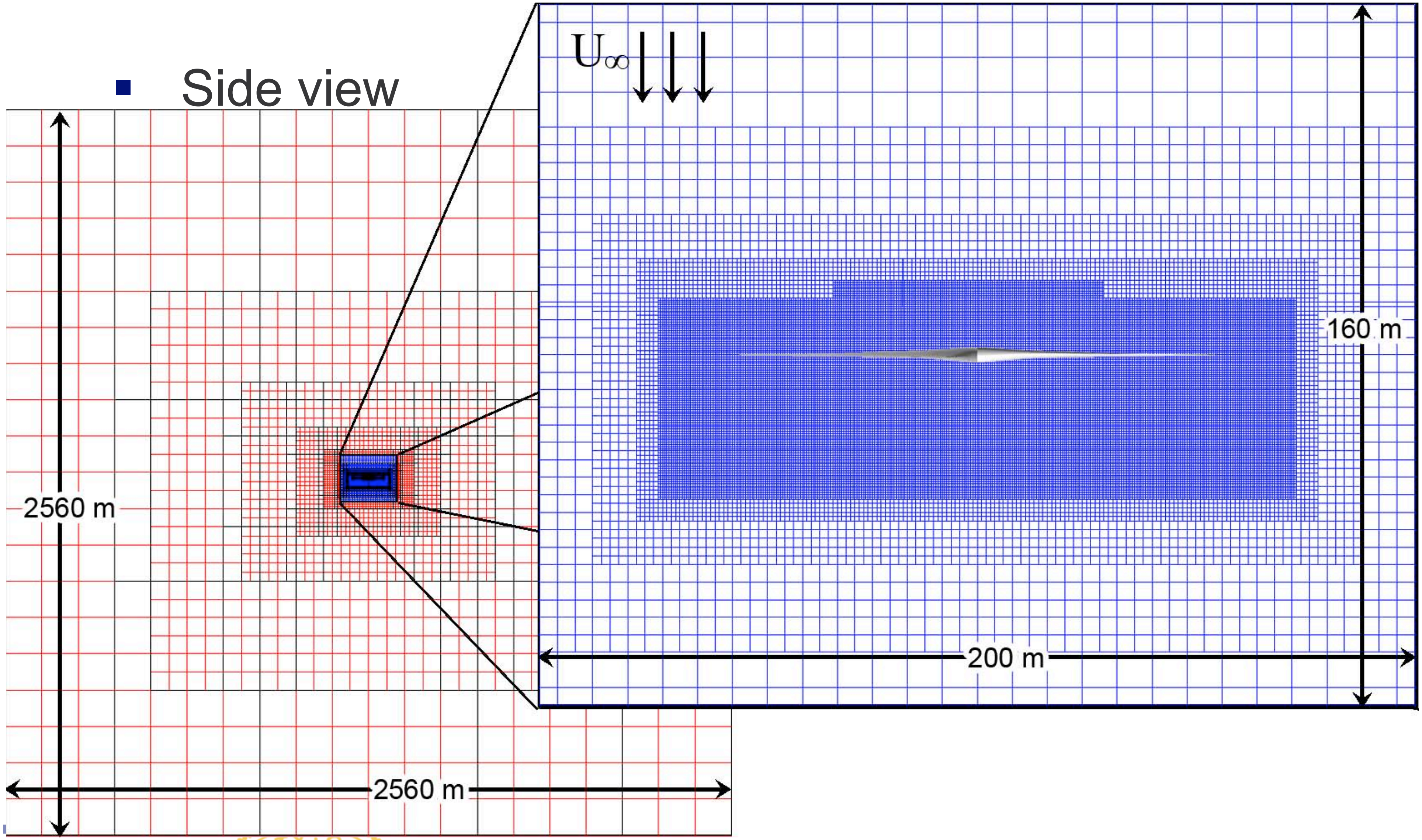

UCDAVIS

NREL 5-MW – Grid Topology

- Baseline ~10D far-field distance
- BRICKS allow for rapid and efficient domain construction
- Improved load balancing

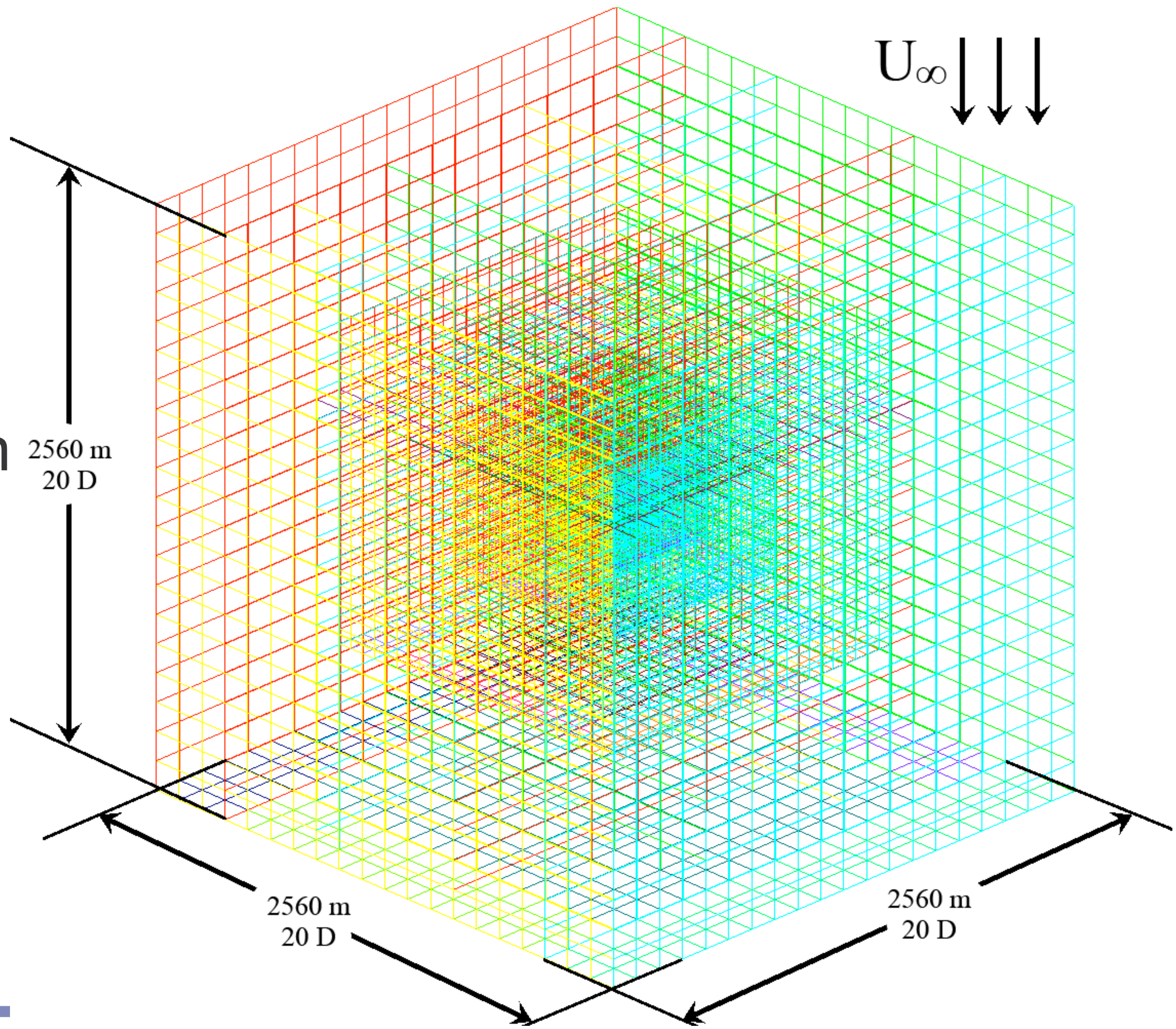

UCDAVIS

NREL 5-MW – U_∞ = 11m/s

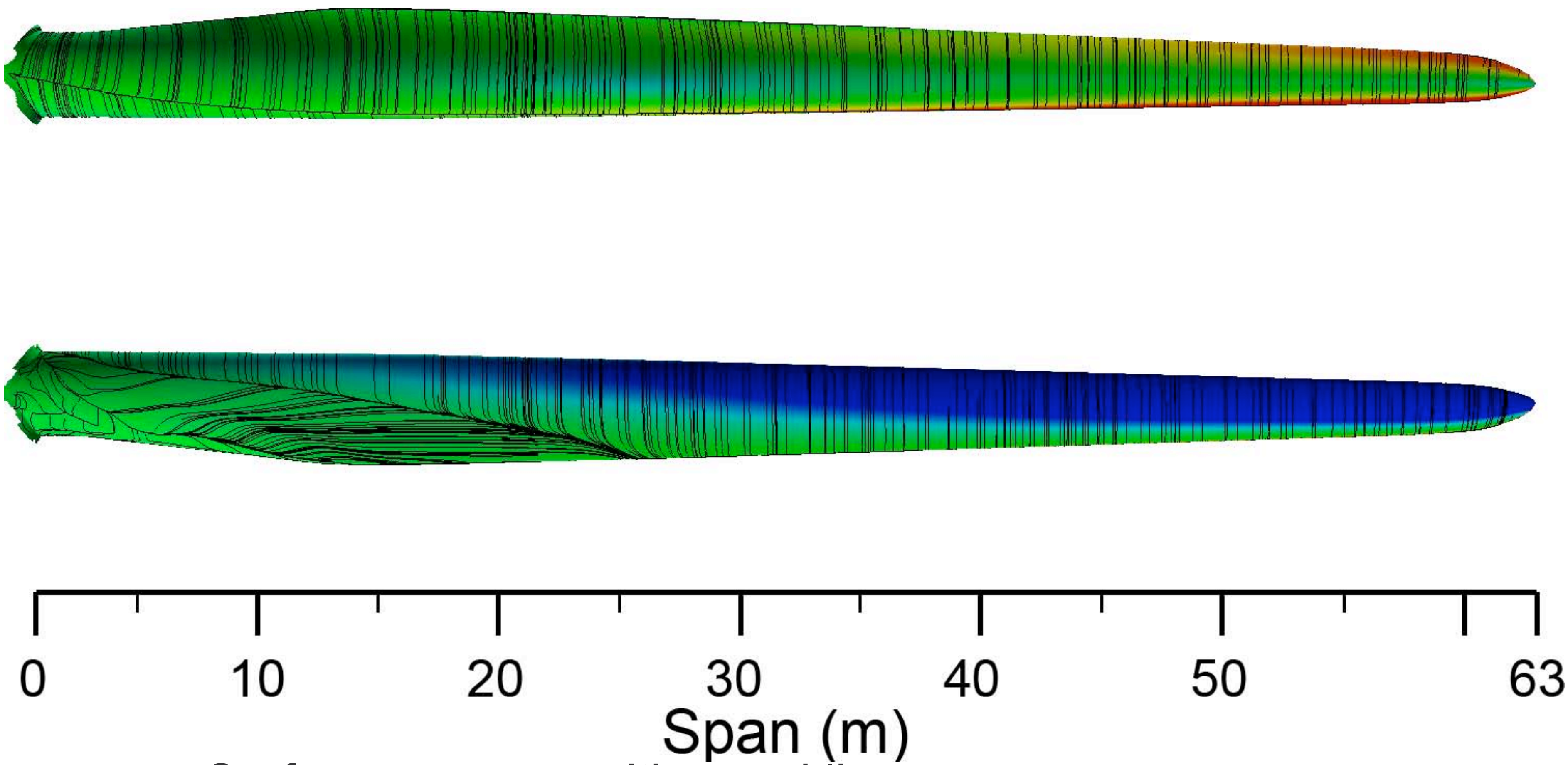

- Surface pressure with streaklines

Ring Fence Geometry

- Uniform height
  - $h_{fence} = 0.05c_{max}$
  - $h_{fence} \approx 0.23$ m
- Centered at max chord
  - $r = 13.7$ m
  - $r/R = 21.7\%$
- Overset grid
  - 201×47×81 points
  - ~5M additional points
  - Point-matched overlap on blade surface
  - Existing blade region IBLANKED

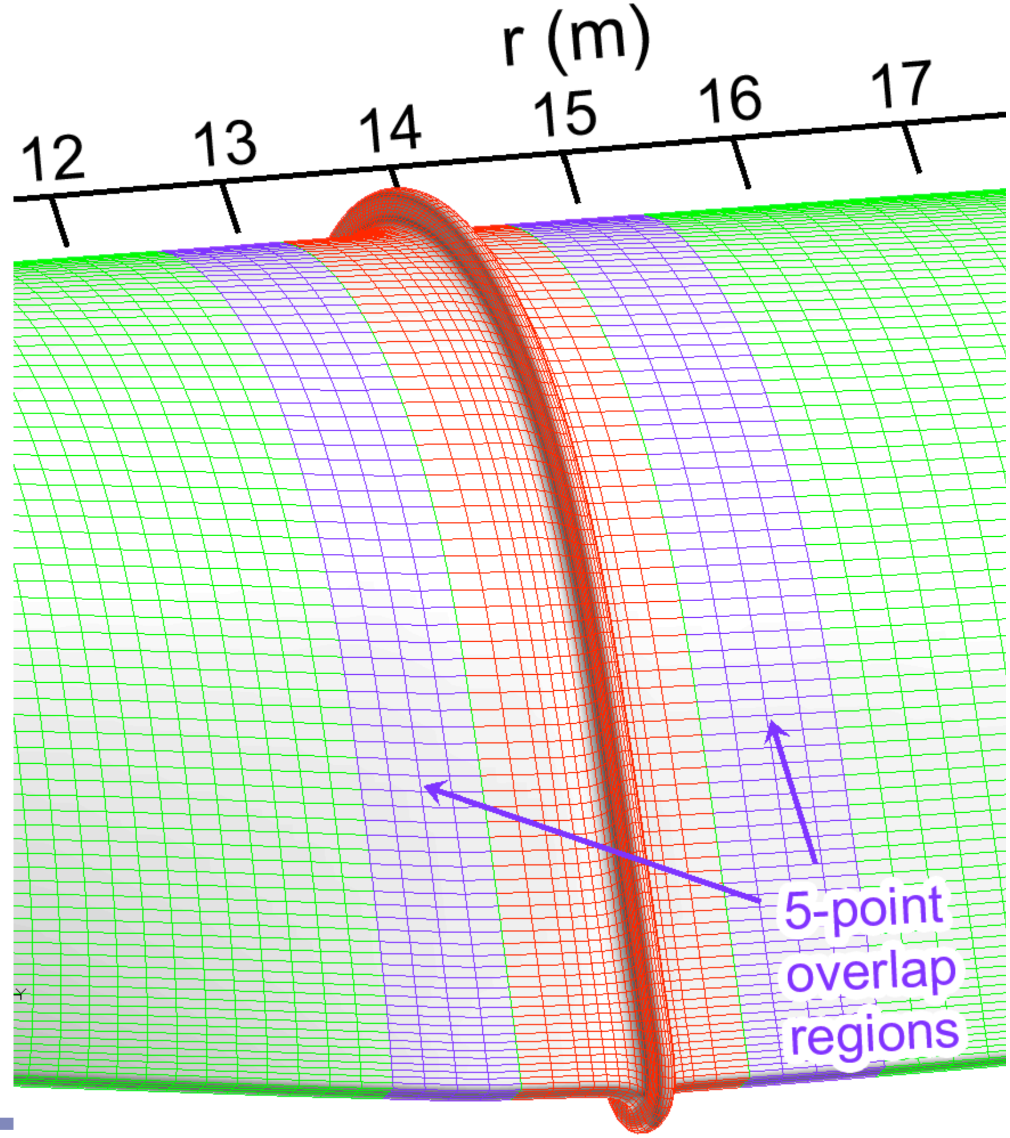

UCDAVIS

Suction Side Streaklines – 8 m/s

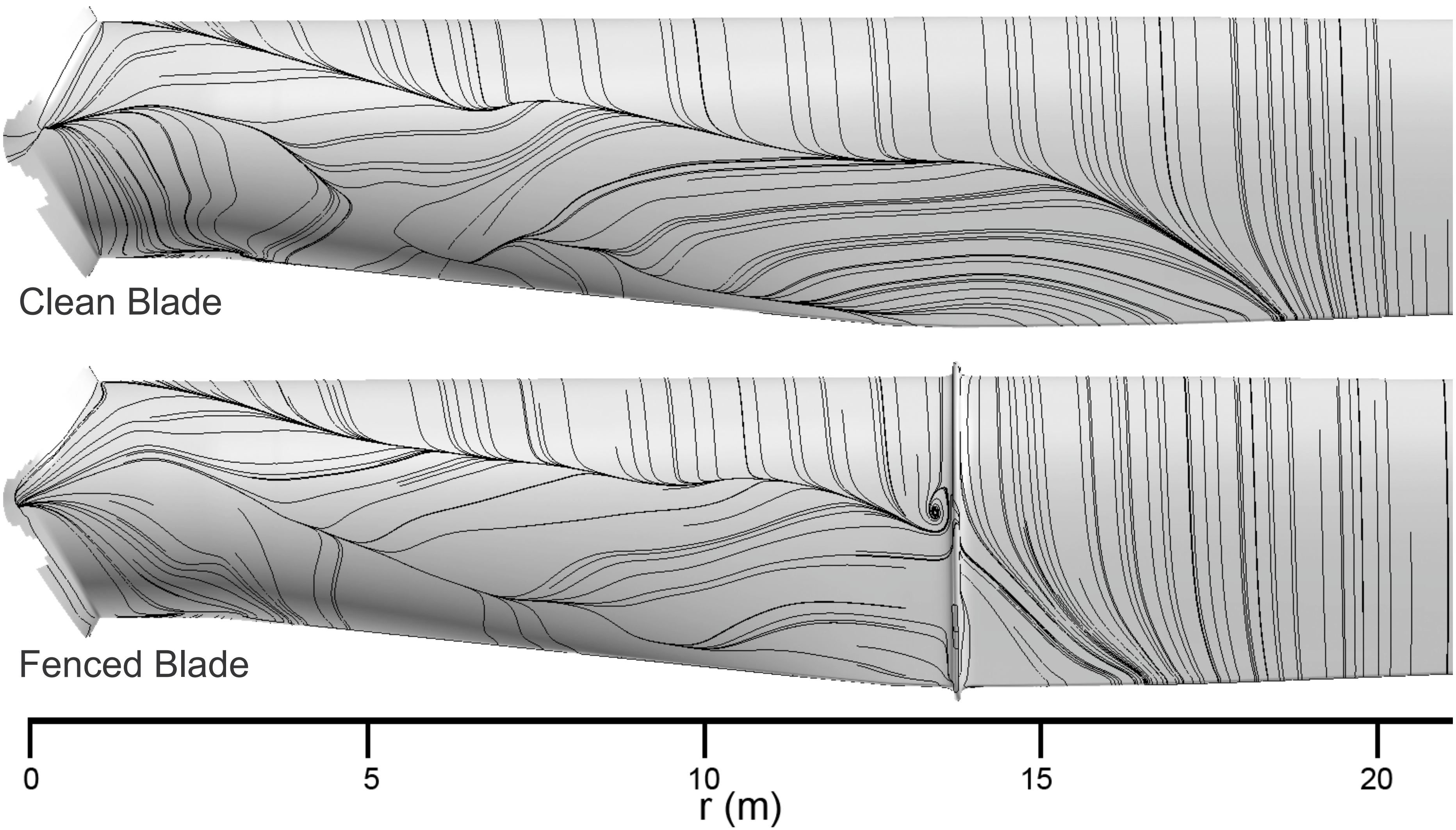

Suction Side Streaklines – 11 m/s

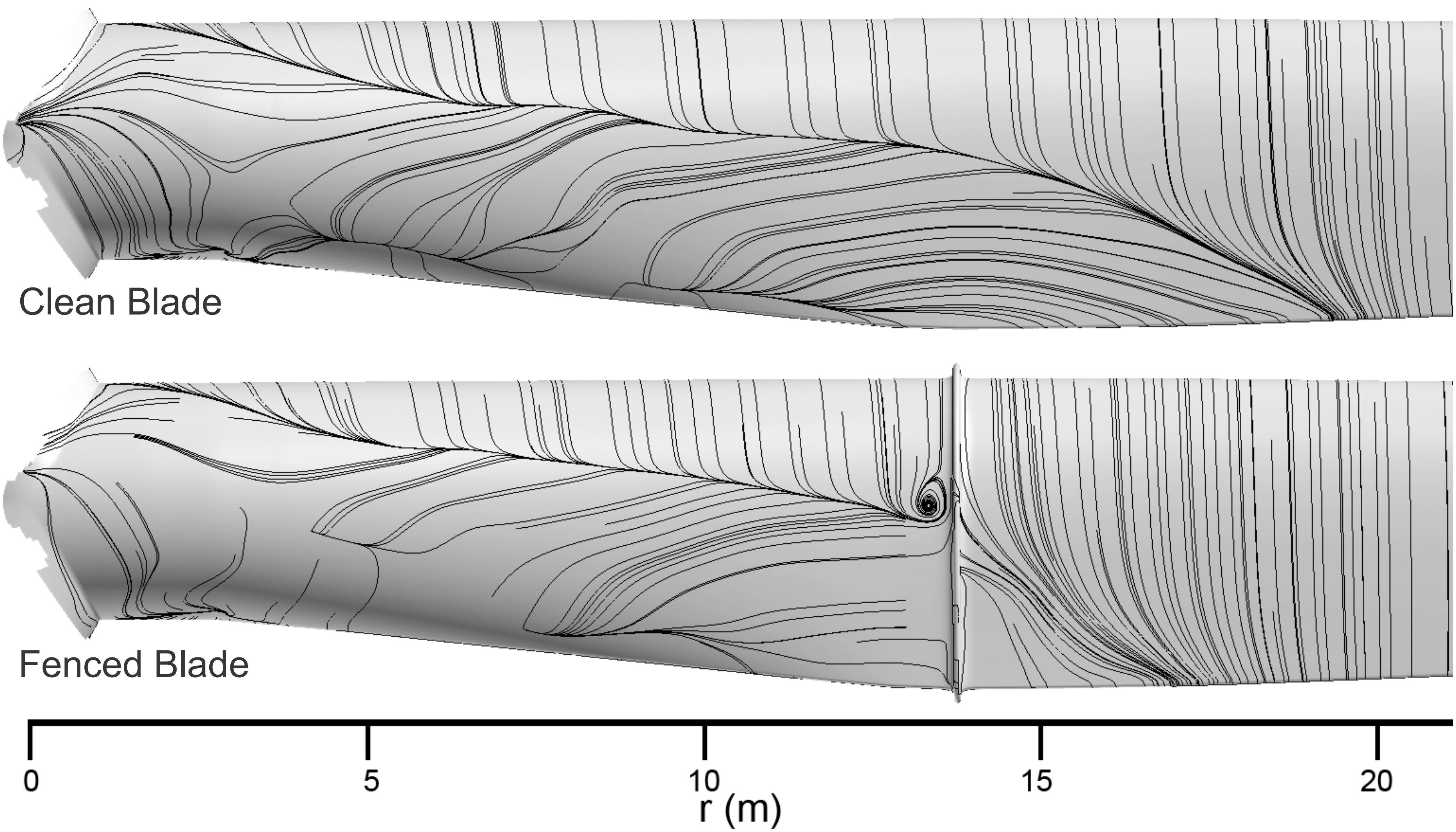

Ring Fence Effect on Rotor Power

Solver Mode	U_∞	*RPM*	$P_{baseline}$ *(kW)*	P_{fenced} (kW)	ΔP (kW)	***% Gain***
Steady	8	9.16	1718	1733	**15.3**	**0.889%**
Time-Acc	8	9.16	1719	1735	**15.3**	**0.888%**
Steady	11	11.89	4650	4679	**28.9**	**0.622%**
Time-Acc	11	11.89	4654	4681	**27.1**	**0.583%**

Inboard Flow Separation Mitigation

- Extensive grid independence and external validation were performed to ensure baseline solution accuracy
- Existence of inboard flow separation was verified
- A framework for detailed study of inboard rotor flows has been established
- A simple fence geometry to limit spanwise flow successfully increased power capture by nearly 1% in Region II

Departing Thoughts

- Wind power can and will continue to play a significant role in the global energy portfolio because it is:
    - Clean, renewable, emission-free
    - A mature and reliable technology
    - Economically viable
- Rotor RD&D is continuing to further reduce wind COE through
    - Further improvements in C_p
    - Reductions in blade loads and mass for given energy capture
    - Improvements in rotor energy capture for given loads and mass
- Overset Grid methodology has been key to the development of technologies and concepts that lead to further reductions in COE